Development of new highly active nano gold catalysts for selective oxidation reactions

Thesis submitted in accordance with the regulations of the

University of Cardiff for the degree of

Doctor of Philosophy

By

Moataz Hashem S. Morad

2014

In The Name Of Allah, The Most Compassionate,
The Most Merciful

To my parents

To my wife

To my brothers and sister

Acknowledgements

I would like to begin with praising and thanking the god, Allah, the almighty for all his bounties upon me and for his assistance in my life and my study which without him this work would not have been achieved.

I would like to thank many people for their help and support during my studies. I would like to greatly thank my supervisor, Prof. Graham Hutchings, for his invaluable support, guidance and encouragement throughout my PhD degree journey. I am also deeply grateful to Dr. Meenakshisundaram Sankar and Dr. Peter J. Miedziak for their supervision, input and support during my PhD study. I would also like to thank my co-supervisor Prof. David W. Knight for his suggestions and invaluable advice throughout this study. I would also like to extend my gratitude to Prof. Christopher Kiely and his group for STEM, Dr. David Morgan for XPS, James Pritchard for H_2O_2 testing and Dr Jennifer Edwards for the thesis correction. I shall also thank the department technical staff in chemistry school. Moreover, I would like to thank all the members of GJH group in lab 1.88, 1.86 and 0.90 for a nice time we spent together with special mention to Salem Bawaked, Mosaed Alhumaimess, Hamed Alshammari and Obaid Aldosari.

Of course, without funding, this research would not have been possible, and so I am incredibly grateful to Umm Al-Qura University, Saudi Arabia.

Finally, I would like to thank my parents and my brothers and my sister for their encouragement and support. I would like to express my deepest gratitude to my wife for endless patience during my study.

Publications

1. **Biotemplated synthesis of catalytic Au–Pd nanoparticles**
   Simon R. Hall, Andrew M. Collins, Natalie J. Wood, Wataru Ogasawara, **Moataz Morad**, Peter J. Miedziak, Meenakshisundaram Sankar, David W. Knight and Graham J. Hutchings. The Royal Society of Chemistry, 2012, 2, 2217-2220.

2. **Synthesis of Stable Ligand-free Gold–Palladium Nanoparticles Using a Simple Excess Anion Method**
   Meenakshisundaram Sankar, Qian He, **Moataz Morad**, James Pritchard, Simon J. Freakley, Jennifer K. Edwards, Stuart H. Taylor, David J. Morgan, Albert F. Carley, David W. Knight, Christopher J. Kiely, and Graham J. Hutchings. ACS Nano, 2012, 6 (8), p 6600–6613.

3. **Selective suppression of disproportionation reaction in solvent-less benzyl alcohol oxidation catalysed by supported Au–Pd nanoparticles**
   Enhong Cao, Meenakshisundaram Sankar, Ewa Nowicka, Qian He, **Moataz Morad**, Peter J. Miedziak, Stuart H. Taylor, David W. Knight, Donald Bethell, Christopher J. Kiely, Asterios Gavriilidis and Graham J. Hutchings. Catalysis Today, 203, 2013, p 146– 152.

4. **Solvent-free aerobic oxidation of alcohols using supported gold palladium nanoalloys prepared by a modified impregnation method**
   Moataz Morad, Meenakshisundaram Sankar, Enhong Cao, Ewa Nowicka, Peter J. Miedziak, David J. Morgan, David W. Knight, Donald Bethell, Asterios Gavriilidis, and Graham J. Hutchings. Catalysis Science & Technology, submitted manuscript ID: CY-ART-03-2014-000387.R2.

Abstract

Gold catalysts have been found to be efficient for many oxidation reactions. The performance of these catalysts depends strongly on the particle size of the Au nanoparticles. However, other factors also have a strong influence on the catalytic activity such as the preparation method and choice of support. The effect of support and the preparation methods has been investigated with regard to the selectivity and the activity of Au catalysts.

The disproportionation of benzyl alcohol has been identified as a source of toluene formation in the solvent free oxidation of benzyl alcohol using supported gold palladium catalysts. The disproportionation reaction of benzyl alcohol oxidation has been performed in a conventional glass stirred reactor. Oxidation and disproportionation reactions respond slightly differently to the changes in reaction parameters, such as oxygen concentration and pressure. When MgO supported gold-palladium catalysts were used for this reaction, the toluene selectivity reduced substantially at the cost of conversion.

The synthesis of bimetallic nanoalloys is of great practical importance as they exhibit size-dependent functional properties, which can be exploited in fields such as catalysis. Conventional chemical impregnation routes for generating supported bimetallic nanoparticles are facile, but often generate materials having broad particle size distributions, which typically exhibit core–shell morphologies and significant compositional variations from particle-to-particle. More complex sol-immobilisation synthesis techniques offer much better control over particle size distribution, but retain stabilising ligands on the surface, which can be deleterious for catalysis. Here, a convenient excess anion modification and post reduction step prior to the impregnation method has been used, which permits the reproducible preparation of supported bimetallic AuPd nanoparticles with a tight particle size distribution comparable to that found for sol-immobilisation materials, but without the complication of ligands adsorbed on the particle surface. These advantageous features of the modified impregnation materials resulting in higher activity and stability compared to the

catalysts prepared using both conventional impregnation and sol-immobilisation methods. Detailed STEM combined with EDX analyses of individual particles have revealed that an increase in anion concentration increases the gold content of individual particles in the resultant catalyst, thus providing a method for controlling/tuning the composition of the nanoalloy particles. The improved activity and stability characteristics of these new catalysts are demonstrated using: (i) the solvent-free aerobic oxidation of benzyl alcohol and (ii) the direct synthesis of hydrogen peroxide as case studies. The study has examined using this modified impregnation catalyst in different Au:Pd ratios for the solvent-free aerobic oxidation of benzyl alcohol. These modified impregnation catalysts have been found to be exceptionally active, mainly with a Au-rich composition, when compared to reduced conventional impregnation catalysts. Moreover, these modified impregnation catalysts have been found to be exceptionally active and stable when evaluated for crotyl alcohol in mild conditions when compared to sol-immobilisation methods.

This new preparation protocol could be beneficial for both the academic research community and the industrial community, with a very convenient and reproducible methodology for preparing supported Au-Pd nanoalloy catalysts with high activity and stability, without using any ligands or stabilisers, while not compromising their catalytic activity.

Table of Contents

Chapter One:

Introduction and literature review

1.1- Introduction

1.1.1- Beginning of catalysis

The history of catalysis began with the first observation of an inorganic catalysis reaction, when alcohol was converted to ether using sulphuric acid in 1552 by Valerius Cordus [1]. Fulhame was the first to present the basic aspects of catalysis in 1794 when he found that water was needed for CO oxidation, and that water was not affected by the chemical reaction [1, 2]. In 1812, the Russian chemist Gottlieb Kirchhoff came to a similar conclusion with respect to the acids used for the hydrolysis of starch to sugars [1, 3, 4]. Sir Humphrey Davy, in 1817, proposed that mixing oxygen with flammable gases when heated at lower than the combustion temperature could lead to an explosion if they were passed over platinum [4]. A year later, Thendard illustrated that hydrogen peroxide decomposed in water; however, it is possible to stabilise hydrogen peroxide in acidic solutions. Moreover, he showed that the rate of decomposition could be decreased by adding noble metals [5, 6]. In 1820, a study was carried out by Edmund Davy into the role of noble metals on alcohol oxidation which could rapidly take place over platinum exposed to air [7]. In 1822, Dobereiner, who burnt oxygen and hydrogen over platinum at room temperature, confirmed the Edmund Davy study [8]. Dulong and Thenard then found that the activity for the reaction of oxygen and hydrogen is dependent on the material used when the tests are carried out with materials other than platinum [3, 9, 10]. Henry, in 1825, discovered that some materials prohibit the combustion of hydrogen, such as hydrogen sulphide. He also found that platinum based catalysts are inactive for CO oxidation [11]. Turner demonstrated the possibility of

combining hydrogen with chlorine when platinum based catalysts are used. Through this discovery, Peregrine Phillips was inspired to develop the first commercial catalytic process by oxidising the sulphur dioxide over platinum based catalysts to give sulphuric acid [12]. After these first important milestones in the history of catalysis, the era of catalysis began, and further investigations have been carried out.

1.1.2- Definition of catalysis

The word catalysis originates from Greek the prefix cata and the verb lysein. Cata means down and the meaning of lysein is split. A catalyst splits the forces that impede the molecules reacting. In 1836, Berzelius coined the word catalysis as he reported: "*I shall therefore call it the catalytic power of substances, and the decomposition by means of this power catalysis, just as we use the word analysis to denote the separation of the component parts of bodies by means of ordinary chemical process. Catalytic power actually means that substances are able to awake affinities which are asleep at this temperature by their mere presence and not by their own affinity*" [13]. He defined a catalyst as a compound which increases the rate of a chemical reaction without being consumed by the reaction [14]. More delicate definitions have been made as a result of developments in understanding the catalysis process. According to G. C. Bond, the catalyst is "a substance that increases the rate at which a chemical system approaches equilibrium, without being consumed in the process" [13]. However, the catalyst will not change the thermodynamics of the reaction or the equilibrium position, because the

effect of the catalyst will be placed on both the forward and reverse reactions (i.e. increasing the rate constant of the reaction K_1 and K_2) [15], as shown below:

$$A \underset{K_2}{\overset{K_1}{\rightleftharpoons}} B$$

The rate constant **k**, is defined by the Arrhenius equation:

$$k = A \,.\, \exp^{(-Ea/RT)}$$

Equation 1.1: Arrhenius equation

Where **A** is the collision frequency, **Ea** is the activation energy (KJ mol^{-1}), **R** is the gas constant (8.314 JK^{-1} mol^{-1}) and **T** is the temperature

Simply, the catalyst provides a new and easier pathway by lowering the activation energy, as shown in **Figure 1.1**. The catalyst, as shown, is not consumed in the reaction, so it does not exist in the final chemical equation and it speeds up the reactions that are kinetically favourable. This suggests that the catalysts cannot catalyse a reaction which is thermodynamically impossible [13].

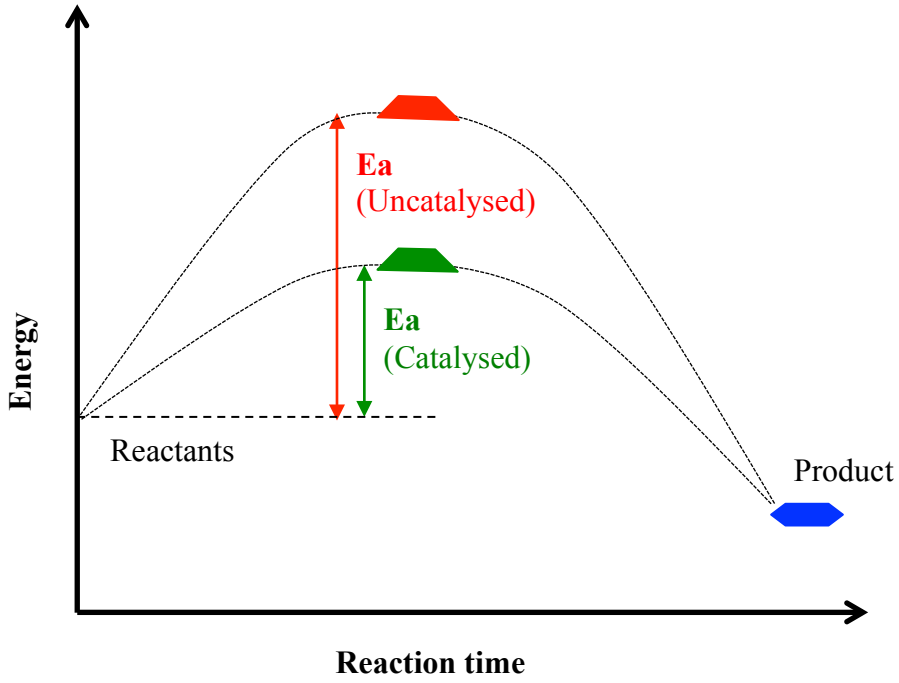

Figure 1.1: A catalyst provides a different path with lower activation energy. The result is an increase in the rate of formation of products

1.1.3- Importance of catalysis

Catalysis is very important in our lives and essential for industry processes. The application of catalysis has been a necessity for industry over the last 150 years. Catalysis has changed our lives, and it is important for many industrial processes in the reality we see around us, for example plastics manufacturing, fuel production and pollution reduction [15]. Approximately 90 % of materials produced are achieved using catalysis at one stage or another. Therefore, the efficacy of a modern chemical industry can be said to be intimately tied to catalysis. Apart from that, catalysis is important in environmental control for example, to convert the emission of hydrocarbons, CO and NO_x into less harmful gases. It is also an extremely active research area. [13, 15, 16].

1.2- Types of catalysis

There are three main types of catalysis: heterogeneous catalysis, homogeneous catalysis and bio-catalysis. The following sections will briefly discuss these types of catalysis. Generally, the first type, bio-catalysis, are considered to be natural catalysts. The second type, homogeneous catalysis, includes mixing the catalyst and reaction in the same phase, usually a liquid phase. In heterogeneous catalysis, the catalyst and reaction mixture are in different phases.

1.2.1- Bio-catalysis

The biocatalyst is an enzyme that is a natural process complex protein that catalyses the reactions in living cell. The backbones of proteins are amino acids, which are linked together by peptide bonds, and these bonds establish the enzyme's structure. A cleft that is surrounded by an array of amino acid residues is usually the active site of an enzyme. As shown in **Figure 1.2**, an enzyme can bind to the substrate. Enzymes use four kinds of interactions to bind their substrates: electrostatic interactions, hydrogen bonding, van der Waals interactions and hydrophobic interactions [16, 17].

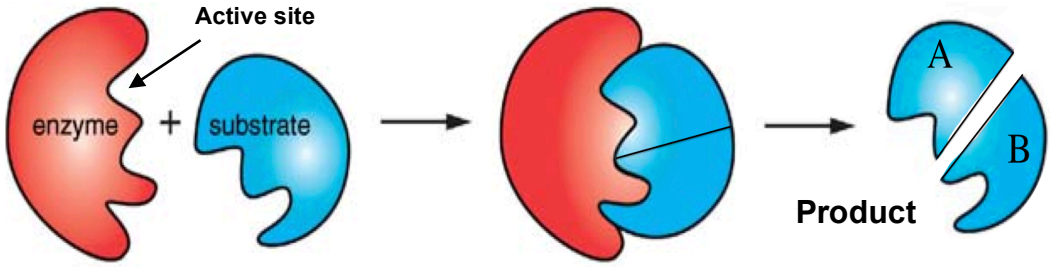

Figure 1.2: Enzyme-substrate binding [17]

Enzymes are extremely efficient and highly selective catalysts, catalysing specific reactions only. This specificity is due to the shapes of the enzyme molecules. An enzyme typically completes 1000 catalytic cycles in one second. Therefore, biocatalysts are extremely important, especially in the pharmaceutical and food industries, as only one compound has the desired activity. As result of this, biocatalysts are used for many drugs, food additives, flavourings, and fragrances [17]. Further advantages of enzymatic reactions are not only for biological systems, as many enzymes are also available as isolated compounds, which catalyse reactions in water and even in organic solvents; however, heating might destroy an enzyme by breaking the weak bonds that hold the active site in its correct configuration [17, 18].

1.2.2- Homogeneous catalysis

In homogeneous catalysis, both the catalyst and the reactant are in the same phase, (e.g. ozone destruction by chloride) [16]. Ozone decomposes spontaneously under the influence of light, but a Cl atom works as a catalyst and accelerates the reaction tremendously, leaving the reaction cycle unaltered. The reaction takes place in the gas phase; the pathway is shown in **Scheme 1.1**:

$$Cl + O_3 \rightarrow ClO_3$$

$$ClO_3 \rightarrow ClO + O_2$$

$$ClO + O \rightarrow Cl + O_2$$

Scheme 1.1: Ozone decomposes by chlorine atoms reacting [16]

Historically, this reaction was important in the prediction of the ozone hole [16]. Industrially, there has been an increase in the number of applications using homogeneous catalysis. The advantage of it is that high selectivity can be achieved, as the active sites of the catalyst are reachable. However, recovery and separation of the catalyst after usage are major disadvantages in homogenous catalysis [19].

1.2.3- Heterogeneous catalysis

In heterogeneous catalysis, the catalyst is present in a different phase from the reaction mixture. The catalytic reaction happens at the catalyst surface on which the reactants temporarily become adsorbed. Impermanent bonds connect the surface to the reactant molecules at the active site where the reaction happens. The product is then desorbed from the catalyst due to the weak bond with the surface. The catalytic oxidation of CO is one example of heterogeneous catalysis. **Figure 1.3** shows the reaction cycle [16].

The catalytic reaction cycle begins with the adsorption of CO and O_2 on the surface of the catalyst, whereby the oxygen molecules become isolated into two O atoms. The adsorbed O atom and the adsorbed CO molecule then react on the surface to form CO_2. The product formed is very stable and unreactive. It interacts weakly with the catalyst surface and it is then desorbed from the catalyst. As a result of the adsorption, sites on the catalyst are independent, so the catalyst becomes available for further reaction cycles [16, 17].

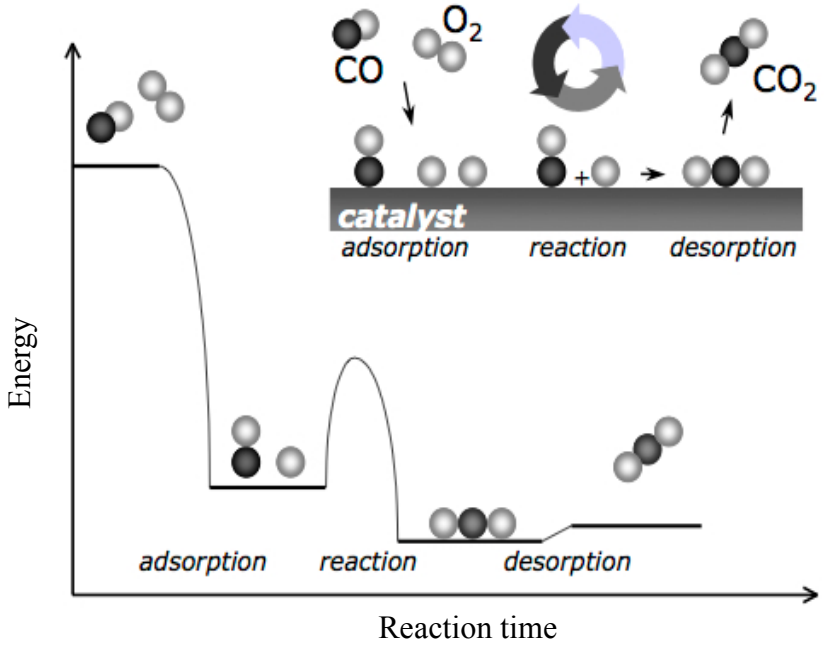

Figure 1.3: Reaction cycle and potential energy diagram for the catalytic oxidation of CO by O_2 [16]

Commonly, catalyst metals are expensive materials (e.g. platinum and gold) so in an economical way the catalyst metals are usually introduced as nanometer-sized particles. The nanometal is supported on an inert material or metal oxide (e.g. TiO_2 and MgO). The reaction will occur on the active surface of the catalyst [16].

Consequently, designing highly active, selective and stable heterogeneous catalysts presents a great challenge in the heterogeneous catalysis community. However, heterogeneous catalysts are important and a highly active academic research area concerns catalysis. Moreover, heterogeneous catalysts are widely used in industry in the production of chemical compounds and in the petrochemical industry; see **Table 1.1** for

the main processes based on heterogeneous catalysis [16, 17, 20]. This thesis will go through the reactions using heterogeneous catalysis.

Table 1.1: Largest processes based on heterogeneous catalysis [16]

Reaction	**Catalyst**
Catalytic cracking of crude oil	Zeolites
Hydrotreating of crude oil	Co–Mo, Ni–Mo, Ni–W (sulfidic form)
Reforming of naphtha (to gasoline)	Pt, Pt–Re, Pt–Ir
Alkylation	H_2SO_4, HF, solid acids
Polymerization of ethylene, propylene, a.o.	Cr, $TiCl_x/MgCl_2$
Ethylene epoxidation to ethylene oxide	Ag
Vinyl chloride (ethylene + Cl_2)	Cu (as chloride)
Steam reforming of methane to CO + H_2	Ni
Water-gas shift reaction	Fe (oxide), Cu–ZnO
Methanation	Ni
Ammonia synthesis	Fe
Ammonia oxidation to NO and HNO_3	Pt–Rh
Acrylonitrile from propylene and ammonia	Bi–Mo, Fe–Sb (oxides)
Hydrogenation of vegetable oils	Ni
Manufacture of sulfuric acid	V_2O_5
Oxidation of CO & hydrocarbons (car exhaust)	Pt, Pd
Reduction of NOx (in exhaust)	Rh, vanadium oxide

1.3- Catalysis by gold

The element gold (Au) has the atomic number 79 with atomic configuration $[Xe]4f^{14}5d^{10}6s^{1}$. Gold is one of the transition metals. It lies in the 11^{th} group of the periodic table along with silver and copper, which due to their ability to form many alloys with many other metals, are called coinage metals [21]. **Table 1.2** shows the physical comparisons that have been made for the three elements of group 11 in the periodic table [21].

Table 1.2: Physical comparisons of the three elements of group 11 in the periodic table

Property	Copper (Cu)	Silver (Ag)	Gold (Au)
Electronic configuration	$[Ar]3d^{10}4s^{1}$	$[Kr]4d^{10}5s^{1}$	$[Xe]4f^{14}5d^{10}6s^{1}$
Atomic weight	63.55	107.86	196.97
Atomic number	29	47	79
MP (°C)	1083	961	1064
BP (°C)	2570	2155	2808
Density (g/ml)	8.95	10.49	19.32
Structure	Fcc	Fcc	Fcc
Electrical resistivity (μohm-cm)	1.673	1.59	2.35
Electronegativity	1.9	1.9	2.4
Electron affinity (kJ mol^{-1})	119	125	223
First ionization energy (kJ mol^{-1})	745	731	890
Metal radius in (12-coordination)/pm	128	144	144
Number of natural isotopes	2	2	1

Gold is considered to be the most electronegative metal, and among other metallic elements, gold is unique as it shows great resistance to oxidation and corrosion [22]. Gold as a bulk material dose not react directly with other electronegative elements (e.g. oxygen and sulphur) due to the high electronegativity of gold, and it will only dissolve in hydrochloric acid when there is a strong oxidising agent such as nitrate ion present (i.e. aqua regia) [21]. The most common oxidation states for gold are +1 and +3 states, and the highest oxidation state is +5 which is seen only in [AuF^{6-}].

In the electronic configuration of copper, silver and gold, these metals have fully occupied d-bands. However, Cu and Ag have low ionisation potentials and the ability to lose electrons, therefore they are potentially able to be catalytically active. In point of fact, industrially, Cu is used for methanol synthesis [23] and Ag is used for ethylene oxide synthesis [24]. On the contrary, Au has a high ionisation potential. Consequently, it has a low attraction to other elements. This was illustrated by early surface science studies and density functional calculations which showed that no dissociative adsorption of H_2 and O_2 happens below 200 °C, which catalytically indicates that Au should be inactive for hydrogenation and oxidation reactions [25, 26]. For these reasons, silver and copper are used in many large processes; moreover, other noble metals such as platinum and palladium are both largely used as catalysts. On the contrary, gold received very little attention in the catalysis community until the 1980s [27]. However, nowadays the interest in gold has increased for industrial and academic chemists. Au has potential applications in material science, medicine and in both homogeneous and heterogeneous catalysis [28].

1.3.1- History of catalysis by gold

In the early history of gold catalysis (about 1960), gold was always regarded as being catalytically inactive [29]. Few references were made to the catalytic power of gold, which is not surprising as it was done using macroscopic gold measurement (wire, foil or powder), not as the measurement of nano gold catalytic power nowadays [29]. The earliest observation was in 1823 by Dulong and Thenard who observed that gold was among the metals that catalysed the decomposition of ammonia; this may have been the first hint that gold might not always exhibit poor activity [9]. This work helped Berzelius to develop the idea of catalytic action. In 1834, Michael Faraday found that at room temperature gold catalysed the reaction of hydrogen with oxygen [29, 30]. 1861 saw the first investigation of gold measurement and the effects of gold on the solubility of hydrogen in palladium, which was carried out by Thomas Graham [31, 32]. The early study of the oxidation of hydrogen by Michael Faraday reaction was implemented again using gold gauze in 1906 [33], and then later in 1925. It was found that gold powder is an effective catalyst [34, 35]. Later, the first report of CO oxidation using gold gauze was observed; it was also noted that gold had mild activity for ethene hydrogenation [36, 37]. In 1973, Bond and co-workers observed that gold in small particles dispersed on SiO_2 or Al_2O_3 successfully catalysed the hydrogenation of alkenes and alkynes [38, 39]. This study proved that Au might be important for gold catalyst activity when dispersed in small nanoparticles. After these previous reports, gold received a large deal of interest after two major discoveries demonstrated that nano-particulate gold may be the best catalyst for certain reactions. These two discoveries were made by: a)

Hutchings, who predicted that gold would be the most active catalyst for ethylene hydrochlorination [40] b) Haruta, who discovered that gold supported catalysts are very active for low temperature CO oxidation [41]. Subsequently, nano-particulate gold catalysts have attracted remarkable attention due to their distinctive catalytic properties. **Figure 1.4** demonstrates the dramatic growth of publications in the field of gold catalysis over the years [42]. There are many applications of gold as a catalyst, such as in chemical industrial processes [43]; environmental control for fuel cells [44], and CO oxidation at low temperatures. Other important industrial applications include fuel cells and car exhaust fumes clean up [42, 45]. The significant applications of the use of gold as a catalyst are in the production of hydrogen peroxide, oxidation of alcohols, oxidation of hydrocarbons and hydrogenation of alkynes [43].

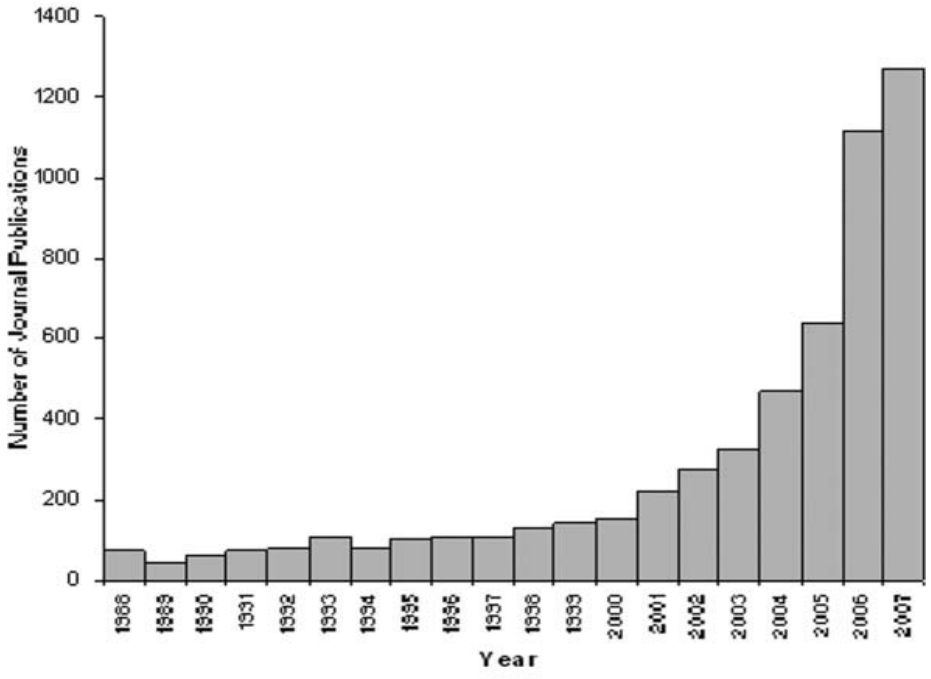

Figure 1.4: Diagram showing the number of publications on "gold catalysis" from 1988 to 2007 [42]

1.3.2- Major preparation methods for gold catalyst

The preparation method and the choice of supports could have an interesting effect on catalyst activity. Gold particle size is very important to obtain an active catalyst, and the preparation method could strongly affect this [43]. The major preparation methods depend on introducing and dispersing gold nanoparticles on supports using a synthesis method such as impregnation, sol immobilisation, deposition–precipitation and co-precipitation. However, introducing gold nanoparticles on the support is considered to be the first main step for the preparation method, which is then followed by drying, calcination or a reduction step in some cases.

1.3.2.1- Conventional wet impregnation method (C_{Im})

The first supported gold catalysts were prepared using the impregnation method [21, 46]. It is the simplest and most straightforward method and can be applied to a number of supports, which is one of the advantages of the method. The impregnation catalyst can be obtained by adding a support to an aqueous solution of gold precursor. The active phase from the gold solution is adsorbed onto the support. Gold chloride ($AuCl_3$) and chloroauric acid ($HAuCl_4$) are the most common aqueous solutions of gold precursors used. Nevertheless, the disadvantage of the method is that it displays only a moderate level of activity for alcohol oxidation [47], which could be due to the large particles ranging from 10-30 nm, and agglomeration of gold pieces during thermal treatment in the final step [46].

1.3.2.2- Sol immobilisation method (S_{Im})

The S_{Im} method immobilises the gold particles on a support from a colloidal suspension using stabiliser ligands and a reducing agent. In a typical preparation, the support is added to the aqueous solution of gold precursor, and a stabiliser ligand such as poly vinyl alcohol (PVA) is added, which works to protect the nanoparticles from sintering. The stabiliser ligand can be removed, after the gold nanoparticles have been supported, by refluxing the catalyst in water, which leads to a more active catalyst for CO oxidation [48]; also, it can be removed with thermal treatment, which leads to sintering of the gold nanoparticles [46]. The advantages of this technique are that the gold is already reduced by a reducing agent ($NaBH_4$) and as the particle size is controlled. The catalysts have a high metal dispersion and metal particles in the 2-6 nm range, which have high catalytic activity for alcohol oxidation [49]. The disadvantages are that it is not as simple as the previous impregnation technique. Moreover, it is not as versatile because a very limited number of supports can be applied, such as activated carbon and TiO_2, whereas it is inapplicable for supports such as SiO_2 and Al_2O_3, because it is highly dependent on the iso-electric point (IEP) of the support [50]. Another disadvantage of the method is that it cannot easily be scaled-up for use on an industrial scale.

1.3.2.3- Deposition – precipitation method (DP)

The DP method is commonly used for preparing small gold particles supported on metal oxides by adding a metal hydroxide or hydrated oxide, which is deposited onto the

surface of the support. Typically, the support is added to an aqueous solution of $HAuCl_4$, and then by adding NaOH or carbonate, the pH of the mixture increases until a fixed value of pH, which is the optimal condition to correspond with the best compromise between gold particle size and gold loading as the pH of a suspension effectively neutralise the surface charge of the particles. After that, the mixture is heated while stirring for 1h. The DP method contains a washing step, which helps to remove sodium and chlorine as much as possible. This is followed by drying and calcined. One of the disadvantages of the DP method is the limitation of the support used, as to adsorb the metal on the surface of support it must involve supports that have a point of zero charge (PZC) greater than five such as MgO, TiO_2, Al_2O_3, ZrO and CeO_2, whereas it is not suitable for supports such as SiO_2, WO_3 and C, as there will be no charge on the surface of support [46].

1.3.2.4- Co-precipitation method (CP)

The CP method performs by adding sodium carbonate to the aqueous solution of gold precursor ($HAuCl_4$) and a metal nitrate so that the metal forms the desired oxide. The CP formation is heated and adjusted to the appropriate pH where precipitation occurs. Then followed by filtered, washed, dried and calcined. This method provides similar parameters to those in the DP method of small gold particles with high dispersion and higher surface area. The disadvantage of this method are the limitation of support and some of the gold particles could be embedded in the bulk of the support [46].

1.4- Selective oxidation by gold and gold-palladium catalyst

1.4.1- Alcohol oxidation

Selective oxidation of alcohols to their corresponding aldehydes is an important chemical transformation and one of the critical challenges facing the academic laboratory and the chemical industry [51]. Several reports propose that catalysis is highly effective and selective for oxidation of alcohols, particularly catalysts using supported gold nanoparticles [51, 52]. The challenges of stable oxidation catalysts are that it has to give not only high conversion but also has to be selective, especially when the molecule contains other oxidisable functional groups, as with allylic alcohol. One way of resolving this challenge was by developing the catalyst through the idea of synthesising a bimetallic catalyst, such as by using Au with Pd in the catalyst, to encourage the catalyst to achieve better activity, selectivity and stability [47].

Aldehydes are valuable, both as intermediates and as high value components, to the perfume industry and pharmaceuticals [53]. Often the process for this type of alcohol oxidation is carried out with the disadvantage of using stoichiometric oxygen electron donors such as chromate or permanganate, which are expensive and have serious environmental issues and toxicity [54, 55]. Therefore, there is a necessity to design a green and economic process for this reaction with high activity and selectivity. Addressing these problems has gained substantial interest in the development of heterogeneous catalysts, which use clean oxidising agents such as molecular O_2, which is not harmful to the environment, rather than the toxic donors [54, 55]. Furthermore,

using solvent free reaction conditions is greener than using solvents. Also, due to the simplicity of the separation of the solid heterogeneous catalysts, they can be reused several times, which is more economic for industry. Due to the importance of alcohol oxidation, oxidation of benzyl alcohol and crotyl alcohol, which both have industrial relevance, have been evaluated using gold and gold-palladium catalysts.

1.4.1.1- Benzyl alcohol oxidation

Gold catalysts have been reported to be considerably effective for the oxidation of alcohols under mild conditions [28], in particular, benzyl alcohol under solvent free conditions using molecular oxygen. However, some reports on the oxidation of benzyl alcohol use a solvent in the presence of molecular oxygen with Pd/C, Pd-Ag/pumice and Ni-hydrotalcite as catalysts [56].

Hutchings and co-workers [57], have demonstrated that supported gold nanocrystal catalysts are effective for this reaction, and they investigated the deposition of gold nanocrystals on several supports synthesised by the co-precipitation and impregnation method. They have reported that both preparation procedures were effective and the catalysts Au/SiO_2, Au/CeO_2 and Au/TiO_2 showed a selectivity of 100% to benzaldehyde and Au/CeO_2 catalyst gave a TOF 150 h^{-1}. The Au with C support catalyst displayed poor activity and selectivity, whilst the Au with more acidic supports, for example Fe_2O_3, showed higher activity, with some selectivity to benzyl benzoate.

Choudhary *et al.* [58], studied Au supported on several oxide supports (MgO, CaO, BaO, Al_2O_3, ZrO_2, La_2O_3, Sm_2O_3, Eu_2O_3, U_3O_8, MnO_2, Fe_2O_3, CoO, NiO, CuO and ZnO) prepared by homogeneous deposition precipitation and evaluated their activity for benzyl alcohol oxidation. The best catalyst performance was Au supported by U_3O_8, which gave a high conversion (53%) and selectivity of 95% to benzaldehyde. The Au/Al_2O_3 catalyst was found to be the best among the catalysts' activity (68.9% conversion), but with the lowest selectivity (65%) to benzaldehyde. On the contrary, the Au/Fe_2O_3 showed the highest selectivity (100%) but with low conversion (16.2%). However, the study of TOF showed that the Au/ZrO_2 catalyst was found to give the highest TOF among all these catalysts. The results of this study clearly demonstrate that the support in gold catalysis could play an important role in deciding both the particle size and catalytic performance.

The effect of support was investigated by Su and collaborators [59] who reported on benzyl alcohol oxidation using an Au monometallic catalyst with gallia polymorphs (α-, β-, and γ-Ga_2O_3) as supports prepared by the homogeneous deposition precipitation method. They demonstrated that the Au/γ-Ga_2O_3 catalyst had much higher activity for benzyl alcohol oxidation and selectivity to benzaldehyde when compared to three catalysts prepared using Au/TiO_2, Au/CeO_2 and Au/Fe_2O_3. They referred the high activity of the catalyst Au/γ-Ga_2O_3 for benzyl alcohol oxidation to the strong interaction between gold nanoparticles and the γ-Ga_2O_3 support.

The authors further demonstrated that mesostructured Ga–Al mixed-oxide solid solutions, which are characterised by unique dehydrogenation properties, could be used

as new attractive supports for active gold catalysts for the liquid-phase aerobic oxidation of alcohols under mild conditions. They showed that $Au/Ga_3Al_3O_9$ could even efficiently catalyse the aerobic oxidation of several alcohols in the absence of water or base conditions [60].

The effect of bimetallic Au-Pd nanocrystal catalysts was reported for the oxidation of benzyl alcohol with O_2 as oxidant under solvent free conditions at 100 °C. Enache *et al.* [47], investigated the effect of synthesised bimetallic Au:Pd supported by TiO_2 prepared by impregnation method, and they found that this catalyst has apparent higher activity for the reaction than both monometallic Au/TiO_2 and Pd/TiO_2 over the period of the reaction time; although at the beginning of the reaction, the bimetallic catalyst gave lower activity than the Pd/TiO_2 and lower selectivity than the Au/TiO_2 catalyst. The characterisation analysis of $Au\text{-}Pd/TiO_2$ catalyst by scanning transmission electron microscopy (STEM) and X-ray photoelectron spectroscopy (XPS) revealed that the introduction of Au to Pd produced an Au rich-core surrounded by a Pd-rich shell. The bimetallic Au-Pd catalysts were prepared using different supports and were investigated for benzyl alcohol oxidation. It was found that the formation of by-products was enhanced when the catalyst was prepared using acidic supports such as Al_2O_3 and Fe_2O_3 as shown in **Table 1.3**.

Table 1.3: The effect of adding Pd to Au supported by different supports on the oxidation of benzyl alcohol to benzaldehyde as reported by Enache *et al.* [47]

Catalyst	0.5 hour		8 hour	
	Conversion (%)	Benzaldehyde selectivity (%)	Conversion (%)	Benzaldehyde selectivity (%)
2.5%Au-2.5%Pd/Al_2O_3	2.6	90.5	83.3	86.6
2.5%Au-2.5%Pd/C	2.9	53.9	69.2	46.4
2.5%Au-2.5%Pd/SiO_2	3.6	97.3	35.7	88.0
2.5%Au-2.5%Pd/Fe_2O_3	3.6	74.9	63.4	66.4
2.5%Au-2.5%Pd/TiO_2	3.7	95.2	74.5	91.6
2.5%Au/ TiO_2	0.6	96.7	15.3	63.9
2.5%Pd/TiO_2	13.4	51.3	60.1	54.4

This investigation led the scientific community to pay more attention to the Au-Pd bimetallic catalyst for alcohol oxidation, in particular for benzyl alcohol oxidation.

Later, Enache *et al.* extended the work, showing the influence of the bimetallic Au-Pd ratio on catalytic performance. This was studied for benzyl alcohol and compared at two different reaction temperatures (100 °C and 160 °C). The catalyst Au-Pd/TiO_2 was prepared using the impregnation method with different Au-Pd ratios and it was found that under these reaction conditions, the 2.5wt%Au+2.5wt%Pd/TiO_2 was the most active catalyst, while the monometallic Au/ TiO_2 catalyst gave the highest selectivity to benzaldehyde [61].

The oxidation of benzyl alcohol has been investigated by Li *et al.* [62] using zeolite-supported Au and Au-Pd catalysts. Three zeolites were investigated (ZSM-5, zeolite b and zeolite Y) and compared with the catalysts prepared by TS-1 and TiO_2 as supports.

They found that with monometallic Au catalysts, the best results are obtained with zeolite b as the support and the conversions were similar to those observed with TiO_2 in terms of turn over frequencies. However, the acidic nature of these supports can catalyse sequential reactions of the reactant and products. The addition of Pd leads to an increase in activity without significantly affecting the selectivity.

More recently, Miedziak *et al.* [63] studied the influence of support morphology and structure on the catalyst activity for benzyl alcohol oxidation. The CeO_2 support was prepared through an antisolvent precipitation technique using supercritical CO_2 and used as support for an Au-Pd catalyst. They demonstrated that the Au-Pd/scCeO_2 catalyst was much more active and stable for the reaction than the catalyst that used non-supercritical CeO_2. Pd and Au were found to be highly dispersed in a regular configuration over scCeO_2. Moreover, the particle sizes of the non-supercritical CeO_2 (unCeO_2) were larger than they were with the scCeO_2. The Au-Pd/scCeO_2 displayed unsettled stability upon reuse the activity increased during the first and second reuse whilst the third reuse was lower than the fresh catalyst.

Investigations into the influence of different catalyst parameters using different methods of gold deposition on U_3O_8 were carried out by Choudhary *et al.* [64] who used the Au/U_3O_8 as catalyst. They found that catalysts containing gold at higher concentrations and with smaller gold particles showed a better process performance of conversion and selectivity. They found that the optimum calcination temperature to achieve that performance was 400 °C. Moreover, the study also showed that benzyl alcohol conversion is largely increased, but the selectivity for benzaldehyde is slightly

decreased, due to the forming of benzyl benzoate by increasing the reaction period and temperature.

Further to this study, Choudhary *et al.* [65] also reported using gold deposition methods on U_3O_8 as support as it showed the best performance for benzyl alcohol oxidation among the supports they investigated in their earlier studies [58, 64]. The study demonstrated that impregnation resulted in the largest gold particles, whereas the homogeneous deposition–precipitation (HDP) method gave the smallest. The gold loading for both HDP and impregnation methods were quantitative, whereas when the methods of deposition–precipitation and co-precipitation were used, the gold loaded on the support was only 60% of the available gold. They reported that the HDP method provided the best performance of conversion, selectivity of benzaldehyde and reusability. The impregnation method produced low activity by reason of the large particle size of gold, although it had similar gold loading to the HDP. The DP and co-precipitation methods produced average activity, as the particle size of gold was average and the gold loading was found to be lower than with the HDP method. The conversion increased as the calcination temperature increased until 400 °C after which it dropped due to the sintering of gold particles that they described.

An investigation into the impact of gold particle size on the catalyst's efficiency was carried out by Wenhao Fang *et al.* [66], who reported on the dehydrogenation of benzyl alcohol in the absence of any oxidant or hydrogen using hydrotalcite-supported gold nanoparticles. They prepared gold catalysis with different supports: Au/Cab-O-Sil, Au/SBA-15, Au/CNT, Au/TiO_2, Au/ZrO_2, Au/La_2O_3, Au/CeO_2, Au/HAP, Au/MgO,

Au/Al_2O_3 and Au/HT using an impregnation method, followed by H_2 reduction at 250 °C. Among these supported Au catalysts, Au/hydrotalcite (Au/HT) exhibited the highest activity (61%) and selectivity as well when compared to Ag/HT and Cu/HT. They also showed that by performing TEM measurements that the size of Au nanoparticles might significantly affect the catalytic performance. The mean size of Au nanoparticles for all these catalysts was between four and 28 nm. However, when preparing the catalysts Au/HT using a deposition–precipitation (DP) method, the TEM of the Au nanoparticles were 1.5–4.5 nm in size and the mean size of Au was calculated to be 2.8 nm by counting ~200 Au nanoparticles. This catalyst gave a significantly higher benzyl alcohol conversion (94%). This study suggests that the choice of a proper support is important for obtaining high activity and selectivity for the Au-catalysts. They also demonstrated that the size of the Au nanoparticles plays a key role in the catalyst's performance.

Hutchings and collaborators [49], explored for the first time, gold supported catalysts prepared by the sol immobilisation technique used for the solvent free oxidation of benzyl alcohol with oxygen. They prepared Au catalysts supported on carbon and titania and these catalysts were found to give a superior catalytic activity for the reaction compared to impregnation method. The characterisation of the catalysts provided a very narrow particle size distribution, also with very small gold particle sizes of 3nm, which led to the TOF ~ 31,900 h^{-1} for the catalyst 1wt%Au/TiO_2. Also, it demonstrated that the gold distribution and the catalyst activity are influenced by supports, which provides clear evidence that the nature of the support is important for gold catalysis.

As the previous investigations show, the addition of Pd to Au led to an increase in the catalytic activity. Consequently, the bimetallic Pd-Au catalyst papered using the sol immobilisation method was evaluated for benzyl alcohol oxidation [67]. The study found that adding Pd to Au supported on C, also led to small gold particles and small particle distribution that led to increased activity when compared to catalysts prepared using the impregnation procedure. The bimetallic catalyst showed significantly high yields of toluene formed by hydrogenolysis when compared with Au or Pd monometallic catalysts. Furthermore, the TOF of Au-Pd/C provided the best performance.

Dimitratos *et al.* [68], extended the work of the sol immobilisation technique to investigate modifying the metal precise order. A gold seed sol or a palladium seed sol was used initially in the catalyst's preparation. The Au–Pd nanocrystalline catalysts supported on TiO_2 and carbon were tested for benzyl alcohol oxidation under solvent-free conditions. Three strategies were formed in the sol immobilisation method: simultaneous formation of the sols for both metals, or initial formation of a seed sol of one of the metals, followed by a separate step in which a coating sol of the second metal is added. They demonstrated that catalysts prepared using the sol immobilisation technique show higher activity when compared with catalysts prepared by impregnation, as lower metal concentrations can be used. The bimetallic catalysts were all more active than the corresponding monometallic catalysts. They showed that for TiO_2-supported catalysts, the order of metal addition in the preparation was not observed to be significant with respect to selectivity or activity. Whereas, carbon

catalysts were more active but less selective when compared at iso-conversion. Moreover, the carbon-supported catalyst was affected by heat treatment, leading to a decrease in the activity by an order of magnitude, whereas the TiO_2-supported catalysts showed a 50% decrease in activity.

Hutchings and co-workers [69] investigated the effect of the metal ratio between Au and Pd bimetallic nanocrystalline catalysts supported on activated carbon *via* a sol immobilisation technique, and explored their use for the oxidation of benzyl alcohol. They showed that the monometallic 1 wt% Au/C was very poor, but on increasing the Pd content, they observed a progressive increase in catalytic activity. Also, the optimum selective oxidation to the aldehyde occurs for the Au/Pd 1:2 molar ratio catalysts. The activities were discussed in terms of the structure and composition of the supported Au-Pd nanoparticles.

The bimetallic sol immobilisation catalyst investigation was carried out with different catalyst methods, and the sol immobilisation was compared to the impregnation and deposition–precipitation methods [70]. The study demonstrated that sol immobilisation catalyst Au-Pd supported on TiO_2 shows the best catalyst performance for activity and selectivity, while the method of impregnation was found to be the least in activity. The activity of the sol immobilisation method was referred to the nano-gold particles and the narrow distribution of the catalyst. Moreover, the catalyst prepared using the impregnation method produced a considerable level of toluene as a by-product, which the authors correlated that to the residual chlorine on the surface of the catalyst, which led to more surface acidity for the catalyst prepared by the impregnation method, and

therefore, selectivity to side reactions. This was minimised in the two other catalysts, as their procedure requires thorough washing.

However, Li *et al.* [62] showed that there are several products that can be produced from benzyl alcohol oxidation, and there are many possible mechanisms for this reaction. The main product of the reaction is benzaldehyde, which can also be oxidised to benzoic acid, as shown in **Scheme 1.2** below:

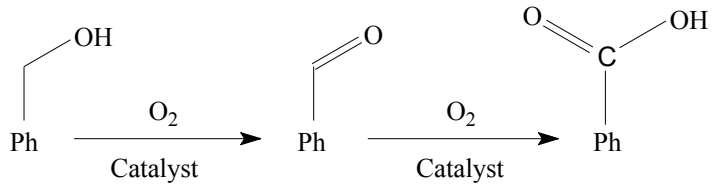

Scheme 1.2: Formation of benzaldehyde and benzoic acid [62]

Moreover, they also showed that there are other by-products that can also be produced from side reactions, which can be formed depending on the reaction conditions and metal catalyst employed. One possibility of the side reactions is the decarbonylation reaction to form benzene [67]. Another side reaction is the condensation reaction between benzaldehyde and benzyl alcohol to form a hemiacetal, which is unstable and further oxidised to an ester as benzyl benzoate, as shown in **Scheme 1.3**.

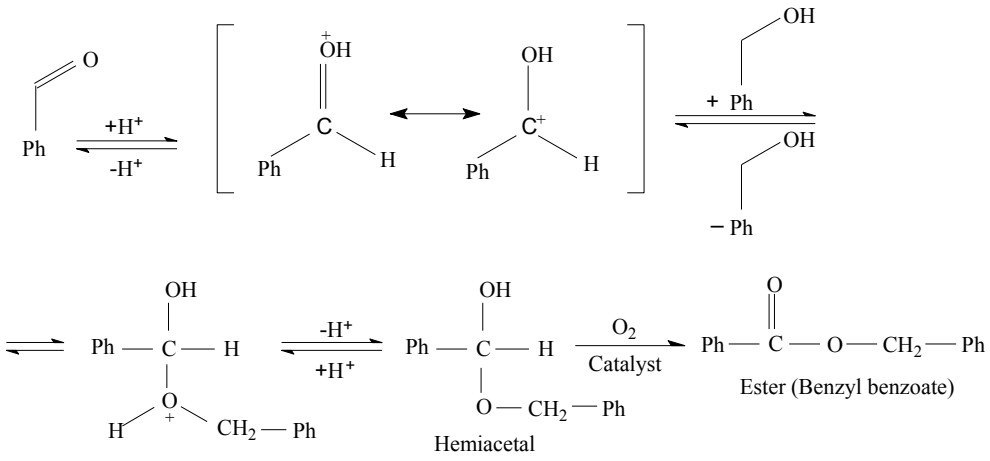

Scheme 1.3: Mechanism of benzyl benzoate formation [62]

Another side reaction that could be observed is the production of dibenzylether (**Scheme 1.4**). However, the acid-basic sites on the catalyst promote these two side reactions.

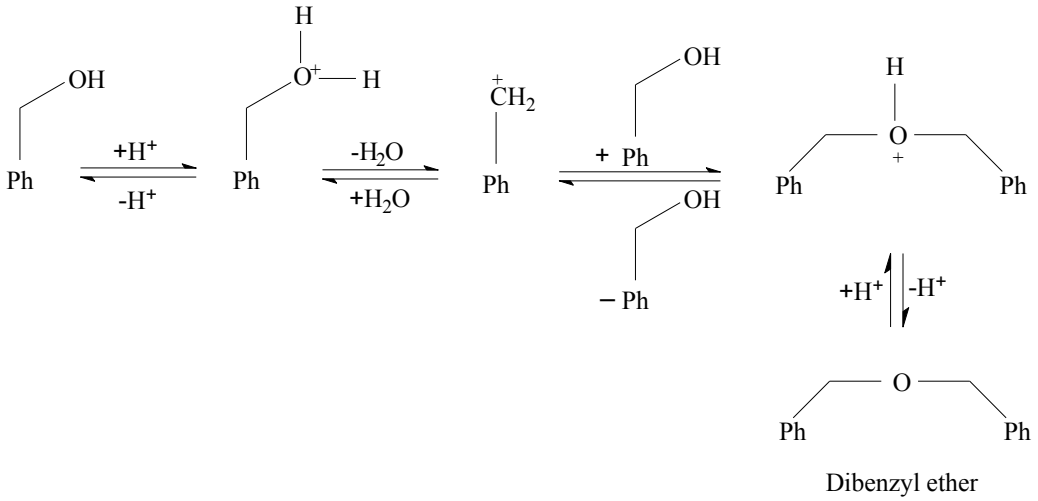

Scheme 1.4: Mechanism of dibenzyl ether formation [62]

The study also debated the possibility of the disproportionation of benzyl alcohol to form benzaldehyde and toluene in equal amounts. They ascribed this reaction to the removal of the oxygen from benzyl alcohol, and subsequently oxidising another

molecule of alcohol to aldehyde (**Scheme 1.5**). However, the metallic sites of the catalyst most probably promote this reaction and also the disproportionation increases with high temperatures and low oxygen pressure.

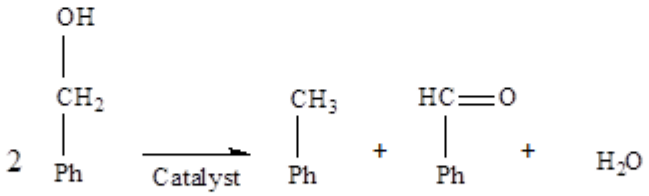

Scheme 1.5: Disproportionation reaction [62]

The very recent disproportionation study carried out by Sankar *et al.* [71, 72], attempted to make sense of the mechanism of benzyl alcohol oxidation by molecular oxygen to benzaldehyde and the by-product toluene. Using gold–palladium alloy nanoparticles for sol immobilisation on different supports as catalysts, they explored the origin of these products using the initial rate measurements and the study of substituent effects. They also examined the effect of changing the nature of the catalyst support. The mechanism suggested multiple chemisorbed states reaction pathways in this heterogeneous system, as well as the oxidation reaction, which gave the source of benzaldehyde. The two new chemisorbed states of the disproportionation pathways are derived from benzyl alcohol the first leading to the other source of benzaldehyde and the second leading to toluene. The authors suggested two possible types of dissociative chemisorption of benzyl alcohol on the metal support surface; the mechanisms are shown in **Scheme 1.6**.

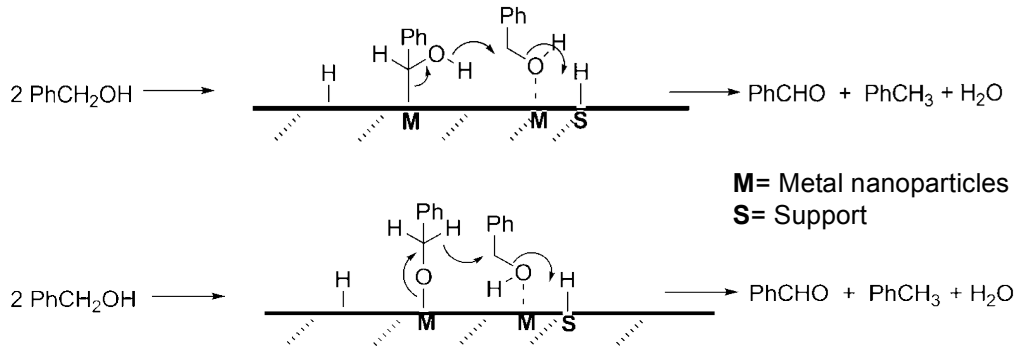

Scheme 1.6: Mechanism of toluene formation [72]

On the other hand, under helium, the selectivity gives rise to benzaldehyde and toluene in roughly equal quantities. The authors also showed that the nature of the support could influence the products and could switch off the disproportionation reaction.

1.4.1.2- Crotyl alcohol oxidation

Crotyl alcohol is an unsaturated alcohol from one of the important families of alcohols, allylic alcohol. An example of allylic alcohol oxidation is crotyl alcohol oxidation to crotonaldehyde, which has industrial relevance. Kawanami and co-workers [73], demonstrated that gold supported on TiO_2 can oxidise crotyl alcohol to the aldehyde with a high conversion rate of 57%, and the crotonaldehyde selectivity was 94%. They used O_2 as oxidant and supercritical CO_2 as a solvent. They indicated that the double bond between C-C might be stabilised by the aldehyde compounds.

Hutchings and collaborators [47] demonstrated that supported bimetallic Au-Pd on TiO_2 is more efficient than monometallic Pd or Au catalysts in alcohol oxidation. Crotyl

alcohol oxidation based on the turnover frequency gave 12600 h^{-1} using Au-Pd/TiO_2. However, they also demonstrated that for crotyl alcohol oxidation using 2.5%Au-2.5%Pd/TS-1 as catalyst, that crotyl alcohol can be converted by 81.9% to crotonaldehyde with a selectivity of 31.5% using H_2O_2 as an oxidising agent [74].

In an XPS study using crotyl alcohol as model, Lee and co-workers [75] proposed that using gold palladium alloys, high palladium surface concentrations should provide the optimum selective oxidation (selox) activity for AuPd alloy nanoparticles with Au_2Pd_3 as the optimum surface alloy composition.

Hou and collaborators [76], used PVP-stabilised 1:3 Au:Pd nanoparticles which gave more activity for crotyl alcohol oxidation and selectivity toward crotonaldehyde than monometallic Au or Pd. Balcha *et al.* [77] extended the study of synthesised PVP stabilised bimetallic AuPd nanoparticle catalysts using co-reduction and sequential reduction routes for aerobic oxidation of crotyl alcohol to crotonaldehyde at room temperature. The structural investigations suggested that sequentially reduced particles have significantly Pd-rich surfaces and Au-rich cores. The sequentially reduced nanoparticles with Pd-rich surfaces 1:3 AuPd system were shown to significantly enhance the activity and selectivity to crotonaldehyde, having a TOF of (306 h^{-1}), and 88% selectivity to crotonaldehyde, which was significantly higher than the TOFs of co-reduced 1:3 AuPd (40 h^{-1}), pure Pd (13 h^{-1}) and Au (12 h^{-1}) nanoparticles.

Bawaked *et al.* [78] reported on the solvent-free oxidation of crotyl alcohol using gold-palladium in different ratios supported on graphite. When Au was present in high concentrations the oxidation reaction to crotonaldehyde was the preferred pathway.

However, when Pd was present in the catalyst, the dominant pathway was isomerisation. They showed that the monometallic Au was observed to have low activity, whereas the activity of crotyl alcohol was significantly higher for the bimetallic catalyst, and it was highly dependent on the ratio between Au and Pd. However, they showed several products that can be produced from crotyl alcohol oxidation reaction, and they suggested a mechanism of this reaction, as shown in **Scheme 1.7.** The products are crotonaldehyde, 3-buten-1ol, 4-hydroxybutan-2-one, butanal, butanoic acid, butane-1,3-diol, butane-1,2-diol, acetic acid, 2-butenoic acid and lactons.

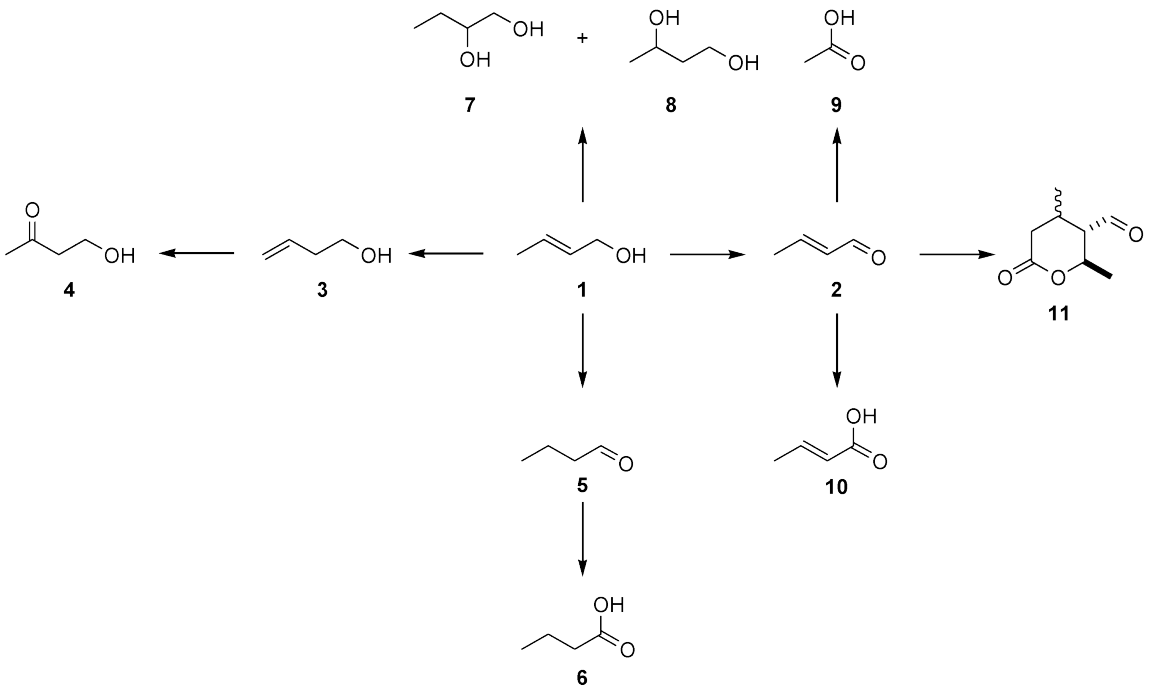

Scheme 1.7: Crotyl alcohol (1) oxidation and isomerisation products. 2-butenal (2), 3-buten-1ol (3), 4-hydroxybutan-2-one (4), butanal (5), butanoic acid (6), butane-1,3-diol (7), butane-1,2-diol (8), acetic acid (9), 2-butenoic acid (10) and lactons (11) [78]

1.4.2- Direct synthesis of hydrogen peroxide

Hydrogen peroxide is a simple molecule with an oxygen-oxygen single bond. H_2O_2 is important for industrial targets such as bleaches and hair dyes [79]. Hydrogen peroxide is also considered to be a strong and green oxidant as water is formed from the oxidation. Therefore, it is used in place of oxygen donors which have serious toxicity issues such as sodium perorbate, sodium chromate or sodium percarbonate [54, 80]. The identification of the synthesis of hydrogen peroxide in a direct route from the reactants of oxygen and hydrogen under non-explosive conditions would be a highly beneficial target. Significant research has been carried out into this reaction, and recently, excellent results have been achieved using gold monometallic and gold palladium bimetallic catalysts. However, a source like halides, were obtained as promoters using a supported Pd catalyst for the reaction [81]. Hutchings and co-workers were the first to find that supported Au catalysts can be very effective for the synthesis of hydrogen peroxide using monometallic gold catalysts supported on alumina. Furthermore, they discovered that the rate of hydrogen peroxide formation could be significantly enhanced by supported bimetallic Au/Pd nanostructures, as shown in **Table 1.4** [82, 83].

Table 1.4: Production of hydrogen peroxide from the reaction of H_2 and O_2 over Au and Au/Pd catalysts at 2 °C in an autoclave reactor using aqueous methanol as solvent

Catalysts	H_2 conversion (%)	H_2O_2 (wt%)	H_2O_2 Selectivity	H_2O_2 production rate mol h^{-1} kg $(cat)^{-1}$ x 10^{-3}
Au/Al_2O_3	6	0.031	53	1530
Pd/Al_2O_3	80	0.0008	1	370
Pd-Au (1:1)/Al_2O_3	63	0.090	14	4460

They showed that a supported Au-Pd catalyst produces significantly more hydrogen peroxide than both monometallic Au or Pd catalysts, denoting a synergetic effect from Au acting as a promoter for the Pd catalyst. In addition, use of supercritical CO_2 as a reaction medium for the formation of hydrogen peroxide has been shown to be a beneficial factor [83].

Ishihara *et al.* [84] studied gold supported on a range of oxide and zeolite supports including silica, alumina, gallia, H-ZMS-5 and H-Y zeolite. Among them, silica was found to be the best support and they also found that adding a small amount of Pd to the Au/SiO_2 catalyst is effective for increasing H_2O_2 formation rate.

Hutchings and co-workers [85] reported that TiO_2-supported Au-Pd for this reaction are very effective. The rates of formation achieved using TiO_2 support were superior to supported Al_2O_3. However, bimetallic catalysts were also more effective than the monometallic ones, with Au:Pd ratio of 4:1 and 1:1 ratio catalysts. The study suggests that the supports play a key role in improving the catalyst's function. The DP preparation method for gold supported on TiO_2 catalyst was also studied, showing considerably less activity for the formation of hydrogen peroxide than those prepared through the impregnation method. The effect of calcination for the catalysts prepared by the impregnation method indicated that the most active catalyst was the one that dried at 100 °C, followed by the catalyst calcined at 200 °C, and the catalyst calcined at 400 °C showed the lowest activity. However, the dried catalyst and the catalyst calcined at 200 °C were not stable when reused due to a significant leaching of the active metals observed. The catalyst calcined at 400 °C was shown to be stable for reuse.

An investigation into the supports was carried out by Li *et al.* [74] who used zeolite supported catalysts over the hydrogen peroxide reaction. They used HZMS-5, zeolite Y, zeolite beta and TS1 as supports. They proved that impregnation was a superior preparation method when compared to the DP method for this reaction. They also studied metals supported on zeolites, which demonstrated that Pd was the most active, followed by Au and Pt catalysts; whereas Cu, Ag, Rh and Ru catalysts showed low activity. Li *et al.* [86] further extended the work on zeolite Y and ZMS-5 and demonstrated that the addition of palladium to the gold catalysts had a synergic effect on the rate of hydrogen peroxide formation. They also studied the bimetallic catalyst prepared using the addition of Ru or Rh to the gold catalyst, indicating no synergic effect observed. Meanwhile there was a synergic effect with the addition of Pt to the gold, but it was not as significant as observed with the Pd catalyst.

In a further investigation by Edwards *et al.* [87], they found that using supported Au-Pd on G60 carbon yields an even more active catalyst than previous catalysts. They ranked the supports previously used in Au-Pd catalysts based on their reactivity as follows: carbon > titania > silica > alumina > iron oxide, proving that the supports play a key role in the catalyst's performance. However, they subsequently [88] studied the same reaction system and found that the carbon-supported catalysts are not core shell in nature, and instead exhibit homogeneous alloy natured bimetallic particles.

The investigation into the preparation method for the hydrogen peroxide synthesis using Au–Pd nanocrystalline catalysts supported on carbon prepared *via* a sol immobilisation technique was reported by Hutchings and collaborators [67]. They compared the activity

of the catalyst with the previous Au–Pd/C catalysts prepared *via* the impregnation method. The sol immobilisation catalyst showed a good performance activity for hydrogen peroxide synthesis as it has great control of the narrower particle size distribution design parameter. They also reported that for the catalyst prepared by sol immobilisation methods [69], the optimum performance for the H_2O_2 synthesis is observed for a catalyst having a Au/Pd 1:2 molar ratio. However, the competing hydrogenation reaction of hydrogen peroxide increases with increasing Pd content, although Pd alone is less effective than when Au is also present.

Ntainjua Li *et al.* [89] used the bimetallic AuPd with a range of supports (Al_2O_3, TiO_2, MgO, and C) prepared through the impregnation method for a hydrogen peroxide study. They reported that support is the crucial parameter with respect to hydrogenation and decomposition activity, as they are the main source for pathways, leading to a loss of selectivity and yield in the reaction. The addition of Au to Pd for catalysts supported on TiO_2 and carbon resulted in a decrease in both H_2O_2 hydrogenation and decomposition, while the reverse effect was observed for the Al_2O_3 and MgO catalysts. They referred to the effects as a function of the basicity of the support.

The synopsis of the important parameters of the previous literature for alcohol oxidation and H_2O_2 synthesis suggest that bimetallic AuPd catalysts are superior to monometallic in catalytic performance. Moreover, the method of synthesis these catalysts are crucial as the important aspect of these catalysts is the size of metal nanopartical, which affect on the catalysts performance. However, selecting the right support is important as it distributes the particles and the nature of support can effect on catalyst selectivity.

1.5- Aim of the study

As addressed in the literature review, the effect of bimetallic used in gold nano-crystal catalysts and the nature of the support may play an important role in catalytic performance. In addition, the catalyst preparation method may lead to developing new green oxidation systems for industrial oxidation targets. Moreover, the application of these catalysts is a promising and challenging topic in heterogeneous gold catalysis. Therefore, the main objectives of this study are to:

1. Study the disproportionation reaction mechanism of the solvent free oxidation of benzyl alcohol using gold palladium catalysts.

2. Study developing the catalyst preparation method, namely the conventional wet-impregnation method, using an excess anion during catalyst preparation; this new design could be used for alcohol oxidation and other applications in green chemistry for industrial purposes.

3. Study the effect of the bimetallic ratio on the gold-palladium catalyst through the modified impregnation method on reaction activity and product selectivity for benzyl alcohol oxidation.

1.6- References

[1] S.J. Green, Industrial Catalysis, The MacMillan Company, New York, 1928.

[2] J.W. Mellor, J. Phys. Chem., 7 (1903) 557-567.

[3] J.R. Partington, A History of Chemistry. Vol. 4, St. Martin's Press, 1964.

[4] G.S.C. Kirchhoff, Schweigers Journal fur Chemie und Physik 4 (1812).

[5] L.J. Thénard, Annales de chimie et de physique, 9 (1818).

[6] L.J. Thénard, Annales de chimie et de physique, 8 (1818).

[7] E. Davy, Philosophical Transactions, (1820).

[8] J.W. Döbereiner, Schweigers Journal fur Chemie und Physik 34 (1822).

[9] L.J.T. Pierre Louis Dulong Annales de chimie et de physique, 23 (1823).

[10] L.J.T. Pierre Louis Dulong annales de chimie et de physique, 24 (1823).

[11] W. Henry, Philosophical Magazine, 65 (1825).

[12] E. Turner, Philosophical journal 11 (1824).

[13] G.C. Bond, Heterogeneous Catalysis: Principles and Applications. 2nd Ed, Clarendon Press, 1987.

[14] J.J. Berzelius, Edinburgh New Philosophical Journal, 21 (1836).

[15] M. Bowker, The Basis and Applications of Heterogeneous Catalysis, Oxford Univ Press, 1998.

[16] I. Chorkendorff, J.W. Niemantsverdriet, Concepts of Modern Catalysis and Kinetics, John Wiley & Sons, 2003.

[17] G. Rothenberg, Catalysis: Concepts and Green Applications, Wiley-VCH Verlag GmbH Co. KGaA, 2008.

[18] I.M. Campbell, Catalysis of Surfaces, Chapman and Hall, 1988.

[19] D.J. Cole-Hamilton, Science (Washington, DC, U. S.), 299 (2003) 1702-1706.

[20] B. Cornils, W.A. Herrmann, Editors, Aqueous-Phase Organometallic Catalysis, 2nd Ed: Aqueous Phase Organometallic Catalysis, Wiley-VCH Verlag GmbH & Co. KGaA, 2004.

[21] G.C. Bond, D.T. Thompson, Catal. Rev. - Sci. Eng., 41 (1999) 319-388.

[22] M. Turner, V.B. Golovko, O.P.H. Vaughan, P. Abdulkin, A. Berenguer-Murcia, M.S. Tikhov, B.F.G. Johnson, R.M. Lambert, Nature (London, U. K.), 454 (2008) 981-983.

[23] G. Ertl, H. Knoezinger, F. Schueth, J. Weitkamp, Editors, Handbook of Heterogeneous Catalysis; Volume 2, Wiley-VCH Verlag GmbH & Co. KGaA, 2008.

[24] H. Kestenbaum, O.A.L. De, W. Schmidt, F. Schuth, W. Ehrfeld, K. Gebauer, H. Lowe, T. Richter, in, Springer-Verlag, 1999, pp. 207-212.

[25] A.G. Sault, R.J. Madix, C.T. Campbell, Surf. Sci., 169 (1986) 347-356.

[26] B. Hammer, J.K. Norskov, Nature (London), 376 (1995) 238-240.

[27] G.J. Hutchings, Catal. Today, 100 (2005) 55-61.

[28] A. Stephen, K. Hashmi, G.J. Hutchings, Angew. Chem., Int. Ed., 45 (2006) 7896-7936.

[29] P.A. Sermon, Gold Bull., 9 (1976) 129-131.

[30] M. Faraday, Experimental Researches in Electricity, J.M. Dent, London, 1914.

[31] T. Graham, Proceedings of the Royal Society of London, 17 (1896).

[32] G. Bond, Gold Bull, 41 (2008) 235-241.

[33] W.A. Bone, R.V. Wheeler, Phil. Trans., 206 (1906) 1-67.

[34] D.L. Chapman, J.E. Ramsbottom, C.G. Trotman, Proc. R. Soc. London, Ser. A, 107 (1925) 92-100.

[35] W.A. Bone, G.W. Andrew, Proc. R. Soc. London, Ser. A, 109 (1925) 459-476.

[36] A.F. Benton, J.C. Elgin, J. Am. Chem. Soc., 49 (1927) 2426-2438.

[37] O. Schmidt, Zeit. phys. Chem, (1925).

[38] G.C. Bond, P.A. Sermon, Gold Bull., 6 (1973) 102-105.

[39] P.A. Sermon, G.C. Bond, P.B. Wells, J. Chem. Soc., Faraday Trans. 1, 75 (1979) 385-394.

[40] G.J. Hutchings, J. Catal., 96 (1985) 292-295.

[41] M. Haruta, N. Yamada, T. Kobayashi, S. Iijima, J. Catal., 115 (1989) 301-309.

[42] G.J. Hutchings, Dalton Trans., (2008) 5523-5536.

[43] C.W. Corti, R.J. Holliday, D.T. Thompson, Gold Bull. (London, U. K.), 35 (2002) 111-117.

[44] C.-J. Zhong, J. Luo, D. Mott, M. Maye, N. Kariuki, L. Wang, P. Njoki, M. Schadt, S.-I. Lim, Y. Lin, Gold-Based Nanoparticle Catalysts for Fuel Cell Reactions, in: B. Zhou, S. Han, R. Raja, G. Somorjai (Eds.) Nanotechnology in Catalysis, Springer New York, 2007, pp. 289-307.

[45] B. Qiao, Y. Deng, Chem Commun (Camb), (2003) 2192-2193.

[46] G.C. Bond, C. Louis, D.T. Thompson, Catalysis by Gold, Imperial College Press, 2006.

[47] D.I. Enache, J.K. Edwards, P. Landon, B. Solsona-Espriu, A.F. Carley, A.A. Herzing, M. Watanabe, C.J. Kiely, D.W. Knight, G.J. Hutchings, Science (Washington, DC, U. S.), 311 (2006) 362-365.

[48] J.A. Lopez-Sanchez, N. Dimitratos, C. Hammond, G.L. Brett, L. Kesavan, S. White, P. Miedziak, R. Tiruvalam, R.L. Jenkins, A.F. Carley, D. Knight, C.J. Kiely, G.J. Hutchings, Nat. Chem., 3 (2011) 551-556.

[49] N. Dimitratos, J.A. Lopez-Sanchez, D. Morgan, A. Carley, L. Prati, G.J. Hutchings, Catal. Today, 122 (2007) 317-324.

[50] M. Haruta, Gold Bull. (London, U. K.), 37 (2004) 27-36.

[51] L.-C. Wang, Y.-M. Liu, M. Chen, Y. Cao, H.-Y. He, K.-N. Fan, J. Phys. Chem. C, 112 (2008) 6981-6987.

[52] A. Abad, C. Almela, A. Corma, H. Garcia, Tetrahedron, 62 (2006) 6666-6672.

[53] E. Garattini, M. Terao, Drug Metabolism Reviews, 43 (2011) 374-386.

[54] A.R. Vaino, J. Org. Chem., 65 (2000) 4210-4212.

[55] R.A. Sheldon, Redox molecular sieves as heterogeneous catalysts for liquid phase oxidations, in: S.T.O.A.M.G. R.K. Grasselli, J.E. Lyons (Eds.) Studies in Surface Science and Catalysis, Elsevier, 1997, pp. 151-175.

[56] V.R. Choudhary, D.K. Dumbre, Catal. Commun., 13 (2011) 82-86.

[57] D.I. Enache, D.W. Knight, G.J. Hutchings, Catal. Lett., 103 (2005) 43-52.

[58] V.R. Choudhary, A. Dhar, P. Jana, R. Jha, B.S. Uphade, Green Chem., 7 (2005) 768-770.

[59] F.-Z. Su, M. Chen, L.-C. Wang, X.-S. Huang, Y.-M. Liu, Y. Cao, H.-Y. He, K.-N. Fan, Catal. Commun., 9 (2008) 1027-1032.

[60] F.-Z. Su, Y.-M. Liu, L.-C. Wang, Y. Cao, H.-Y. He, K.-N. Fan, Angew. Chem., Int. Ed., 47 (2008) 334-337.

[61] D.I. Enache, D. Barker, J.K. Edwards, S.H. Taylor, D.W. Knight, A.F. Carley, G.J. Hutchings, Catal. Today, 122 (2007) 407-411.

[62] G. Li, D.I. Enache, J. Edwards, A.F. Carley, D.W. Knight, G.J. Hutchings, Catal. Lett., 110 (2006) 7-13.

[63] P.J. Miedziak, Z. Tang, T.E. Davies, D.I. Enache, J.K. Bartley, A.F. Carley, A.A. Herzing, C.J. Kiely, S.H. Taylor, G.J. Hutchings, J. Mater. Chem., 19 (2009) 8619-8627.

[64] V.R. Choudhary, R. Jha, P. Jana, Green Chem., 9 (2007) 267-272.

[65] V.R. Choudhary, D.K. Dumbre, Appl. Catal., A, 375 (2010) 252-257.

[66] W. Fang, Q. Zhang, J. Chen, W. Deng, Y. Wang, Chem. Commun. (Cambridge, U. K.), 46 (2010) 1547-1549.

[67] J.A. Lopez-Sanchez, N. Dimitratos, P. Miedziak, E. Ntainjua, J.K. Edwards, D. Morgan, A.F. Carley, R. Tiruvalam, C.J. Kiely, G.J. Hutchings, Phys. Chem. Chem. Phys., 10 (2008) 1921-1930.

[68] N. Dimitratos, J.A. Lopez-Sanchez, D. Morgan, A.F. Carley, R. Tiruvalam, C.J. Kiely, D. Bethell, G.J. Hutchings, Phys. Chem. Chem. Phys., 11 (2009) 5142-5153.

[69] J. Pritchard, L. Kesavan, M. Piccinini, Q. He, R. Tiruvalam, N. Dimitratos, J.A. Lopez-Sanchez, A.F. Carley, J.K. Edwards, C.J. Kiely, G.J. Hutchings, Langmuir, 26 (2010) 16568-16577.

[70] P.J. Miedziak, Q. He, J.K. Edwards, S.H. Taylor, D.W. Knight, B. Tarbit, C.J. Kiely, G.J. Hutchings, Catal. Today, 163 (2011) 47-54.

[71] S. Meenakshisundaram, E. Nowicka, P.J. Miedziak, G.L. Brett, R.L. Jenkins, N. Dimitratos, S.H. Taylor, D.W. Knight, D. Bethell, G.J. Hutchings, Faraday Discussions, 145 (2010) 341-356.

[72] M. Sankar, E. Nowicka, R. Tiruvalam, Q. He, S.H. Taylor, C.J. Kiely, D. Bethell, D.W. Knight, G.J. Hutchings, Chem. - Eur. J., 17 (2011) 6524-6532.

[73] X. Wang, H. Kawanami, S.E. Dapurkar, N.S. Venkataramanan, M. Chatterjee, T. Yokoyama, Y. Ikushima, Appl. Catal., A, 349 (2008) 86-90.

[74] G. Li, J. Edwards, A.F. Carley, G.J. Hutchings, Catalysis Communications, 8 (2007) 247-250.

[75] A.F. Lee, S.F.J. Hackett, G.J. Hutchings, S. Lizzit, J. Naughton, K. Wilson, Catal. Today, 145 (2009) 251-257.

[76] W. Hou, N.A. Dehm, R.W.J. Scott, J. Catal., 253 (2008) 22-27.

[77] T. Balcha, J.R. Strobl, C. Fowler, P. Dash, R.W.J. Scott, ACS Catal., 1 (2011) 425-436.

[78] S. Bawaked, Q. He, N.F. Dummer, A.F. Carley, D.W. Knight, D. Bethell, C.J. Kiely, G.J. Hutchings, Catal. Sci. Technol., 1 (2011) 71-83.

[79] P.B. Walsh, Tappi J., 74 (1991) 81-83.

[80] D.G. Lee, U.A. Spitzer, J. Org. Chem., 35 (1970) 3589-3590.

[81] J. Wanngard, in, Eka Chemicals AB, Swed. . 1998, pp. 5 pp.

[82] P. Landon, P.J. Collier, A.J. Papworth, C.J. Kiely, G.J. Hutchings, Chem. Commun. (Cambridge, U. K.), (2002) 2058-2059.

[83] P. Landon, P.J. Collier, A.F. Carley, D. Chadwick, A.J. Papworth, A. Burrows, C.J. Kiely, G.J. Hutchings, Phys. Chem. Chem. Phys., 5 (2003) 1917-1923.

[84] T. Ishihara, Y. Ohura, S. Yoshida, Y. Hata, H. Nishiguchi, Y. Takita, Appl. Catal., A, 291 (2005) 215-221.

[85] J.K. Edwards, B.E. Solsona, P. Landon, A.F. Carley, A. Herzing, C.J. Kiely, G.J. Hutchings, Journal of Catalysis, 236 (2005) 69-79.

[86] G. Li, J. Edwards, A.F. Carley, G.J. Hutchings, Catalysis Today, 122 (2007) 361-364.

[87] J.K. Edwards, A. Thomas, B.E. Solsona, P. Landon, A.F. Carley, G.J. Hutchings, Catalysis Today, 122 (2007) 397-402.

[88] J.K. Edwards, A. Thomas, A.F. Carley, A.A. Herzing, C.J. Kiely, G.J. Hutchings, Green Chemistry, 10 (2008) 388-394.

[89] E. Ntainjua N, J.K. Edwards, A.F. Carley, J.A. Lopez-Sanchez, J.A. Moulijn, A.A. Herzing, C.J. Kiely, G.J. Hutchings, Green Chemistry, 10 (2008) 1162-1169.

Chapter two:

Experimental

Technique

2.1- Introduction

Experimental techniques represent a very important aspect of chemistry. Many characterisation techniques have been used in catalysis research, with the intent to uncover the mystery behind the reactant mechanism, and analyse the catalyst composition and look at catalyst behaviour [1]. This chapter describes in detail the experimental techniques, catalyst preparation methods and the experimental conditions used for catalyst testing, with a description of the reactor that was used. This chapter will also provide the methods used for analysing and quantify the products after reaction, and finally, the basic principles of the characterisation techniques that have been used to examine the catalysts.

2.2- Catalyst preparation methods

2.2.1- Sol immobilisation method (S_{Im})

In a typical catalyst, synthesis using the S_{Im} method is used to prepare, for example, a Au+Pd bimetallic catalyst with 1:1 weight ratio of the metals in 1% weight of support. The catalyst was prepared using aqueous solutions of $PdCl_2$ (Sigma Aldrich) with a palladium concentration of 6 mg/ml and $HAuCl_4.3H_2O$ (Sigma Aldrich) with a gold concentration of 8.9 mg/ml. The required amount of PVA Polyvinylalcohol (Sigma Aldrich) 1 wt% solution MW = 10000, 80% hydrolysed (Au+Pd) (wt/wt) = 1.3) was added to the aqueous mixture solutions of $PdCl_2$ (1.66 ml) and $HAuCl_4$ (1.123 ml). A

freshly prepared solution of $NaBH_4$ (0.1 M of $NaBH_4$ / (Au+Pd) (mol/mol) = 5) was then added to form a dark-brown sol. After 30min of sol generation, the colloid was supported by adding 1.98 g of a support material or a metal oxide, for example TiO_2, Degussa P25. The suspension was acidified to pH 1, through the drop-wise addition of concentrated H_2SO_4, which was added under vigorous stirring. After 2h, the slurry was filtered, and the catalyst was washed thoroughly with 2L of distilled water and then dried at 110 °C for 16hrs prior to use. In a similar way, monometallic supported 1% (Au), 1% (Pd) and bimetallic 1% (Au-Pd) with different ratios were also prepared [2].

2.2.2- Conventional wet impregnation method (C_{Im})

Typically, in the C_{Im} method, the metal precursors are wet impregnated on to the solid support or a metal oxide. The synthesis involved using the C_{Im} method to prepare, for example, a Au+Pd bimetallic catalyst with 1:1 weight ratio of the metals in 1% weight of support such as TiO_2, Degussa P25; the metal precursors were solid $PdCl_2$ (Sigma Aldrich) and an aqueous solution of $HAuCl_4.3H_2O$ (Sigma Aldrich). The requisite amount of solid $PdCl_2$ (0.016 g) was added to a predetermined volume of an aqueous solution of $HAuCl_4.3H_2O$ 8.9 ml (1.123 ml) and stirred vigorously at 80 °C for a few minutes until the palladium salt had apparently dissolved. After that, the requisite amount of the support, 1.98 g, was added to this solution under vigorous stirring conditions. The solution was agitated in this way until it formed a paste, which was then dried at 110 °C for 16h and then calcined in static air at 400 °C for 3h or was reduced at

400 °C for 4h under 5% H_2 in Ar. In a similar way, monometallic supported 1% (Au), 1% (Pd) and bimetallic 1%(Au-Pd) with different ratio were also prepared [3].

2.2.3- Modified impregnation method (M_{Im})

The new method of modified impregnation catalyst synthesis is similar to the C_{Im} catalyst method, for example, a Au+Pd bimetallic catalyst with 1:1 weight ratio of the metals in 1% weight of support. The catalyst was prepared using an aqueous solution of $HAuCl_4.3H_2O$ (Sigma Aldrich) as a gold precursor and was dissolved in deionised water to form a solution with a gold concentration of 8.9 mg/ml. The $PdCl_2$ (Sigma Aldrich) salt was dissolved in a 0.58M aqueous HCl solution (36% concentration HCl, diluted using the requisite amount of deionised water) with gentle warming and vigorous stirring to form a solution with a Pd concentration of 6 mg/ml. This solution was cooled and used as the palladium precursor. In a typical synthesis run, the requisite amount of gold solution (1.123 ml) and palladium solution (1.66 ml) were poured into a clean 50ml round bottom flask fitted with a magnetic stirrer bar (**Figure 2.1**). The volume of the solution was adjusted using deionised water to a total volume of 15ml. The flask was then immersed into an oil bath sitting on a magnetic stirrer hot plate. The solution was stirred vigorously at 1000rpm and the temperature of the oil bath was raised from 27 °C to 60 °C over a period of 10 min. At 60 °C, the amount of support material required was calculated so as to have a total final metal loading of 1% wt. 1.98g of support material or the metal oxide used, for example TiO_2, Degussa P25, was

added slowly over a period of 8-10min with constant stirring. After the completion of the addition of the support material, the slurry was stirred at 60 °C for an additional 15min. Following this, the temperature of the oil bath was raised to 95 °C and the slurry was stirred at that temperature for a further 16h until all the water had evaporated, leaving a dry solid. Subsequently, the solid powder was transferred into a mortar and pestle and was ground thoroughly to form a uniform mixture. This was stored and designated as a "dried only" sample. 400mg of the unreduced sample was transferred and spread out over a glass calcination boat (13cm in length). This boat was then put inside a calcination furnace fitted with an inlet and outlet valve. The temperature of the furnace was raised from 30 °C to 400 °C at a heating rate of 10 °C /min under a steady flow of 5%H_2 in Ar. The sample was reduced at 400 °C for 4h under 5%H_2 in Ar or calcined in static air at 400 °C for 3h. Finally, the furnace was cooled and this "reduced" sample was used as the M_{Im} catalyst or "calcined" as calcined M_{Im} catalyst.

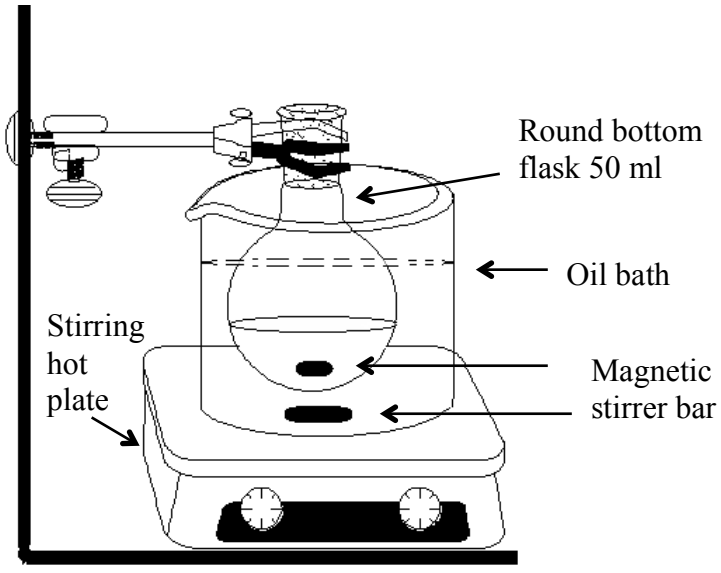

Figure 2.1: Schematic diagram of preparing the M_{Im} catalysts

2.3- Catalyst testing

2.3.1- Alcohol oxidation using glass stirred reactor (GSR)

Oxidations of alcohols were carried out in a Radleys carousel reactor, which is a 50mL glass stirred reactor (GSR); a diagram of the reactor is shown in **Figure 2.2**.

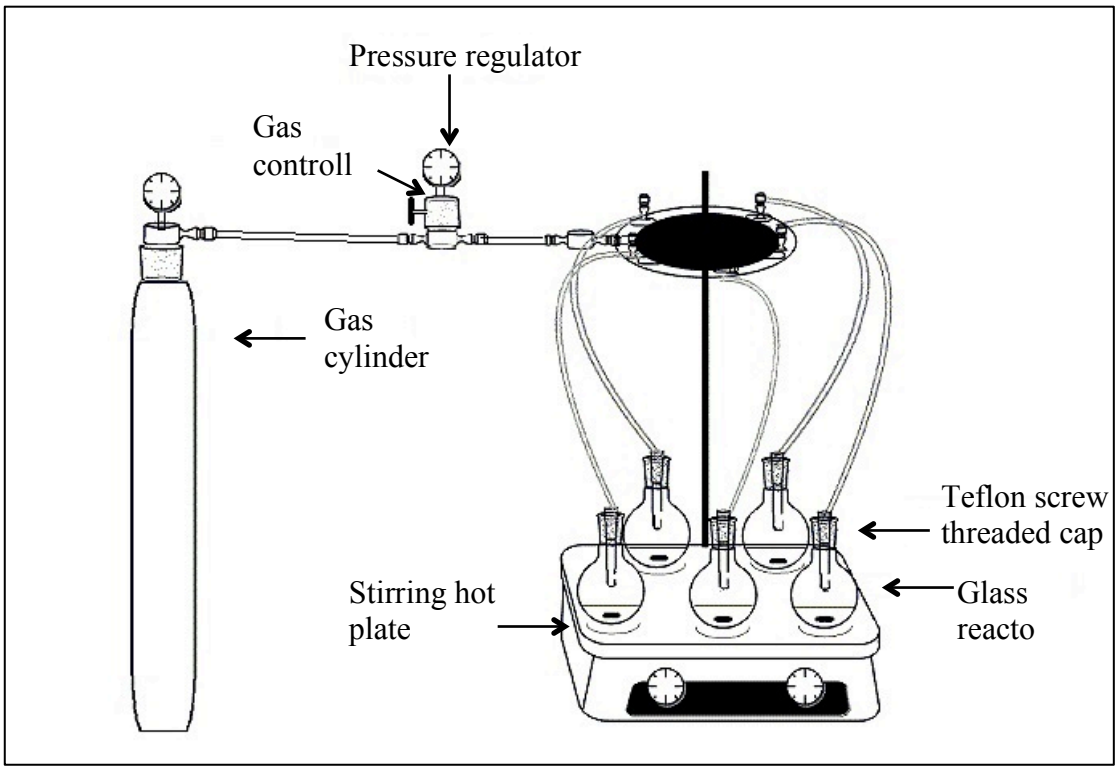

Figure 2.2: Schematic diagram of the Radleys carousel glass stirred reactor

In a typical reaction, the requisite amount of catalyst and substrate were charged into the reactor at room temperature, which was then purged with the required gas (e.g., O_2 or He) three times, before the reactor was sealed using a Teflon screw threaded cap. The reactor was always connected to the gas-line to ensure the consumed O_2 or He would be topped-up. The pressure was monitored using the pressure gauge fitted in the inlet line

to ensure that there was no change in the pressure during the course of the reaction. The reactor with the reaction mixture was loaded into a pre-heated heating block, which was maintained at the reaction temperature. The reaction started by commencing stirring inside the reactor with a magnetic bar at 1000 rpm. After a specific time, the stirring was stopped and the reactor was immediately cooled in an ice bath. After cooling for 10 min, the reactor was opened slowly and the contents were centrifuged. An aliquot of the clear supernatant reaction mixture (0.5 mL) was then diluted with an internal standard material (0.5 mL of mesitylene) for GC analysis. This experimental method in this thesis is the standard reaction protocol for oxidation of alcohols.

2.3.2- Catalyst reusability procedure for glass reactor

Reusability of catalysts was examined, as it is a key feature of green chemistry and one of the advantages for economic purposes. The reuse study was carried out using the same catalyst procedure as standard reaction conditions for oxidation of alcohols, but in the reuse experiments, larger amounts of the catalyst were used (100 mg instead of 20 mg) as there is a possibility that some of the catalyst will be lost in the later washing step. After the reaction, the catalyst was collected through the centrifuging of the reaction mixture. The catalyst, after separation, was washed with the acetone six times and left to dry at a room temperature for 16 hours to remove the acetone. The dried catalyst was collected from the centrifuge tube and left in an oven for 1 h at 80 °C prior to use for the first reuse.

2.3.3- Direct synthesis of hydrogen peroxide H_2O_2

Direct synthesis of hydrogen peroxide from hydrogen and oxygen was carried out by James Pritchard from the *School of Chemistry, Cardiff University, UK,* using standard experimental conditions reported in numerous publications [4-6]. Catalyst testing was performed using a stainless steel autoclave (Parr Instruments) with a nominal volume of 100 ml and a maximum working pressure of 14 MPa. The autoclave was equipped with an overhead stirrer (0−2000 rpm) and had provision for the measurement of temperature and pressure. Following the standard reaction conditions employed previously, the autoclave was charged with the catalyst (0.01 g) and solvent (5.6 g MeOH and 2.9 g H_2O), and purged three times with 5%H_2/CO_2 (3 MPa), before being filled with 5% H_2/CO_2 and 25% O_2/CO_2 to give a hydrogen/oxygen ratio of 1:2 at a total pressure of 3.7 MPa. Stirring (1200 rpm) was commenced on reaching the desired temperature (2 °C), and experiments were carried out for 30min. The H_2O_2 yield was determined by titration of aliquots for the final filtered solution with acidified $Ce(SO_4)_2$ (7×10^{-3} mol/L). $Ce(SO_4)_2$ solutions were standardised against $(NH_4)_2Fe(SO_4)_2\cdot6H_2O$ using ferroin as an indicator.

2.4- Analysis of reaction products

2.4.1- Gas chromatography (GC)

2.4.1.1- Background

The reaction mixture solutions were analysed using gas chromatography, which is widely used in academic and industrial laboratories. It is a way to separate and quantify the constituents of the chemical reaction. The GC consists of an injector port, a carrier gas called mobile phase, columns called the stationary phase and detectors, as shown in **Figure 2.3**.

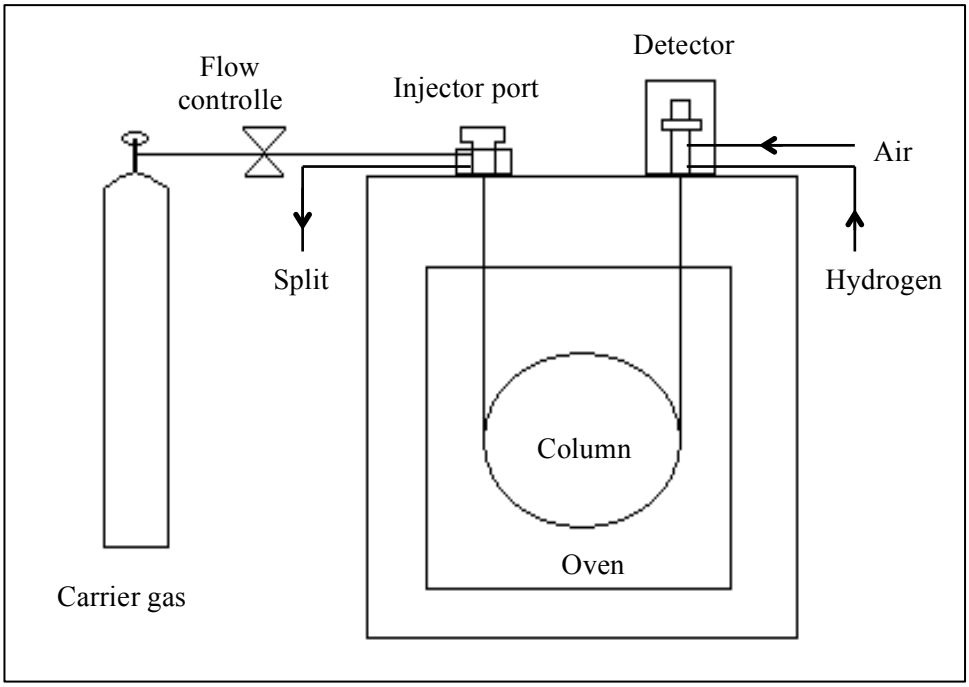

Figure 2.3: Schematic diagram of gas chromatography (GC)

The sample is injected into an injection port and the sample is introduced through a syringe and injected through a septum. The sample was heated and mixed

homogeneously with the carrier gas. Then it was carried by the gas carrier through an inert packing. At the split point, the sample was split into two parts using the variable flow rates of the carrier gas; then most of the homogenised mixture passed through the split outlet to the waste vent, while a small enough amount of homogenised mixture entered the column.

There are two types of GC column, packed and capillary, which are commonly used for separation in GC. Generally, packed columns are made of a fine inert solid material coated with liquid phase, as in a stationary phase. Capillary columns consist of a capillary tube, and their inner walls are lined with a fine layer of material, for example polyamide. Due to the sensitivity and high resolution of capillary columns, it is the most commonly used column in gas chromatography. The length of the column, and the wall composition and the polarity, are causes of separating the components. When the column has separated, the sample components are then analysed by a detector [7].

There are two detectors commonly used in GC- the flame ionization detector (FID) and the thermal conductivity detector (TCD). The TCD detector is less sensitive but it is suitable for all compounds, and therefore, it is widely used for gas analysis. The FID is very sensitive to hydrocarbons so it is has been used extensively in research. A FID is made of a stainless steel chamber (jet). The gas flow exiting the column passes through this jet, is mixed with hydrogen as fuel and air, and is burned at the jet's tip (**Figure 2.4**). Carbon atoms produce CH radicals that produce CHO^+ ions and electrons in flame. The resulting electron current is converted into a voltage, which is amplified and then converted into a digital signal. The signal for each component is shown as a peak and

the area of the peak is divided by a relative sensitivity factor and corrected with the response factor (RF) of the compound to obtain the true number of the count [8, 9].

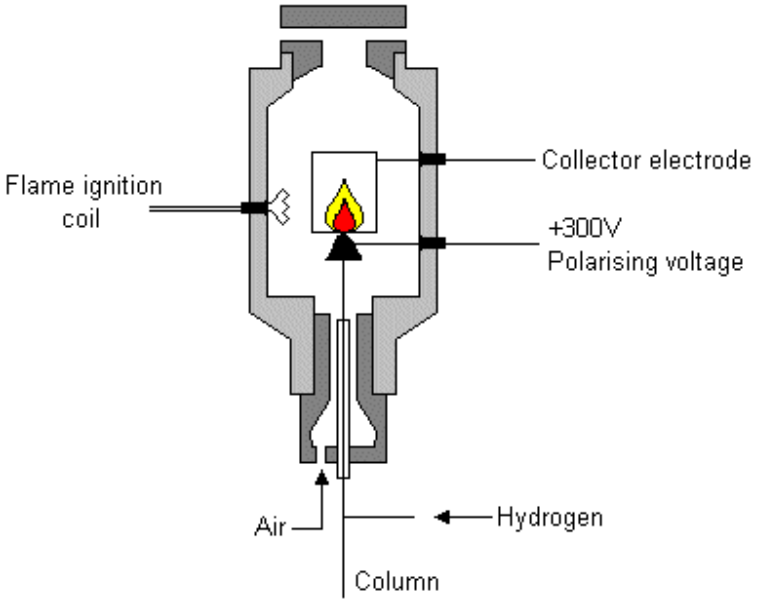

Figure 2.4: Schematic diagram of Flame Ionisation Detector (FID)

2.4.1.2- Experimental

The GC analysis in this study was conducted using GC (Varian star CP-3800) with a CP-wax 52 column (capillary column, 25m, 0.35mm ID, 0.2 micron) and a FID detector. A sample (0.02µl) was automatically injected into the GC using a micro syringe.

2.4.1.3- Internal standard

An internal standard was added to the reaction mixture samples. The analyte chosen for the internal standard needed to have a predictable and different retention time and area similar to the sample products mixture, allowing it to be used to determine whether abnormalities had occurred. The standard chosen was mesitylene, as it is does not interfere with the reaction, and is eluted from the column at a different retention time to the sample products mixture. 0.5ml of internal standard solution was added to 0.5 ml of the sample mixture at the end of the reaction.

2.4.1.4- Quantification of products after reaction

The response factor (RF) of each product was calculated by finding the ratio of a known amount of product over a constant amount of internal standard (mesitylene). Six different solutions were made up of internal standard and all the different products. For example, one of the six solution calibrations was made up to represent 20% conversion, containing the starting material with the products, assuming the selectivity percentage of each product was 20%. This sample mixture was added to mesitylene (0.5ml). The next solution was made up and contained the same mixture but for 40% conversion of the starting material and the products with mesitylene (0.5ml). The six different calibration solutions (0%, 20%, 40%, 60%, 80% and 100% of conversion) were injected for GC calibrations. The signal area of each compound from the GC shows as a peak; the peak area is divided by the signal peak area of the internal standard to obtain the

normalised area. **Figure 2.5** shows the line calibration curve that can be obtained from the ratio between the calibration concentration of each compound and the normalised area of each compound to obtain the response factor (RF).

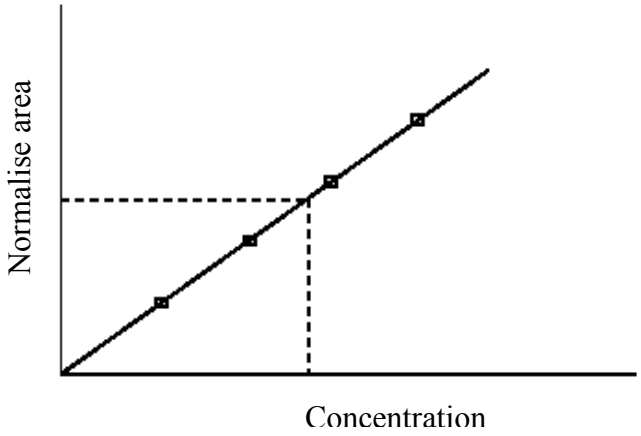

Figure 2.5: Example of calibration curve line in GC

Calculations of conversion, selectivity, yield and TON (turnover number) and TOF (turnover frequency) have been made using these formulas:

$$\textbf{Conversion (\%)} = \frac{\textbf{Mols of substrate consumed}}{\textbf{Starting mols of substrate}} \times \mathbf{100}$$

$$\textbf{Selectivity to X product (\%)} = \frac{\textbf{Mols of X product formed}}{\textbf{Mols of substrate consumed}} \times \mathbf{100}$$

$$\textbf{Yield to X product (\%)} = \frac{\textbf{The Conversion} \times \textbf{The Selectivity to X product}}{\mathbf{100}}$$

$$\textbf{TON} = \frac{\textbf{Mols of substrate consumed}}{\textbf{Mols of metal}}$$

$$\textbf{TOF} = \frac{\textbf{TON}}{\textbf{Reaction time (min)}} \times \mathbf{60}$$

2.5- Catalyst characterisation

2.5.1- X-Ray powder diffraction (XRD)

2.5.1.1- Background

Since Wilhelm Röentgen discovered X-rays in 1895, X-ray powder diffraction (XRD) has become a common technique for the determination of crystalline material, as it provides useful information for the identification of crystalline compounds by their diffraction pattern [10]. Therefore, it is used in the study of heterogeneous catalysts. Sir W.H. Bragg and his son Sir W.L. Bragg developed the technique of XRD in 1913. The basic equation, called the Bragg's Law, refers to the simple equation shown by **Equation 2.1**:

$$n\lambda = 2d \sin\theta$$

Equation 2.1 Bragg's Law

Where **n** is an integral number, **λ** is the wavelength of the X-rays, **d** is the interplanar spacing generating the diffraction and **θ** is the glancing angle.

The X-ray diffraction equipment comprises mainly of an X-ray source. Simply, it is a sample holder and detector for detecting the diffracted X-rays. The generated X-rays are aimed towards the sample (**Figure 2.6**).

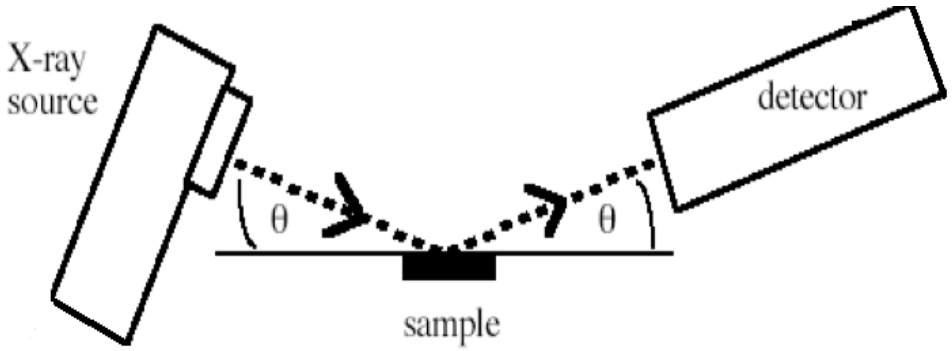

Figure 2.6: Schematic of the X-ray tube, the X-ray detector and the sample (θ: glancing angle)

The crystalline materials on its three-dimensional structures can be defined as regular repeating planes of atoms that form a crystal lattice. When an X-ray beam incidents on planes of atoms on a pair of parallel P1 and P2 (as in **Figure 2.7**), the distance between them is the interplanar spacing **d**. Part of the X-ray beam will be diffracted. The diffracted X-rays waves will interfere constructively and give a diffraction line for a particular angle of beam incidence, which can be observed and detected as it satisfies Bragg's Law (**Equation 2.1**).

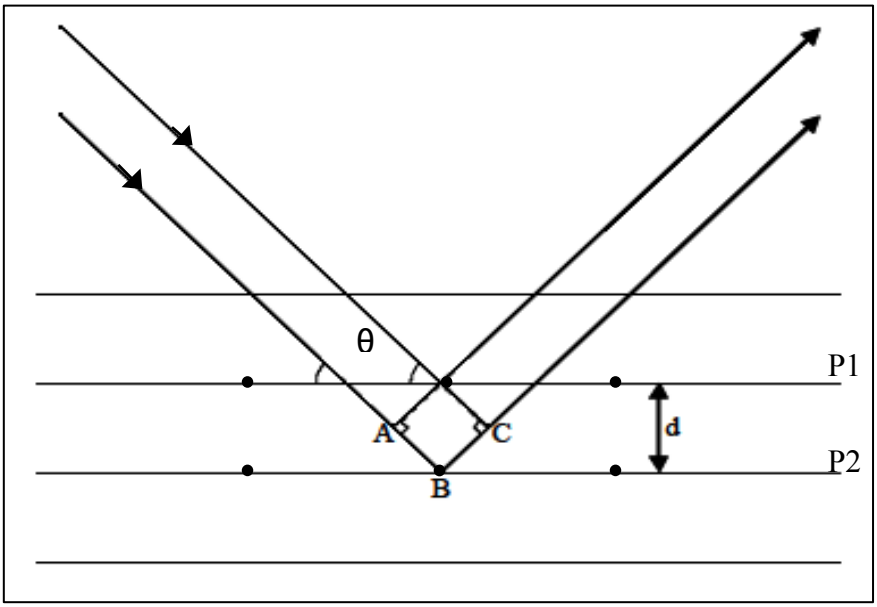

Figure 2.7: A demonstration of Bragg's equation

So the difference in length between the X-rays is AB + BC which is equivalent to:

$$\mathbf{AB + BC = 2d \sin\theta}$$

$$\mathbf{AB + BC = n\lambda}$$

$$\mathbf{n\lambda = 2d \sin\theta}$$

Since we Know **λ** and **θ,** the **d** spacing can be calculated [11].

2.5.1.2- Experimental

In this study, powder X-ray diffraction (XRD) patterns were recorded using a Panalytical X'pert Pro diffractometer using Ni filtered CuK_{α} radiation (operating at 40 kV, 40 mA). Scans were in the range 10–80^{o} 2θ.

2.5.2- X-Ray photoelectron spectra (XPS)

2.5.2.1- Background

K. Siegbahn and his group developed X-Ray photoelectron spectroscopy (XPS) in the mid 1960's. In 1981, he was awarded the noble prize for his extensive work in developing XPS to become a useful analytical technique [12]. XPS is also known as electron spectroscopy for chemical analysis (ESCA) and can provide information for studying the surface composition and oxidation state of supported catalysts. This technique relies on the photoelectric effect. The basic set up for XPS is shown in **Figure 2.8**, and it is made up of an x-ray source, an electron energy analyser and a high vacuum chamber holding the sample.

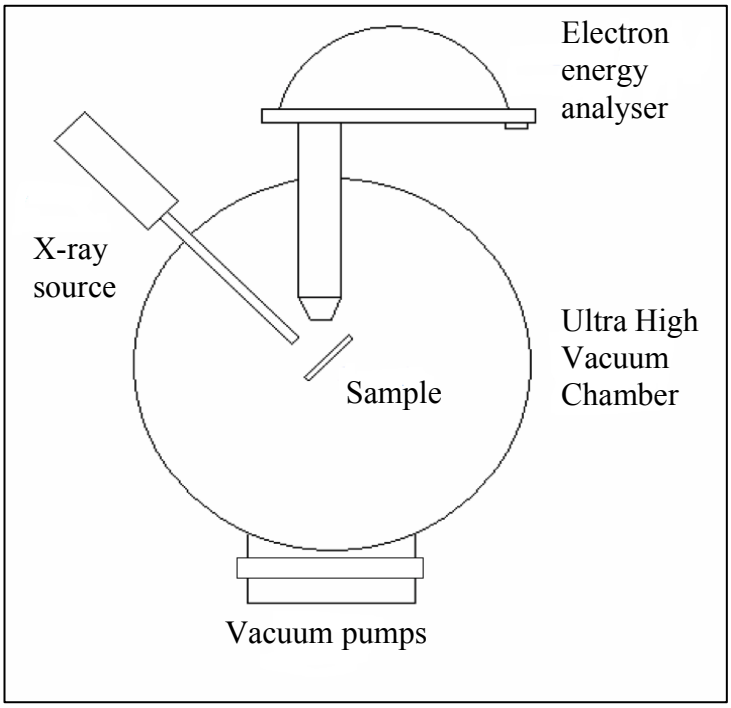

Figure 2.8: The basic set up for X-ray photoelectron spectroscopy

XPS uses X-ray radiation to examine core-levels of the elements on the surface. When a photon with energy hυ hits the sample and is absorbed by an atom, it interacts with the inner shell electrons, which are ionised. A core or valence electron with binding E_b is ejected with kinetic energy E_k expressed as shown in **Equation 2.2**:

$$\mathbf{E_k = h\upsilon - E_b - \Phi}$$

Equation 2.2

Where $\mathbf{E_k}$ is the kinetic energy of the photon ejected, $\mathbf{h\upsilon}$ is the x-ray energy of the photon, $\mathbf{E_b}$ is the binding energy of the parent atom relative to the ejected electron, and $\mathbf{\Phi}$ is the work function (see **Figure 2.9**).

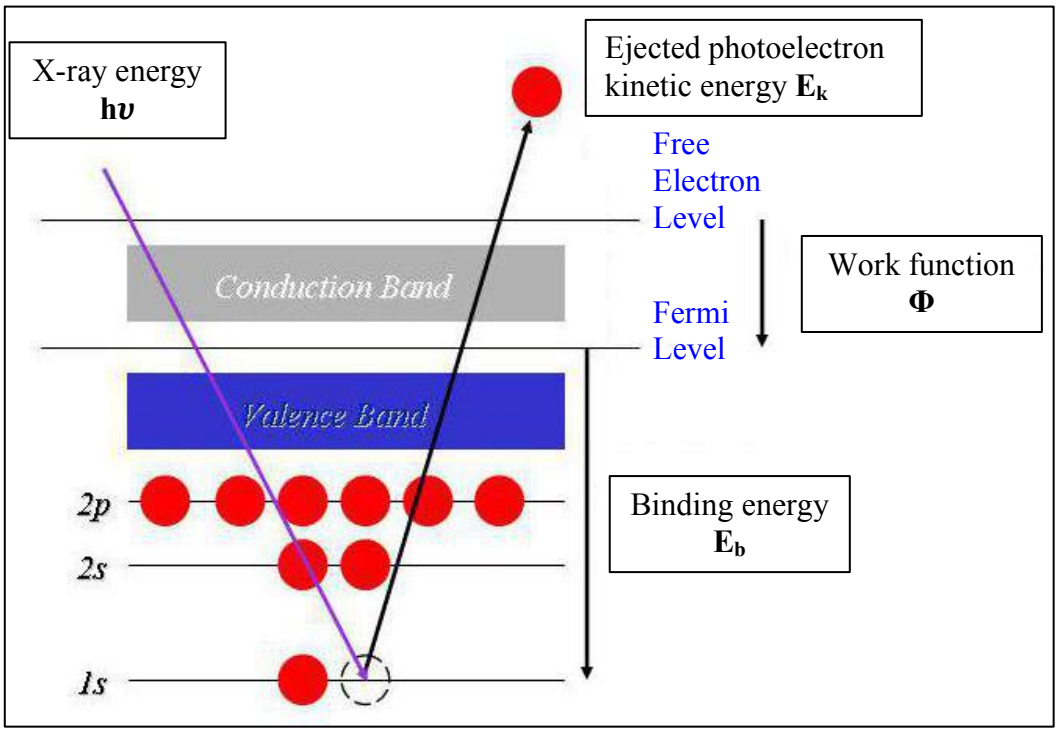

Figure 2.9: Ejected electron by X-ray photon

The difference between the photon energy and the ejected electron kinetic energy is roughly equal to the binding energy of that electron. The work function (**Φ**) is generally less than <2eV and often ignored. Calculating the $\mathbf{E_k}$ kinetic energy and measuring the $\mathbf{E_b}$ binding energy will produce an imprint of the parent atom. Therefore, each element will give rise to a characteristic set of peaks in the photoelectron spectrum at kinetic energies determined by the respective binding energies and the photon energy. **Figure 2.10** shows example of the XPS for palladium (Pd) metal, where the most intense peak at ca. 335 eV is attributed to emission from the 3*d* levels of the Pd atoms, while the 3*p* and 3*s* levels give rise to the peaks at ca. 534/561 eV and 673 eV respectively.

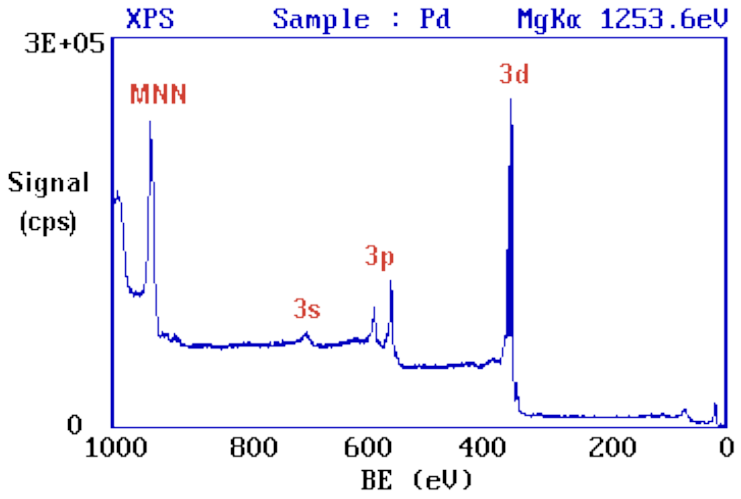

Figure 2.10: Example of XPS spectrum of a Pd metal sample

2.5.2.2- Experimental

Quantitative data can be obtained from peak areas, and identification of chemical states often can be made from exact measurements of peak positions and separations, as well as from certain spectral features. The following principles are used to provide accurate quantification: standardized set of sensitivity factors, transmission function of the spectrometer (detection efficiency) and corrections for geometric asymmetry (related to the angle between the X-ray source and the analyser). As show in **Equation 2.3:**

$$I_x = k \times n_x \times \sigma \times \lambda \times T$$

Equation 2.3

Where $\boldsymbol{I_x}$ is peak area, $\boldsymbol{k}$ is instrumental factors (*e.g.* analysed area, photon flux constant for given operation mode), $\boldsymbol{n_x}$ is atomic density of analyte in sample, σ is ionisation cross-section (probability of ionisation), λ is inelastic mean free path (IMFP) and $\boldsymbol{T}$ is transmission function (detection efficiency).

$$n_x = \frac{I_x}{k \times \sigma \times \lambda \times T}$$

Elemental sensitivity factor, S

$$n_x = \frac{I_x}{S}$$

Describing relative concentration of observed elements as a number fraction by:

$$C_x = \frac{n_x}{\sum n_i} = \frac{I_x / S_x}{\sum I_i / S_i}$$

The XPS analysis work was carried out by Dr. David Morgan from *School of Chemistry, Cardiff University* using a Kratos Axis Ultra DLD spectrometer. Samples were mounted using double-sided adhesive tape, and binding energies referenced to the C1-sbinding energy of adventitious carbon contamination taken to be 284.7 eV. Monochromatic AlK_{α} radiation was used for all analysis. The intensities of the Au(4f) and Pd(3d) features were used to derive Pd:Au surface molar ratios.

2.5.3- Electron microscopy (SEM, TEM and STEM)

2.5.3.1- Background

Scanning electron microscopy (SEM) is an important technique for catalysts characterisation. It is a type of electron microscopy which electrons are used as an alternative source of light to produce images. Therefore, SEM can present high quality images with detailed information about the macroscopic morphology of the catalyst because of the enormous depth of focus on the sample compared to optical microscopy and when coupled with energy-dispersive X-ray spectroscopy (EDX or XEDS), the chemical composition can be analysed [13].

Typically, electrons beam are generated by a metallic filament cathode, which heated in vacuum by passing a voltage to it. Normally tungsten is used as filament because of the highest melting point and lowest vapour pressure. The electrons condensed and focused by lenses and emitted towards the sample. Pairs of scanning coils, an objective lens and apertures are participate in focusing and deflecting the beam, allowing it to scan a

rectangular area of the sample. The interaction between the electrons primary beam and the sample causes emission of electrons from the sample surface and reflected electrons. The electrons emitted from the sample have high electron energy and are called backscatter electrons (BSE), which mainly used for showing the contrast in chemical components. Secondary electrons are reflected electrons have low energy than the backscatter electrons as a result of the inelastic interaction of the primary beam with the sample where significant energy loss was occurred. However a secondary electrons detector collects these electrons. Both electrons secondary and backscatter are converted to a signal then sent to a viewing screen.

Transmission electron microscopy (TEM) is a useful technique to determine the size, shape and compositions in heterogeneous catalysis because of its high resolution[14]. It is operates on the same basis principle as the light microscope using electrons instead of light. Electrons emitted from a gun through electromagnetic lenses and can be focused into a fine beam. The interaction of this beam gave several types of electrons, which reflected from the sample surface and disappear. The electrons that transmit through the sample are magnified by electromagnetic lenses and then hit a fluorescent screen are generate the TEM image. Based on atom density metals generally have a higher electrons density than supports, therefore they appear darker in the TEM image.

Scanning transition electron microscopy (STEM) is also a type of electron microscopy and similar to SEM. STEM provides useful information for the characterisation of nanostructures, and it provides a range of different imaging modes. Furthermore, it can provide information on elemental composition and electronic structure at the ultimate

sensitivity for a single atom. Advantages of using STEM over SEM because of higher magnification 1,000,000x of STEM compared to 100,000x of SEM, and the higher spatial resolution can be achieved allowing for analysis on the atomic scale, such as a few nanometers, compared to a few micrometers using an SEM which is very helpful for characterising nanoparticle catalysts.

In scanning transmission electron microscopy (STEM), a focused beam of electrons generated by a lanthanum hexaboride filament is focused into a narrow spot and scanned over the surface of thin specimens of the sample. The transmitted electron signal is detected to form an image by the annular dark field (ADF) detector, which is the method, used to map the sample and is very sensitive to variations in atomic number of atoms contained in the sample. **Figure 2.11** shows a schematic of the main components of a high-resolution dedicated STEM system [15-17]. A high angle annular dark field detector (HAADF) is used to collect electrons, which are not Bragg scattered, with high efficiency all the electrons scattered to identify the chemical component. Atomic resolution images are produced, where the contrast is directly related to the atomic number (Z-contrast image). Other detectors are used such as an energy dispersive X-ray (EDX or XEDS) detector to give information of elemental analysis and chemical composition. The EDX system commonly used system in both SEMs and TEMs for detecting the X-rays that are generated and emitted from the sample. The EDX system is composed of three basic parts: a detector, a pulse processor and a multi-channel analyser or computer display. Typically, the detector is based on a semiconductor device, usually a crystal of silicon or Si(Li) detector. The crystal absorbs

the energy of incoming X-rays by ionization, generating free electrons in the crystal that become conductive and produce an electrical charge bias. The X-ray absorption then converts the energy of individual X-rays into electrical voltages of proportional size; the electrical pulses correspond to the characteristic X-rays of the element, which each element has a unique atomic structure allowing unique set of peaks on its X-ray spectrum [18].

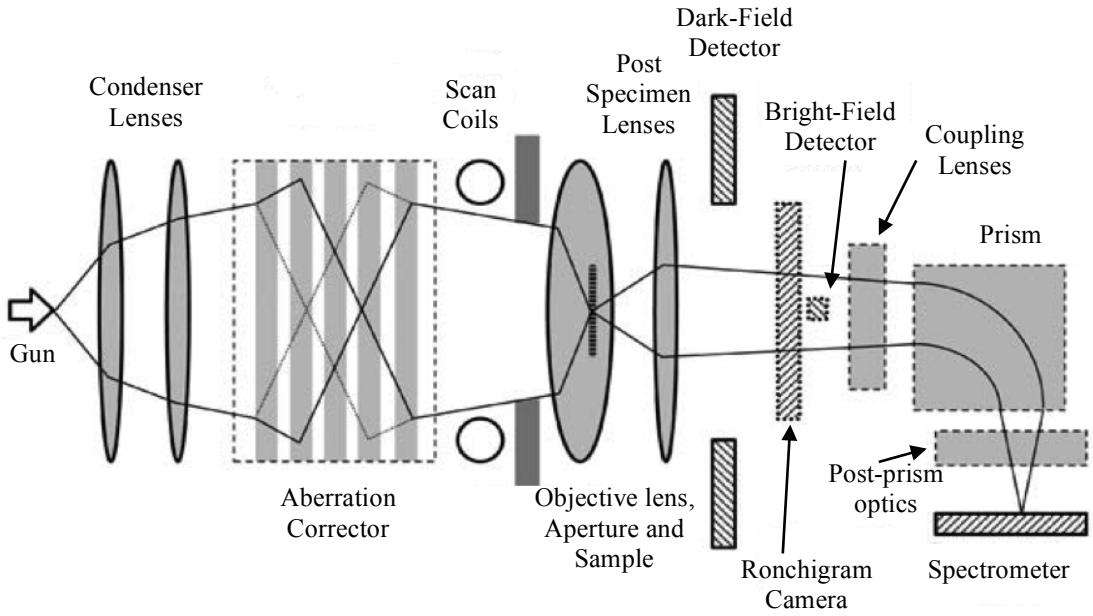

Figure 2.11: Schematic showing the main components of a high-resolution dedicated STEM [17]

2.5.3.2- Experimental

In this study, samples for examination by transmission electron microscopy were prepared by dry dispersing the catalyst powder onto a holey carbon film supported by a 300 mesh copper TEM grid. STEM high angle annular dark field (HAADF) images and X-ray energy-dispersive spectra of nanoparticles were obtained using an aberration corrected JEOL 2200FS STEM operating at 200kV. Selected sample powders were also dispersed on an Al-stub and examined in a Hitachi 4300LV SEM equipped with an EDAX energy dispersive X-ray spectrometer. Professor Christopher Kiely and his group in *the material science department at the Lehigh University in the USA* obtained the STEM images.

2.6- References

[1] A. Bruckner, Catal. Rev. - Sci. Eng., 45 (2003) 97-150.

[2] S. Meenakshisundaram, E. Nowicka, P.J. Miedziak, G.L. Brett, R.L. Jenkins, N. Dimitratos, S.H. Taylor, D.W. Knight, D. Bethell, G.J. Hutchings, Faraday Discuss., 145 (2010) 341-356.

[3] D.I. Enache, J.K. Edwards, P. Landon, B. Solsona-Espriu, A.F. Carley, A.A. Herzing, M. Watanabe, C.J. Kiely, D.W. Knight, G.J. Hutchings, Science (Washington, DC, U. S.), 311 (2006) 362-365.

[4] J.K. Edwards, B. Solsona, N.E. Ntainjua, A.F. Carley, A.A. Herzing, C.J. Kiely, G.J. Hutchings, Science (Washington, DC, U. S.), 323 (2009) 1037-1041.

[5] J.K. Edwards, A.F. Carley, A.A. Herzing, C.J. Kiely, G.J. Hutchings, Faraday Discuss., 138 (2008) 225-239.

[6] R.C. Tiruvalam, J.C. Pritchard, N. Dimitratos, J.A. Lopez-Sanchez, J.K. Edwards, A.F. Carley, G.J. Hutchings, C.J. Kiely, Faraday Discuss., 152 (2011) 63-86.

[7] D.J. Butcher, Microchem. J., 87 (2007) 91.

[8] D.C. Harris, Quantitative Chemical Analysis, 7th Edition ed., W. H. Freeman and Company, 2007.

[9] R. Kellner, a. et, Editors, Analytical Chemistry. A Modern Approach to Analytical Science. 2nd Newly Revised Edition, WILEY VCH, 2004.

[10] B.D. Cullity, S.R. Stock, Elements of X-Ray Diffraction, 3rd Edition, Prentice Hall, 2001.

[11] D.L. Andrews, A.A. Demidov, An Introduction to Laser Spectroscopy; Second Edition, Kluwer Academic/Plenum Publishers, 2002.

[12] G. Rothenberg, Catalysis: Concepts and Green Applications, Wiley-VCH Verlag GmbH Co. KGaA, 2008.

[13] D.A.M. Monti, A. Baiker, Journal of Catalysis, 83 (1983) 323-335.

[14] N.W. Hurst, S.J. Gentry, A. Jones, B.D. McNicol, Catalysis Reviews, 24 (1982) 233-309.

[15] A.V. Crewe, J. Wall, J. Langmore, Science, 168 (1970) 1338-1340.

[16] Weilie Zhou, Z.L. Wang, Scanning Microscopy for Nanotechnology Techniques and Applications, 1st edition, 1st edition ed., Springer, 2007.

[17] M. Varela, A.R. Lupini, B.K. van, A.Y. Borisevich, M.F. Chisholm, N. Shibata, E. Abe, S.J. Pennycook, Annu. Rev. Mater. Res., 35 (2005) 539-569, 512 plates.

[18] Mihail Nazarov, D.Y. Noh, New Generation of Europium- and Terbium-Activated Phosphors, Pan Stanford Publishing, 2011.

Chapter three:

Selective suppression of disproportionation reaction in solvent-less benzyl alcohol oxidation catalysed by supported Au-Pd nanoparticles

3.1- Introduction

Selective oxidation of alcohols, using molecular oxygen, has received considerable attention in the recent past due to its potential application in the production of intermediates in the fine chemicals and fragrance industries [1-3]. Many heterogeneous catalysts have been reported to be active for this transformation and recently supported gold nanoparticles have been shown to be highly effective [4-6]. With respect to gold catalysis, it is known that this reactivity is due to small gold nanoparticles; their interface with the supporting matrix is also important [7-10]. Recently, Hutchings and co-workers reported a twenty five fold increase in turnover frequency for the oxidation of alcohols by adding small amounts of palladium to supported gold catalysts, and they have demonstrated that these catalysts could be used for the solvent-free aerobic oxidation of alcohols [11]. Subsequently, bimetallic gold–palladium catalysts have been utilised for the oxidation of a wide range of substrates including aliphatic alcohols, polyols and alkyl aromatics [12-14]. Benzyl alcohol has long been used as a model substrate for selective oxidation [15-17]. Earlier investigations into the solvent-free aerobic oxidation of this substrate using supported gold–palladium catalysts resulted in the detection of many products, including toluene, benzoic acid, benzyl benzoate and dibenzyl ether, besides the desired product, benzaldehyde [15-18]. Detailed knowledge of the origins of these products is crucial to fine-tune the catalyst to obtain the most important product, benzaldehyde, in high yield by suppressing the formation of by-products. Benzaldehyde and benzoic acid are formed by the sequential oxidative dehydrogenation and further oxidation of benzyl alcohol, as shown in **Scheme 3.1**.

Dibenzyl ether is formed through the dehydration of benzyl alcohol, and benzyl benzoate is reported to be formed either *via* hemiacetal from benzaldehyde or by the esterification of benzoic acid by the substrate benzyl alcohol [12, 18, 19]. There has been a long ongoing debate about the origin of the other major by-product: toluene [12, 20-22]. Baiker *et al.* proposed hydrogenolysis of benzyl alcohol as the origin of toluene, but many other groups proposed a disproportionation mechanism of benzyl alcohol as the origin of toluene [12, 20-22]. Disproportionation of benzyl alcohol results in an equimolar mixture of benzaldehyde and toluene, as shown in **Scheme 3.2**.

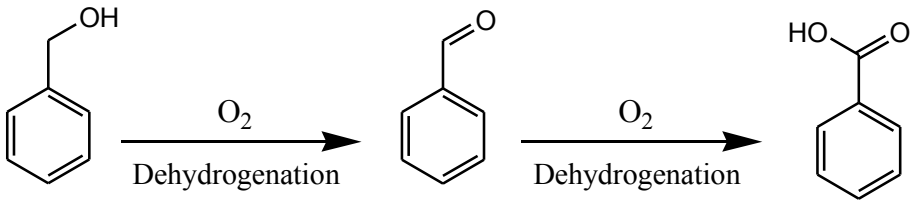

Scheme 3.1: Dehydrogenation of benzyl alcohol to benzaldehyde and further oxidation to benzoic acid

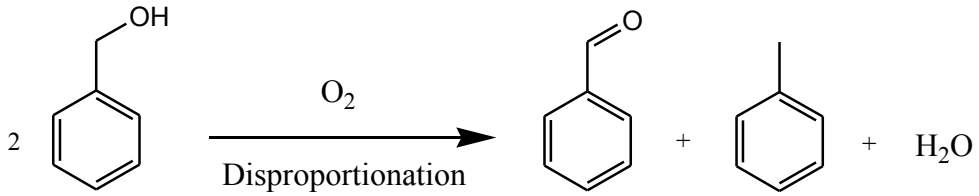

Scheme 3.2: Disproportionation of two moles of benzyl alcohol leading to equimolar amounts of toluene and benzaldehyde

Since benzaldehyde is formed by both oxidation as well as disproportionation reactions, it becomes difficult to study this disproportionation reaction under aerobic conditions, where both oxidation as well as disproportionation reactions are active [23]. Hutchings

and co-workers recently reported a methodology that will be used in this study to quantify these two reactions separately, even under such aerobic conditions. Based on this methodology, in this current study, it has been found that the oxidation and disproportionation reaction could have different active sites in the supported gold palladium catalysts; with metal sites for the oxidation reaction and metal–support interface sites for the disproportionation reaction. It has also been demonstrated that by changing the support, it is possible to either switch-on or switch-off this disproportionation reaction and thus toluene formation [23].

3.2- Experimental

3.2.1- Catalyst preparation

Catalysts were prepared using the sol immobilisation method. 1%AuPd/TiO_2 and 1%AuPd/MgO were synthesised according to this method, as described in detail in chapter 2 (section 2.2.1).

3.2.2- Catalyst testing

Benzyl alcohol oxidation was carried out in a Radleys carousel glass stirred reactor (GSR) described in detail in chapter 2 (section 2.3.1) and the quantification procedure of the sample reaction described in chapter 2 (section 2.4.1.4).

3.2.3- Catalyst characterisation

The catalysts were characterised using scanning transmission electron microscopy (STEM) as described in chapter 2 (section 2.5.3).

3.3- Results and discussion

3.3.1- Effect of temperature on disproportionation of benzyl alcohol

A solvent-free benzyl alcohol reaction, under aerobic conditions (1 bar of O_2), was performed using a 1%Au–Pd/TiO_2 catalyst, prepared using the sol-immobilisation technique, in a GSR at different temperatures (80, 100 and 120 °C) in a time online study (15, 30, 45, 60 and 75 min). Conversion and selectivity were calculated using the procedure described in chapter 2 (section 2.4.1.4). According to **Scheme 3.2**, the number of moles of benzyl alcohol consumed in disproportionation is twice the number of moles of toluene formed. From this value, a disproportionation turnover number (TON_D) was calculated using **Equation 3.1**. Benzaldehyde is formed from both the reactions; the moles of benzaldehyde formed by disproportionation are equal to the number of moles of toluene formed. Through subtraction, the moles of benzaldehyde formed by the oxidation reaction (**Scheme 3.1**) can then be calculated and converted into an oxidation turnover number (TON_O) using **Equation 3.2**. The total turnover number (TON_{total}) was calculated using **Equation 3.3** [23].

Equation 3.1

$$\mathbf{TON_D = \frac{2 \times mol\ of\ toluene}{mol\ of\ metal}}$$

Equation 3.2

$$\mathbf{TON_O = \frac{mol\ of\ benzaldehyde - mol\ of\ toluene}{mol\ of\ metal}}$$

Equation 3.3

$$\mathbf{TON_{Total} = \frac{mol\ benzyl\ alcohol\ converted}{mol\ of\ metal}}$$

The results of the conversion and selectivity are presented in **Table 3.1**; the calculations of TON_D, TON_O and TON_{Total} are shown in the figures (**Figure 3.1, Figure 3.2** and **Figure 3.3)**. With an increase in temperature, there is an overall increase in TON_{Tot}, mostly because of the higher contribution from TON_D as compared to TON_O. Besides toluene and benzaldehyde, other products including benzene, dibenzyl ether, benzoic acid and benzyl benzoate were also detected, but at very low concentrations (< 3% molar selectivity). The amount of toluene increases with increasing temperature, as shown in **Table 3.1**. The results of TON_D came near to equivalent amounts of TON_O (**Figure 3.2**) and have increased with temperature to more than the amount of TON_O in **Figure 3.3**. This proves that, under aerobic conditions, oxidation is not the only active reaction, and it indicates that disproportionation could be the cause of toluene formation, as opposed to previous claims that toluene is formed by hydrogenolysis of benzyl alcohol [17, 22].

Initially, an increase in oxidation was observed from 80 °C to 120 °C, followed by a substantial increase in the disproportionation reaction (TON_D), which was observed with an increase in the reaction temperature. It is notable that the TON_D tends to stop after 60 min of reaction time with the 80 °C as shown in **Figure 3.1**, it is possibly because of increasing the aldehyde formation led to poison the formation of toluene. At reaction temperatures above 100 °C, any increase in the overall reaction (TON_{Tot}) is exclusively because of an increase in the disproportionation reaction and not the oxidation reaction. This suggests that raising the temperature is not the correct approach to increase the yield of the desired benzaldehyde product.

Table 3.1: Temperature effect on conversion and selectivity data for the oxidation of benzyl alcohol using 1%Au-Pd/TiO_2 sol immobilisation method in a time online study at 80, 100 and 120 °C [a]

Catalyst	Temp. (°C)	Time (h)	Conversion (%)	Selectivity (%)					
				Benzaldehyde	Toluene	Benzene	Benzoic acid	Benzyl benzoate	DBE
1%Au-Pd/TiO_2	80	0	**0**						
		15	**2.5**	80.6	13	0	0.5	0.4	1
		30	**4.6**	83.7	14.8	0	0	0.5	0.8
		45	**7.5**	78	17.8	3.4	0	0.5	0.5
		60	**8.4**	83.6	14.3	1.3	0	0.7	0.4
		75	**12**	86.2	11.2	1.8	0	1	0.3
1%Au-Pd/TiO_2	100	0	**0**						
		15	**9.7**	71.8	24.8	2.7	0	0.2	0.4
		30	**12.7**	75.8	21.8	1.5	0	0.3	0.5
		45	**17.7**	77.3	21.8	0.5	0	0.3	0.5
		60	**21.3**	78.6	20.2	0.3	0	0.3	0.5
		75	**26.2**	82.2	16.6	0.3	0	0.3	0.4
1%Au-Pd/TiO_2	120	0	**0**						
		15	**19.1**	68.8	30	0.2	0	0.2	0.5
		30	**28.1**	70	28.6	0.3	0	0.3	1
		45	**36.5**	70.7	27.4	0.4	0	0.3	1.2
		60	**39.4**	74.4	24.7	0.4	0	0.3	0.6
		75	**49.4**	74.7	24.1	0.5	0	0.3	0.6

[a] Reaction conditions: 0.02g catalyst, 1 bar of O_2, 2g benzyl alcohol and stirring at 1000 rpm

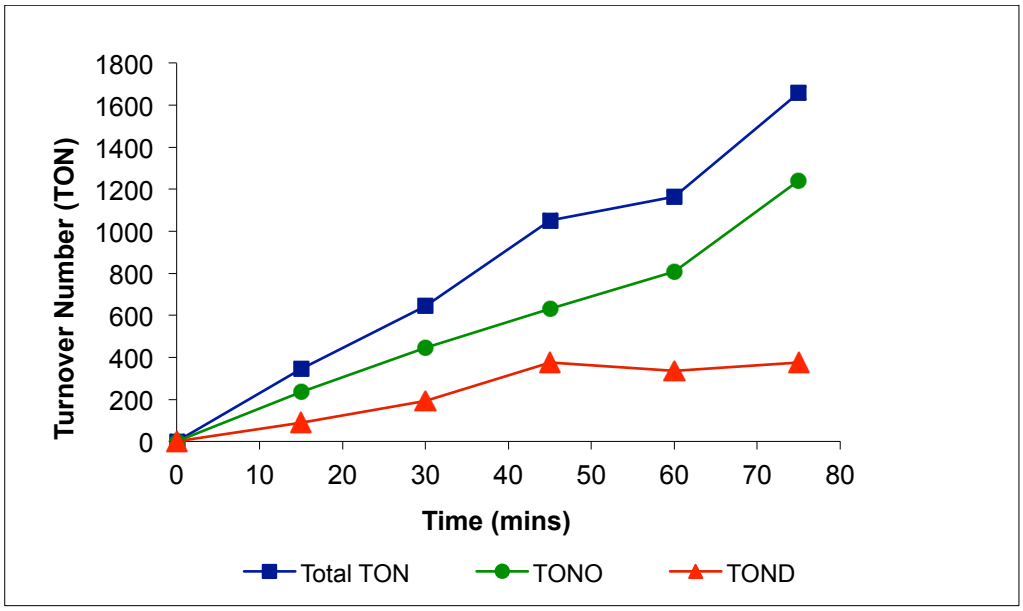

Figure 3.1: Temperature effect on oxidation (TON_O), disproportionation (TON_D) and the total turnover number (TON_{Tol}) 1 bar of O_2 in a time online study at 80 °C

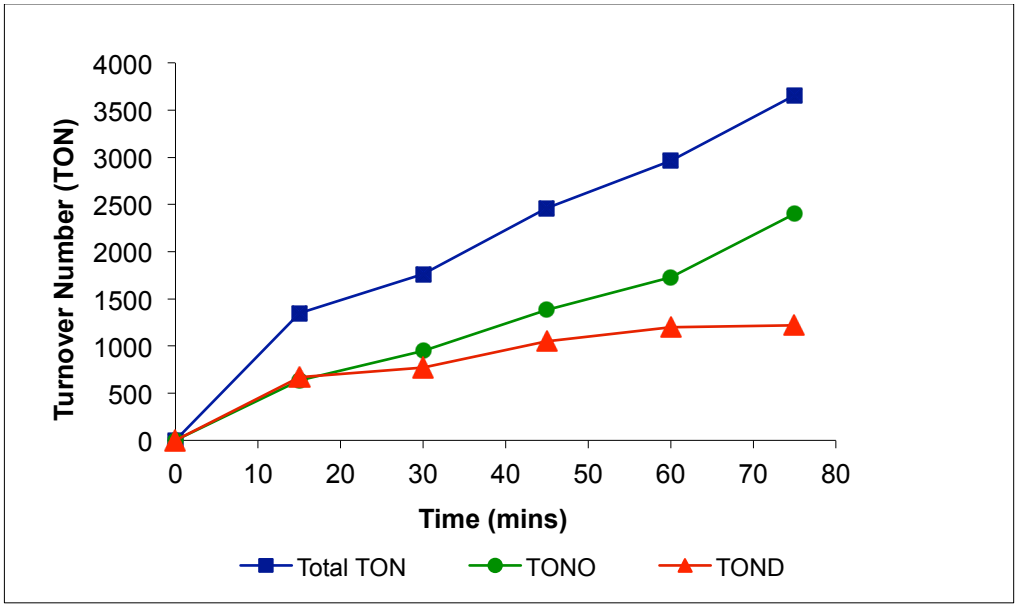

Figure 3.2: Temperature effect on oxidation (TON_O), disproportionation (TON_D) and the total turnover number (TON_{Tol}) 1 bar of O_2 in a time online study at 100 °C

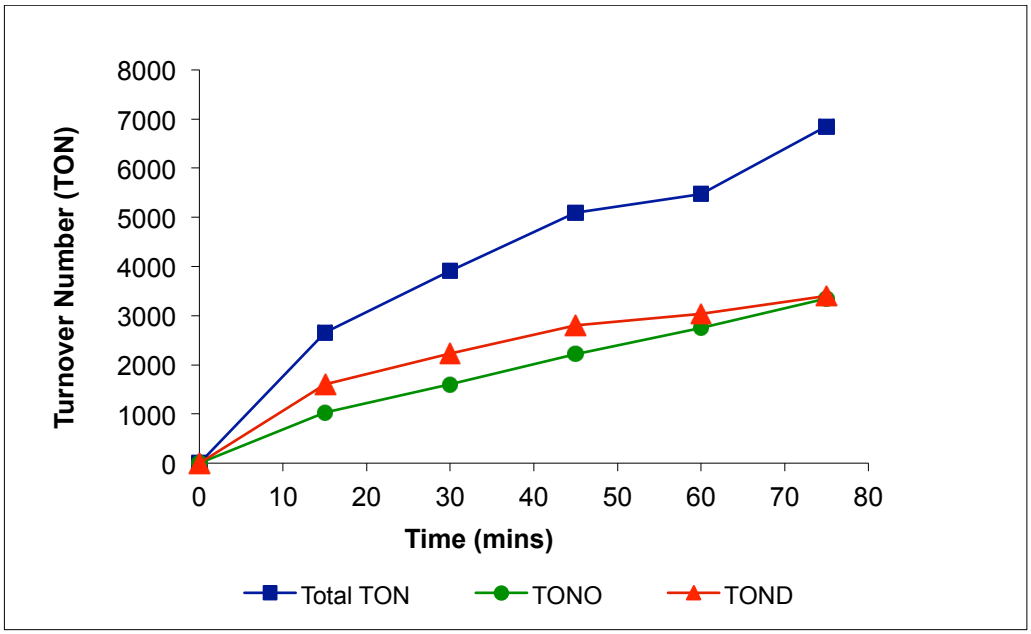

Figure 3.3: Temperature effect on oxidation (TON_O), disproportionation (TON_D) and the total turnover number (TON_{Tol}) 1 bar of O_2 in a time online study at 120 °C

3.3.2- Oxidation versus disproportionation of benzyl alcohol under anaerobic conditions

The data provided in previous study proves that disproportionation of benzyl alcohol is not the only reaction that is active under aerobic conditions. To further investigate this, anaerobic conditions have been used in this reaction instead of O_2, such as in the presence of He alone or in air condition; the reaction was carried out in a time online study (15, 30, 45, 60 and 75 min). Besides disproportionation, oxidative dehydrogenation of benzyl alcohol to benzaldehyde occurs, and in fact becomes the most favoured reaction. With the help of the TON quantification methodology, it has become easier to study the response of these two reactions separately to reaction

parameters. With the air and the anaerobic conditions, the product mixture comprised of near equivalent amounts of benzaldehyde and toluene (as show in **Table 3.2**) in the presence of He and air. The calculations for TON_D, TON_O and TON_{Total} are shown in (**Figure 3.4** and **Figure 3.5**)**.** In the presence of He and air there were clear differences in the amount of TON_D in anaerobic conditions. The TON_{Tot} was not equivalent to TON_D under air and anaerobic conditions, as there was a small positive value for TON_O attributed to the adsorbed O_2 on the surface of the catalyst, which could not be removed [23]. This study, in conjunction with the temperature study, proves that under air and anaerobic conditions, disproportionation is the only active reaction and it proves that it is the source of toluene and it is not formed by hydrogenolysis of benzyl alcohol [17, 22]. Stoichiometrically, oxygen is not involved in the disproportionation reaction, but on comparing the TON_D data at the temperature of 120 °C between aerobic (shown in **Table 3.1** and **Figure 3.3**) and anaerobic conditions with the two reactions in the presence of He or air (shown in **Table 3.2)** and (**Figure 3.4** and **Figure 3.5**), it is evident that oxygen has a substantial promotional effect on the disproportionation reaction [23].

Table 3.2: Conversion and selectivity data for the oxidation of benzyl alcohol using 1%Au-Pd/TiO_2 sol immobilisation method in the presence of He and air [a]

Catalyst	Atmosphere	Time (h)	Conversion (%)	Selectivity (%)					
				Benzaldehyde	Toluene	Benzene	Benzoic acid	Benzyl benzoate	DBE
1%Au-Pd/TiO_2	Air	0	**0**						
		15	**11.1**	57.4	41	0.7	0	0.2	0.6
		30	**15**	58	40.2	0.6	0	0	0.6
		45	**21.1**	56.4	40.3	2.4	0	0	0.8
		60	**22.2**	56.4	40.5	2	0	0.1	1
		75	**27.2**	58.6	40	0.3	0	0.1	1
1%Au-Pd/TiO_2	He	0	**0**						
		15	**4.6**	54.4	39.2	5.8	0	0	0.5
		30	**7.5**	50	39.2	10.3	0	0	0.3
		45	**8**	54	46	0	0	0	0
		60	**8.3**	52.3	41.6	5.8	0	0	0.2
		75	**10.2**	51.6	44.3	3.7	0	0	0.3

[a] Reaction conditions: 0.02g catalyst, 1 bar pressure, 2g of benzyl alcohol, 120 °C and stirring at 1000 rpm

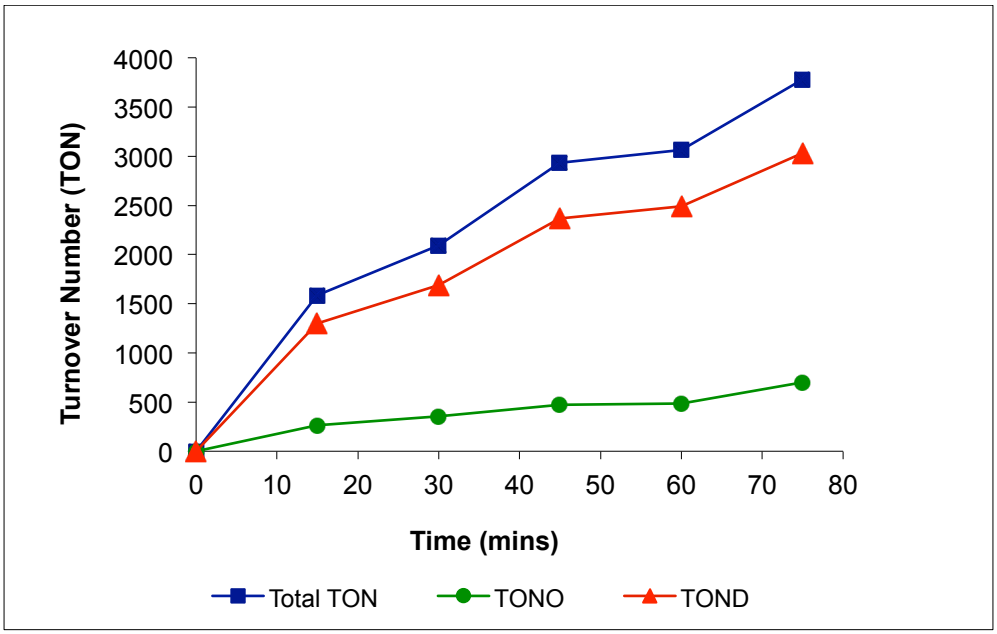

Figure 3.4: Air conditions effect on oxidation (TON_O), disproportionation (TON_D) and the total turnover number (TON_{Tol}) in a time online study at 120 °C

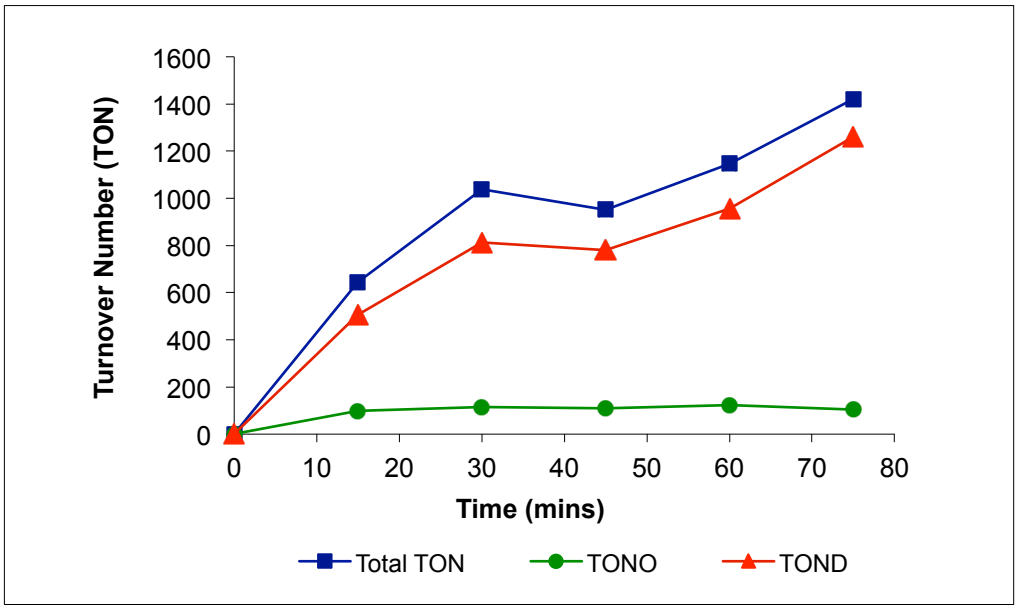

Figure 3.5: Anaerobic conditions effect on oxidation (TON_O), disproportionation (TON_D) and the total turnover number (TON_{Tol}) 1 bar of He in a time online study at 120 °C

3.3.3- Effect of reaction pressure

The oxidation of benzyl alcohol using 1%AuPd/TiO_2 catalyst was examined further at different O_2 pressures. A study of 1 bar of oxygen at 120 °C from the data shown in previous studies (**Table 3.1** and **Figure 3.3**) were compared under the same conditions at 120 °C using 2 bars of oxygen in a time online study (15, 30, 45, 60 and 75 min). This is shown in **Table 3.3**, and was followed by a further increase in O_2 pressure to 3 bars; the figures show the clear effect of the TON calculations (**Figure 3.7** and **Figure 3.7**). However, the TON_D reached a maximum in pure O_2 at 1 bar, and then decreased with further increases in O_2 pressure to 2 bars and 3 bars. The results show that the oxidation reaction and hence the benzaldehyde formation was promoted by increasing O_2 concentrations. It was also noted that the oxidation TON (TON_O) and the total TON (TON_{Tot}) increased gradually with O_2 pressure within the pressure range studied. The dependence of TON_D on O_2 pressure suggests that there may be two different mechanisms for these disproportionation reactions, one anaerobic and the other promoted by oxygen; the complexity of the dependence arising from the interaction between the two disproportionation routes, at least when carried out on AuPd/TiO_2 catalysts.

Table 3.3: Conversion and selectivity data for the oxidation of benzyl alcohol using 1%Au-Pd/TiO_2 sol immobilisation method in different O_2 pressures [a]

Catalyst	O_2 Pressure (bar)	Time (h)	Conversion (%)	Selectivity (%)					
				Benzaldehyde	Toluene	Benzene	Benzoic acid	Benzyl benzoate	DBE
1%Au-Pd/TiO_2	2	0	**0**						
		15	**17.4**	72.5	26	0.3	0	0.3	0.8
		30	**25.6**	75.2	23.4	0.4	0	0.3	0.6
		45	**34.7**	75.9	22.6	0.5	0	0.3	0.6
		60	**37.4**	79	19.6	0.5	0	0.4	0.6
		75	**50.8**	80	19	0.5	0	0.3	0.4
1%Au-Pd/TiO_2	3	0	**0**						
		15	**18.5**	77.4	22.5	0	0	0	0
		30	**28**	80.1	18.5	0.5	0	0.3	0.5
		45	**39**	80.2	18.4	0.4	0	0.4	0.5
		60	**45.3**	82.7	16	0.5	0	0.4	0.4
		75	**53.3**	84.6	14.1	0.5	0	0.4	0.3

[a] Reaction conditions: 0.02g catalyst, 2g of benzyl alcohol, 120 °C and stirring at 1000 rpm

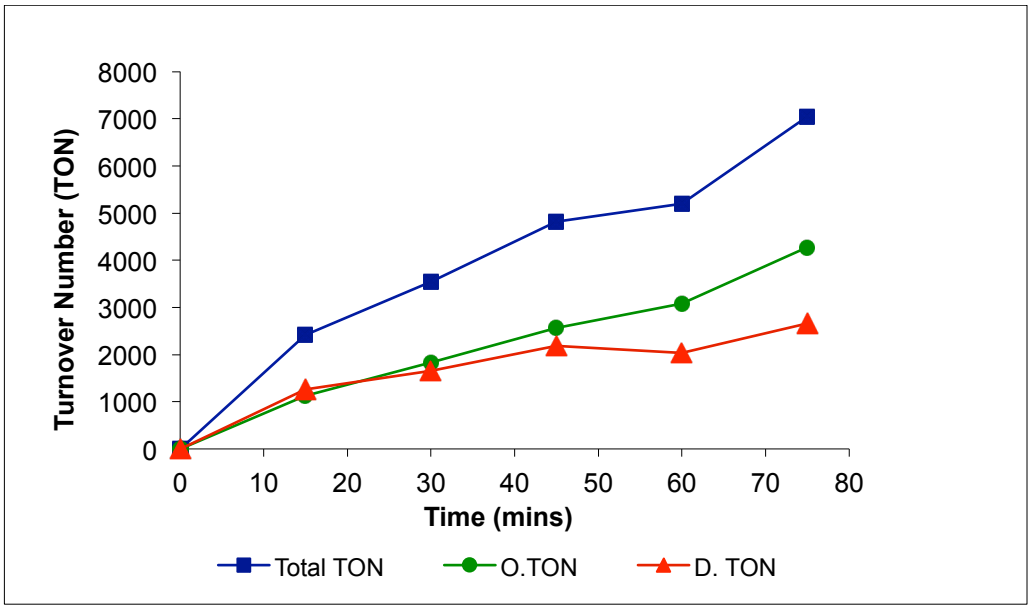

Figure 3.6: Atmospheric effects on oxidation (TON_O), disproportionation (TON_D) and the total turnover number (TON_{Tol}) 2 bar of O_2 in a time online study at 120 °C

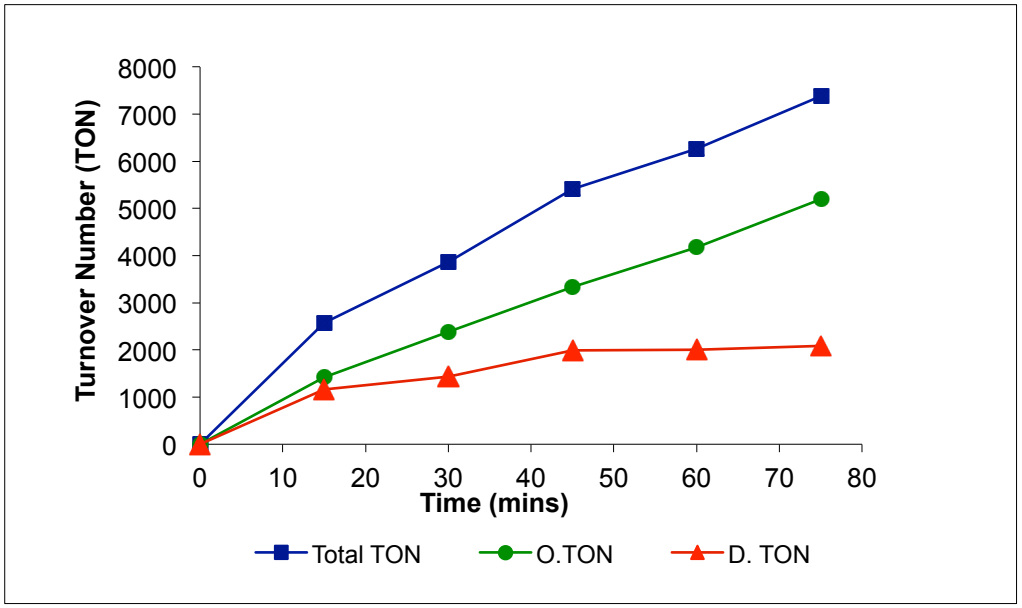

Figure 3.7: atmospheric effects on oxidation (TON_O), disproportionation (TON_D) and the total turnover number (TON_{Tol}) 3 bar of O_2 in a time online study at 120 °C

3.3.4- Effect of the support

In a previous study, Hutchings and co-workers reported that MgO and ZnO supported gold palladium catalysts completely switched-off the disproportionation reaction [23]. In this study, the same catalyst (1%AuPd/MgO) has been tested in a GSR for the oxidation of benzyl alcohol under aerobic pure O_2 conditions at a temperature of 120 °C. The results are listed in **Table 3.4**, and the TON calculation is presented in **Figure 3.8**. With the time online study, the alcohol conversions and selectivity of aldehyde have increased, but the selectivity to the toluene remains constant without any substantial changes. The MgO supported catalysts displayed lower activity compared to their TiO_2 analogues. At 120 °C, the 1%AuPd/TiO_2 catalyst resulted in approximately 50% conversion, whereas the 1%AuPd/MgO catalyst gave approximately 20% conversion, but with a substantial increase in benzaldehyde selectivity of around 75% for the TiO_2 supported catalyst to 95% for the MgO supported catalyst. This is because the TiO_2 supported catalysts promote both oxidation and disproportionation reactions. Consequently, the overall higher activity for the TiO_2 supported catalyst is due to the additive contribution of both reactions, whereas the MgO supported catalyst only selectively promotes the oxidation reaction. Detailed quantitative studies indicate that the interfacial sites between the nanoparticles and supports play a crucial role in the disproportionation reaction [23]. By changing the support from TiO_2 to MgO there is a complete switch-off in the disproportionation reaction, and thus in toluene selectivity. The reason for this observed difference between the TiO_2 and MgO supported catalysts is speculated to be the mode of adsorption of the benzyl alcohol molecules at the metal–

support interface for the disproportionation reaction. This difference in the mode of adsorption is attributed to the higher basicity of the MgO support [23].

Table 3.4: Conversion and selectivity data for the oxidation of benzyl alcohol using 1%Au-Pd/MgO sol immobilisation method [a]

Catalyst	Time (h)	Conversion %	Selectivity (%)					
			Benzaldehyde	Toluene	Benzene	Benzoic acid	Benzyl benzoate	DBE
1%Au-Pd/MgO	0	0						
	15	5.7	96.6	0.4	1.4	0.5	1	0
	30	8.1	97	0.4	1.5	0	1	0
	45	10.5	96.5	0.4	2	0.1	1	0
	60	15.7	96.4	0.4	2	0.1	1.1	0
	75	18.2	96.1	0.5	2.5	0.1	1	0

[a] Reaction conditions: 0.02g catalyst, 1 bar of O_2, 2g benzyl alcohol, 120 °C and stirring at 1000 rpm

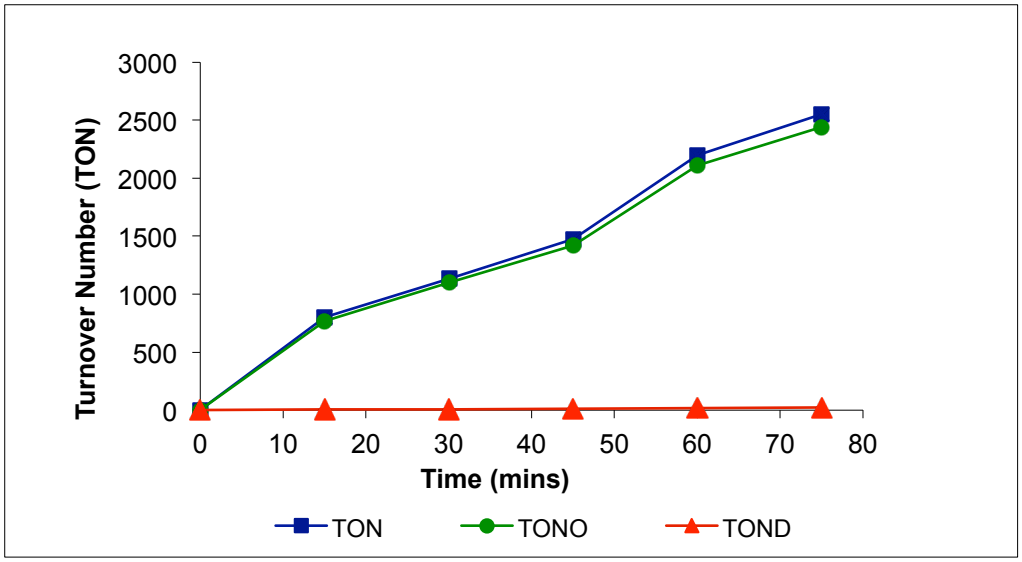

Figure 3.8: Supports effect on oxidation (TON_O), disproportionation (TON_D) and the total turnover number (TON_{Tol}) 1 bar of O_2 in a time online study at 120 °C

3.3.5- Scanning transmission electron microscopy (STEM)

The 1%Au–Pd/TiO_2 and 1%Au–Pd/MgO catalysts have been extensively studied previously [18, 23-25] and it has been found that particle size and composition are important factors for catalytic performance, and for that reason these studies have been extended by the scanning transmission electron microscopy (STEM) described in detail in chapter 2 (section 2.5.3). Representative STEM-HAADF images and corresponding particle size distributions for the TiO_2 supported catalyst and the MgO supported catalyst are presented in **Figure 3.9** (a,b) and **Figure 3.10** (a,b) respectively. It is clear that there is no major difference between the metal particle size distributions for these two catalysts only there are more sub-2 nm particles in for catalytic performance. This is hardly surprising as both these catalysts were derived from the same starting colloids, which were subjected to an identical thermal treatment. Detailed higher resolution HAADF and XEDS studies indicate that the metal particles were Au-Pd alloys in both catalyst systems (**Figure 3.9** (c,d) and **Figure 3.10** (c,d)). Furthermore, on both supports, there is a tendency for the colloidal metal particles to wet the underlying oxide, as evidenced by particle flattening and surface faceting [23]. This intimate wetting contact creates a large number of interface sites and provides good anchoring of the alloy particle to the support. These electron microscopy results imply that the difference in promotional behaviour for the disproportionation reaction between these two catalysts is not simply because of any gross particle size differences, but is much more subtle in origin, and it may be related to the redox behaviour or surface compositional characteristics of the oxide support.

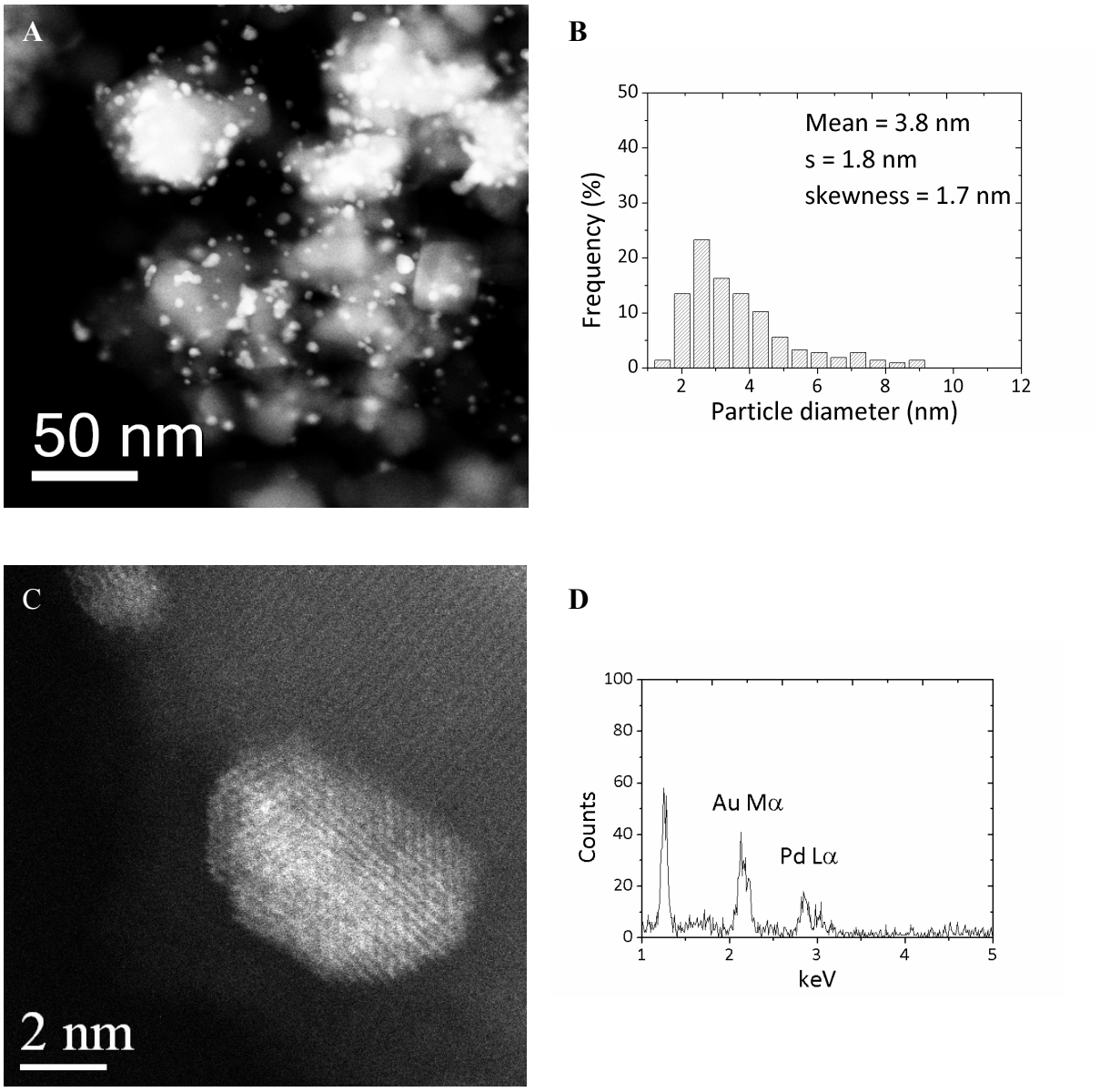

Figure 3.9: (a) STEM-HAADF image and (b) corresponding particle size distribution for 1%AuPd/TiO_2 catalyst prepared by sol immobilisation. (c) Atomic resolution HAADF image of a typical metal nanoparticle and (d) its corresponding XEDS spectrum confirming that it is an alloy of Au and Pd

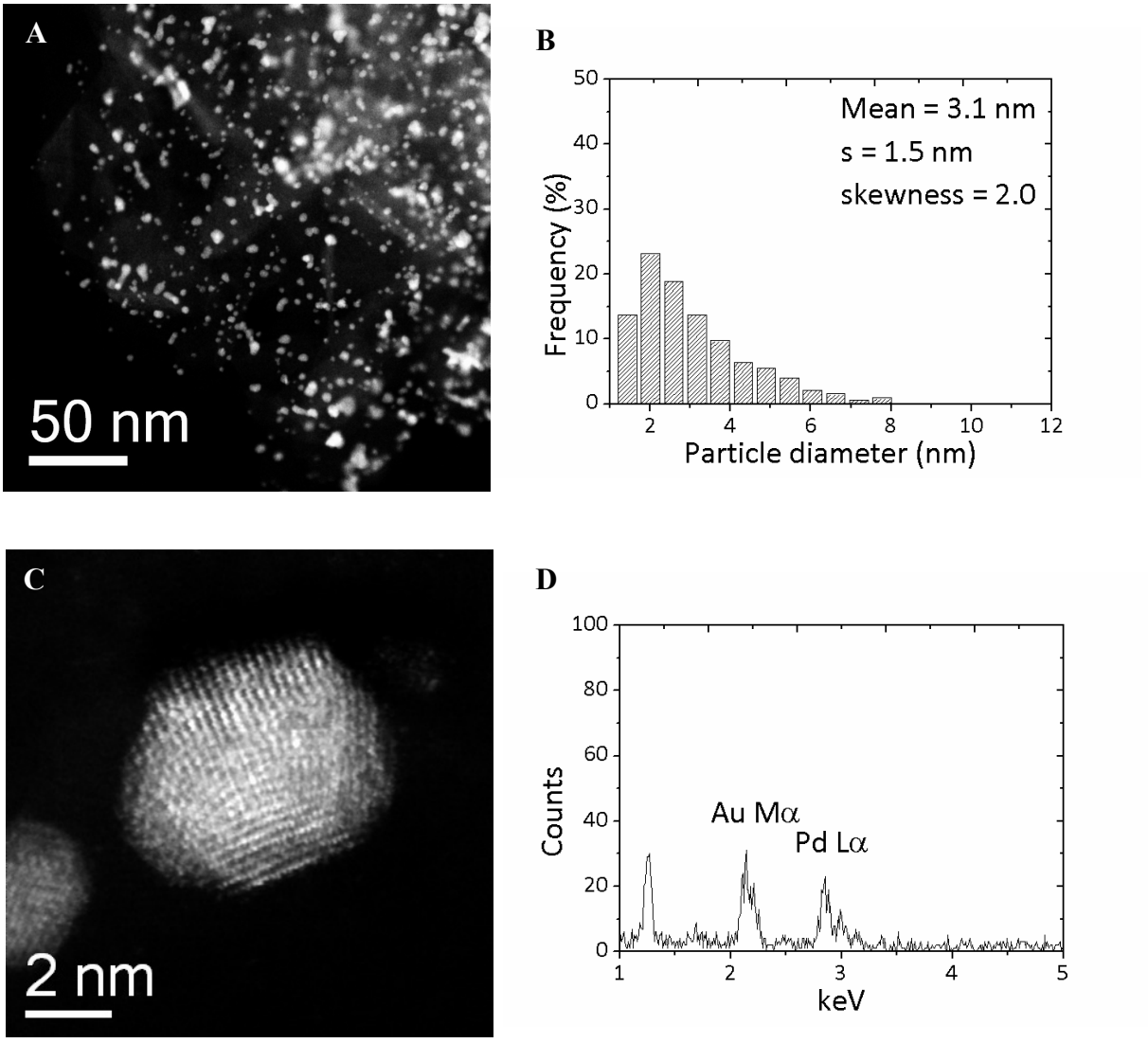

Figure 3.10: (a) STEM-HAADF image and (b) corresponding particle size distribution for 1%AuPd/MgO catalyst prepared by sol immobilisation (c) Atomic resolution HAADF image of a typical individual metal nanoparticle and (d) its corresponding XEDS spectrum confirming that it is an alloy of Au and Pd

3.4- Conclusions

The disproportionation of benzyl alcohol on a 1%AuPd/TiO_2 catalyst was confirmed experimentally in a glass stirred reactor under anaerobic conditions to produce equimolar amounts of benzaldehyde and toluene, which proved that it is the source of toluene. The disproportionation reaction is promoted by increases in O_2 concentration/pressure up to 1 bar, but this promotion effect is reduced by further increases in O_2 pressure. This dependence of the disproportionation reaction on O_2 pressure may imply the existence of two mechanisms of disproportionation- one aerobic and the other anaerobic. Moreover, increasing the temperature promotes the disproportionation and the consequence of toluene formation. However, this study also indicates that the support plays an important role in the formation of products, as it can stop the disproportionation and the formation of toluene, and a consequence of this the selectivity is an increase in aldehyde. The characterisation of the catalysts suggests that the difference in promotional conductance for the disproportionation reaction for these AuPd supported TiO_2 and MgO catalysts is not simply because of any differences in particle size, but it could be related to the redox conductance or surface compositional characteristics of the oxide support.

3.5- References

[1] G.C. G. Cainelli, Chromium Oxidations in Organic Chemistry 1st edition, 1st ed., springer, Berlin, (1984).

[2] R.A. Sheldon, J.K. Kochi, Metal-Catalyzed Oxidations of Organic Compounds, Academic Press, (1981).

[3] J.-E. Baeckvall, Editor, Modern Oxidation Methods, Wiley-VCH Verlag GmbH & Co. KGaA, (2004).

[4] T. Mallat, A. Baiker, Chem. Rev. (Washington, DC, U. S.), 104 (2004) 3037-3058.

[5] P.C. Della, E. Falletta, L. Prati, M. Rossi, Chem. Soc. Rev., 37 (2008) 2077-2095.

[6] A. Corma, H. Garcia, Chem. Soc. Rev., 37 (2008) 2096-2126.

[7] N. Lopez, J.K. Norskov, Surf. Sci., 515 (2002) 175-186.

[8] M.P. Casaletto, A. Longo, A.M. Venezia, A. Martorana, A. Prestianni, Appl. Catal., A, 302 (2006) 309-316.

[9] Z. Zhou, S. Kooi, M. Flytzani-Stephanopoulos, H. Saltsburg, Advanced Functional Materials, 18 (2008) 2801-2807.

[10] A. Abad, P. Concepcion, A. Corma, H. Garcia, Angew. Chem., Int. Ed., 44 (2005) 4066-4069.

[11] D.I. Enache, J.K. Edwards, P. Landon, B. Solsona-Espriu, A.F. Carley, A.A. Herzing, M. Watanabe, C.J. Kiely, D.W. Knight, G.J. Hutchings, Science (Washington, DC, U. S.), 311 (2006) 362-365.

[12] S. Meenakshisundaram, E. Nowicka, P.J. Miedziak, G.L. Brett, R.L. Jenkins, N. Dimitratos, S.H. Taylor, D.W. Knight, D. Bethell, G.J. Hutchings, Faraday Discuss., 145 (2010) 341-356.

[13] L. Kesavan, R. Tiruvalam, R.M.H. Ab, S.M.I. bin, D.I. Enache, R.L. Jenkins, N. Dimitratos, J.A. Lopez-Sanchez, S.H. Taylor, D.W. Knight, C.J. Kiely, G.J. Hutchings, Science (Washington, DC, U. S.), 331 (2011) 195-199.

[14] A. Villa, N. Janjic, P. Spontoni, D. Wang, D.S. Su, L. Prati, Appl. Catal., A, 364 (2009) 221-228.

[15] K. Yamaguchi, N. Mizuno, Angewandte Chemie International Edition, 42 (2002) 1480-1483.

[16] V.R. Choudhary, D.K. Dumbre, Catalysis Communications, 12 (2011) 1351-1356.

[17] D. Ferri, C. Mondelli, F. Krumeich, A. Baiker, J. Phys. Chem. B, 110 (2006) 22982-22986.

[18] E. Cao, M. Sankar, S. Firth, K.F. Lam, D. Bethell, D.K. Knight, G.J. Hutchings, P.F. McMillan, A. Gavriilidis, Chemical Engineering Journal, 167 (2011) 734-743.

[19] D. Enache, D. Knight, G. Hutchings, Catal Lett, 103 (2005) 43-52.

[20] S. Hladiy, M. Starchevskyy, Y. Pazderskyy, L. Yaroslav, in, BASF A.-G., Germany . (2001), pp. 10 pp.

[21] G. Kovtun, T. Kameneva, S. Hladyi, M. Starchevsky, Y. Pazdersky, I. Stolarov, M. Vargaftik, I. Moiseev, Advanced Synthesis & Catalysis, 344 (2002) 957-964.

[22] D.M. Meier, A. Urakawa, A. Baiker, Analyst, 134 (2009) 1779-1780.

[23] M. Sankar, E. Nowicka, R. Tiruvalam, Q. He, S.H. Taylor, C.J. Kiely, D. Bethell, D.W. Knight, G.J. Hutchings, Chemistry – A European Journal, 17 (2011) 6524-6532.

[24] N. Dimitratos, J.A. Lopez-Sanchez, D. Morgan, A.F. Carley, R. Tiruvalam, C.J. Kiely, D. Bethell, G.J. Hutchings, Physical Chemistry Chemical Physics, 11 (2009) 5142-5153.

[25] R.C. Tiruvalam, J.C. Pritchard, N. Dimitratos, J.A. Lopez-Sanchez, J.K. Edwards, A.F. Carley, G.J. Hutchings, C.J. Kiely, Faraday Discuss., 152 (2011) 63-86.

Chapter four:

Synthesis of stable ligand-free gold palladium nanoparticles using a simple excess anion method

4.1- Introduction

Supported gold nanoparticles have been found to be effective in a number of applications, including CO oxidation [1], acetylene hydrochlorination [2], environmental catalysis [3-7], energy processing [8, 9] and chemical synthesis [10-14]. For a number of reactions, it has been reported recently that bimetallic catalysts exhibit a significant increase in activity as compared to their monometallic analogues [15-18]. For instance, supported gold-palladium catalysts have been found to be very effective for aerobic oxidation reactions [15] and for the direct synthesis of hydrogen peroxide [13]. An important aspect of these catalysts is the size of the supported metal nanoparticles: gold nanoparticles are extremely active catalysts, whereas bulk gold is chemically inert. The method of synthesis of these catalysts is therefore crucial [19]. Many methods for preparing highly active heterogeneous gold and gold-alloy catalysts have been reported to date [20], including deposition-precipitation [1, 21]; chemical vapour deposition [22]; ligand-assisted synthesis [23]; sol-immobilisation or colloidal deposition [24, 25]; impregnation [26], and incipient wetness [27]. However, all these methods display one or more of the following disadvantages: (i) a lack of reproducibility of the catalytic activity, (ii) a complex synthesis procedure, (iii) a lack of stability under reaction conditions, or (iv) the synthesis method is applicable/active only for a very specific reaction/support combination. Consequently, considerable effort is still being expended to discover a simple and effective method for the reproducible preparation of highly active and stable gold-based nanoparticulate catalysts [28, 29].

Conventional wet-impregnation (C_{Im}) is the simplest method of making supported Au-Pd nanoparticles based catalysts, but it suffers from the great disadvantage of generating other materials which display only a moderate level of activity, for example the direct synthesis of hydrogen peroxide or the solvent-free oxidation of alcohols [15, 30]. For oxide-supported AuPd alloy nanoparticles, detailed analysis of the material by aberration corrected scanning transmission electron microscopy indicates that the bimetallic nanoparticles comprised an Au-rich core and Pd-rich shell, with particle sizes typically ranging from 1 to 10 nm, together with occasional very large particles (>>10nm); also, the smaller particles are the most catalytically active [15, 31]. In an attempt to eliminate the catalytically inactive larger particles many more sophisticated preparation methods have been reported in the literature. One such method is sol immobilisation (S_{Im}) [24, 25] whereby colloidal nanoalloys with a narrow metal alloy particle-size distribution are prepared using stabiliser ligands and a reducing agent; the colloidal particles being subsequently immobilised onto a metal oxide support. Although this technique results in catalysts having metal particles in the 2-6 nm range which have a high catalytic activity, this synthetic method is not as simple and versatile as the impregnation technique [32]. Another practical limitation of the sol-immobilisation methodology is that it can only be used to prepare Au-Pd catalysts on a very limited number of supports, such as activated carbon and TiO_2, because the efficiency of deposition or immobilisation of these preformed colloids is highly dependent on the iso-electric point (IEP) of the support [32]. Furthermore, S_{Im} requires the use of polymeric stabiliser ligands and organic reducing agents both of which can remain on the surface of the nanoparticles and are potentially deleterious for catalysis

[24, 25, 33]. In addition to these disadvantages, the sol-immobilisation method cannot easily be scaled-up for use on an industrial scale. Very recently, a supra-molecular route has been reported for the synthesis of core-shell nanoparticle catalysts. It is based on an anion coordination protocol by binding the shell metal to the surface of the primary metal core before reduction, but once again this methodology uses a complicated synthesis procedure for the stabiliser ligand [23]. In this study these problems have been addressed and a catalyst synthesis method has been defined, which is as versatile and simple as the impregnation method, but results in catalysts as active as those made *via* sol-immobilisation. Here in this study, it is apparent that by adding an excess of anionic ligands of the metal precursors during an impregnation type catalyst synthesis, and employing a subsequent high-temperature heat treatment in a reducing atmosphere, nanoalloy particles with a very tight particle size and compositional distribution are obtained. These are found to be exceptionally active and stable as catalysts for solvent-free aerobic oxidation of benzyl alcohol, as shown in this study, and also for the direct synthesis of hydrogen peroxide [34].

4.2- Experimental

4.2.1- Catalyst preparation

The catalysts 0.5wt%Au+0.5wt%Pd/TiO_2 were prepared using three different preparation methods in this study using the sol-immobilisation S_{Im} method as described in chapter 2 (section 2.2.1); conventional impregnation C_{Im} method as described in chapter 2 (section 2.2.2), and modified impregnation M_{Im} method as described in chapter 2 (section 2.2.3).

4.2.2- Catalyst testing

The catalysts were evaluated for solvent-free aerobic oxidation of benzyl alcohol in a 50 mL glass stirred multi-pot (Radleys carousel) reactor system. Details of the reactor set-up and reaction procedure are presented in chapter 2 (section 2.3.1), and the samples' reaction analysis and quantification procedure is also presented in chapter 2 (section 2.4.1.4). The catalysts were also evaluated for the direct synthesis of hydrogen peroxide. Details of the reactor set-up and the reaction procedure are presented in chapter 2 (section 2.3.3).

4.2.2- Catalyst characterisation

The catalysts were characterised using scanning transmission electron microscopy (STEM), as described in chapter 2 (section 2.5.3); X-ray photoelectron spectroscopy (XPS) as described in chapter 2 (section 2.5.2), and powder X-ray diffraction (XRD) as described in chapter 2 (section 2.5.1).

4.3- Results and discussion

4.3.1- Modified impregnation (M_{Im}) strategy

The results of the interaction between chloride and gold nano-particles generally have a negative effect on catalytic activity as suggesting that the presence of chloride ion enhances mobility and agglomeration of gold species during thermal treatment and remain one of the most important aspects of the wet chemical synthesis for gold-based catalysts [5, 35-38]. Many previous reports have correlated the decrease in the catalytic activity of supported gold-based catalysts with the presence of chloride ions in the catalyst. Hence, many studies have been directed at removing these chloride ions, with the aim of making the catalysts more active [39]. Contrary to this, some previous attempts at using excess chloride ions to reduce the particle size of the supported noble-metal nanoparticles based catalysts have also been reported. However, this method has been limited to the incipient wetness technique and efforts to use excess chloride ions in other methods have proved to be unsuccessful [27, 40].

Against this background, this chapter will present a modified impregnation method denoted as M_{Im} whereby an excess of Cl^- ions are utilised to prepare highly active and stable supported gold-palladium nanoparticle based catalysts while synthesising the bimetallic catalysts from their precursors ($HAuCl_4$ and $PdCl_2$). Then the excess ions of Cl^- were introduced by adding the requisite amount of aqueous HCl into the aqueous wet-impregnation medium. It is considered that the abundance of Cl^- ions present in the aqueous medium facilitates the formation of the $AuCl_4^-$ species for the gold precursor and, most importantly, the $PdCl_4^{2-}$ species for the palladium precursor. It is important to note that the $PdCl_4^{2-}$ species is soluble in water, whereas $PdCl_2$ is sparingly soluble in water. A study by Adhikari [41] for the sorption tests with various metal were conducted in hydrochloric acid medium, it is important to note the most stable forms of the metals Au(III) and Pd(II) the species distribution in acidic chloride media are shown in **Figure 4.1**. Illustrating that Au(III) and Pd(II) exist mostly as anionic chloro-complexes such as $AuCl_4^-$ and $PdCl_4^{2-}$ respectively in the strong acidic conditions of the experiment. It is also proposed that the co-existence of these two species in the aqueous medium facilitates the formation of a more homogeneous mixture of the two metal ions, thereby enabling improved dispersion during the impregnation stage. In the absence of an excess of chloride ions, (*i.e.* the C_{Im} route) a $[Au(OH)_x(Cl)_{4-x}]^-$ gold precursor forms (where x is always >1) and the palladium precursor tends to form insoluble salts. The presence of this combination of species poses a problem for the conventional C_{Im} method, and leads to ineffective adsorption onto the support, which can result in the formation of some very big metallic particles, which are essentially inactive as catalysts.

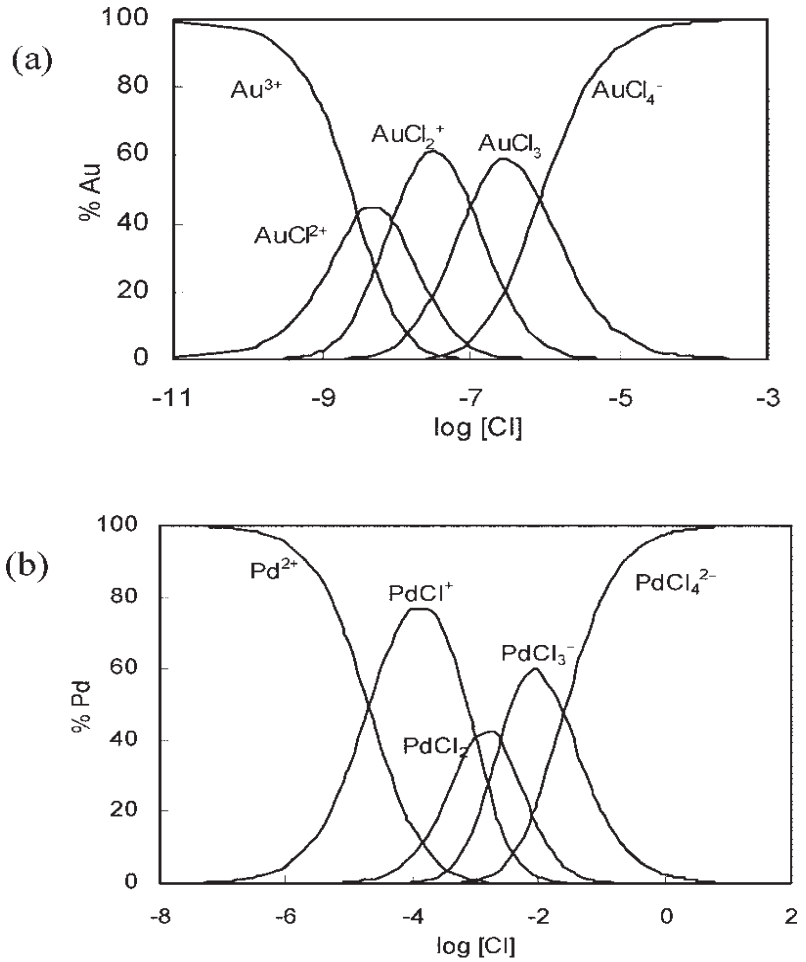

Figure 4.1: Chemical speciation diagrams of Au(III) and Pd(II) ions with respect to chloride concentration [41]

Crucially, it should be noted that the as-synthesised and dried material prepared by the M_{Im} route then needs to be heated at 400 °C in a stream of 5% H_2 in Ar in order to observe the best catalytic activity. This gas-phase reduction step serves to substantially decrease the number of chloride ions present in the final catalyst.

4.3.2- Comparison of the catalytic properties of supported AuPd nanoparticles prepared by M_{Im}, S_{Im} and C_{Im}

To demonstrate the efficacy of this new M_{Im} preparation method, the catalysts prepared- M_{Im}, S_{Im} and C_{Im}- were tested for the selective aerobic oxidation of alcohols at 120 °C, and it is well known as in chapter three that supported gold-palladium nanoparticles are very active in this reaction [15]. For a judicious comparison, catalysts were prepared with identical metal content (0.5wt%Au and 0.5wt%Pd) on the same support TiO_2. The results are presented in **Table 4.1** where the molar conversions for these reactions are presented along with the corresponding selectivity for benzaldehyde (main-product) and toluene (by-product). There are slight differences in the catalytic activities of the catalysts prepared by the three different methodologies and these followed the order: $M_{Im} > S_{Im} > C_{Im.}$ The activity of M_{Im} was slightly higher compared to the S_{Im} catalysts, but both are equally active (within experimental error-limits). In addition to that, S_{Im} has given the lowest selectivity to benzaldehyde, which could suggest that the S_{Im} catalyst is active for the competing disproportionation reaction as explained in previous chapter, which toluene disturbs benzaldehyde selectivity by resulting in the formation of an equimolar mixture of toluene and benzaldehyde [42, 43]. This comparability of activity demonstrates the superiority of the current modified impregnation methodology over the other methodologies, especially the S_{Im} method, which has been reported to be exceptionally active [44]. The enhanced catalytic activity of the M_{Im} catalyst is may be due to an optimised nanostructure compared to the corresponding S_{Im} and C_{Im} catalysts which will be discussed in detail later in the chapter.

Table 4.1: Solvent-less aerobic oxidation of benzyl alcohol using 0.5%Au 0.5%Pd/TiO_2 prepared by three different methods [a]

Preparation Method	Time (h)	Conversion (%)	Selectivity (%)	
			Benzaldehyde	Toluene
Modified Impregnation (M_{Im})	20	27	78	20.3
	30	40	74.7	24
	60	55	74	24.4
Sol Immobilization (S_{Im})	20	22	66.6	32
	30	36	64.5	34
	60	53	66.1	31.6
Conventional Impregnation (C_{Im})	20	10	81	16.9
	30	22.5	81	16
	60	45	80.8	16.8

[a] Reaction conditions: 0.02g catalyst, 1 bar of O_2, 2g benzyl alcohol, 120 °C and stirring at 1000 rpm

To demonstrate the efficacy of the new M_{Im} preparation method, James Pritchard from the *School of Chemistry, Cardiff University* has studied direct synthesis of hydrogen peroxide over the M_{Im} catalyst, and it has been found that the 0.5%Au-0.5%Pd/TiO_2 M_{Im} catalyst was nearly four times more effective than the 0.5%Au-0.5%Pd/TiO_2 C_{Im} catalyst, with an activity of 99 mol H_2O_2 kg-cat^{-1} h^{-1} [34]. This catalyst is considerably more active than the previous best and stable 2.5%Au-2.5%Pd/TiO_2 prepared by the C_{Im} calcined catalyst (64 mol H_2O_2 kg-cat^{-1} h^{-1}), even though the new M_{Im} catalyst contains five times less metal [45]. The 0.5%Au-0.5%Pd/TiO_2 C_{Im} calcined catalyst gives less

activity (23 mol H_2O_2 kg-cat^{-1} h^{-1}) compared to the material prepared by the sol immobilisation method (32 mol H_2O_2 kg-cat^{-1} h^{-1}); moreover, the S_{Im} catalyst is found to lose activity upon reuse, whereas the C_{Im} catalyst is stable for several reuse cycles, as will be shown later on in this study [34, 46].

The comparison between M_{Im} and C_{Im} catalysts for benzyl alcohol oxidation and H_2O_2 synthesis produced results (as shown in **Table 4.2**), which indicate agreement for both evaluated benzyl alcohol and direct synthesis of hydrogen peroxide. Reducing the catalyst under 5% H_2/Ar leads to increasing the activity and stability of both catalysts. Dried only catalysts are inactive for benzyl alcohol oxidation and not stable for H_2O_2 synthesis, whereas the calcined catalysts are less active than reduced catalysts for both benzyl alcohol and for H_2O_2 synthesis [34].

Table 4.2: Comparison of M_{Im} and C_{Im} catalysts for benzyl alcohol oxidation and H_2O_2 synthesis: The effect of preparation methods and heat treatment [a]

Catalyst	Preparation method & Heat Treatment	Benzyl alcohol Conversion (%)	H_2O_2 Productivity (molH_2O_2/kg-cat/h)
0.5%Au+0.5%Pd / TiO_2	C_{Im} - Dried at 110 °C	10	118
	C_{Im} - Calcined at 400 °C	45	23
	C_{Im} - Reduced at 400 °C	54	68
	M_{Im} - Dried at 95 °C	8	96
	M_{Im} - Calcined at 400 °C	27.5	36
	M_{Im} - Reduced at 400 °C	55	99

[a] Reaction conditions of H_2O_2: 5% H_2/CO_2 and 25% O_2/CO_2, 50% H_2/O_2 at 3.7 MPa, MeOH (5.6g), H_2O (2.9g), catalyst (0.01g), 2 °C, 1200 rpm, 30 min. Reaction conditions of benzyl alcohol: 0.02g catalyst, 1 bar of O_2, 2g benzyl alcohol, 120 °C, stirring at 1000 rpm and 1hr of reaction time

Qian He, from the *Department of Materials Science and Engineering, Lehigh University, USA,* examined the catalysts using high angle annular dark field (HAADF) imaging and STEM-XEDS studies. He compared the morphologies of 0.5wt%Au+0.5wt%Pd/TiO_2 catalysts prepared by the C_{Im} and M_{Im} (0.58 M HCl) preparation routes under three distinct conditions *viz,* dried-only; calcined at 400 °C; and reduced in 5 %H_2/Ar. Representative data for these C_{Im} and M_{Im} samples are shown in **Figures 4.2** and **4.3** respectively. The dried-only C_{Im} (**Figures 4.2 (a, b)**) and dried-only M_{Im} (**Figures 4.3 (a, b)**) materials show rather similar morphologies with numerous 1-2 nm Pd-rich clusters and atomically dispersed species, as well as occasional large (μm-scale) gold-rich particles which originate from a poor dispersion of the gold component. After calcination in air at 400 °C (C_{Im} – **Figures 4.2 (c, d)**; M_{Im} – **Figures 4.3 (c, d)**) some sintering occurs and both materials show 5-10 nm particles, which have a distinct Au-rich core and Pd-rich shell morphology. In addition, there are still numerous Pd-rich clusters and atomically dispersed species remaining on the TiO_2 supports. If the C_{Im} and M_{Im} dried-only materials are subjected to a 400 °C reducing (5 %H_2/Ar) treatment instead of calcination (C_{Im} – **Figures 4.2 (e, f)**; M_{Im} – **Figures 4.3 (e, f)**) then all the clusters and atomically dispersed species are now absent and have been efficiently subsumed into the larger random alloy particles. However, the reduced C_{Im} and M_{Im} materials do show a distinct difference in AuPd particle size distribution, with mean values of 4.7 and 2.9 nm respectively. All these catalysts, C_{Im} calcined, C_{Im} reduced, M_{Im} calcined and M_{Im} reduced, were evaluated for benzyl alcohol oxidation and hydrogen peroxide synthesis; the results are presented in **Table 4.2**. For both C_{Im} and M_{Im} catalysts, the reduced materials have different catalytic activity compared to

their calcined analogues: C_{Im} (calcined) and C_{Im} (reduced) catalysts have activities of 45% and 54% respectively; M_{Im} (calcined) and M_{Im} (reduced) catalysts have activities 27.5% and 55% respectively. The difference in catalytic activity between the M_{Im} and C_{Im} catalysts could be because of the "excess" anion effect where the difference between "calcined" and "reduced" catalysts within the set could be because of the structural differences of the nanoalloys. This suggests that the random alloy structures are catalytically more active compared to the core-shell morphologies [46].

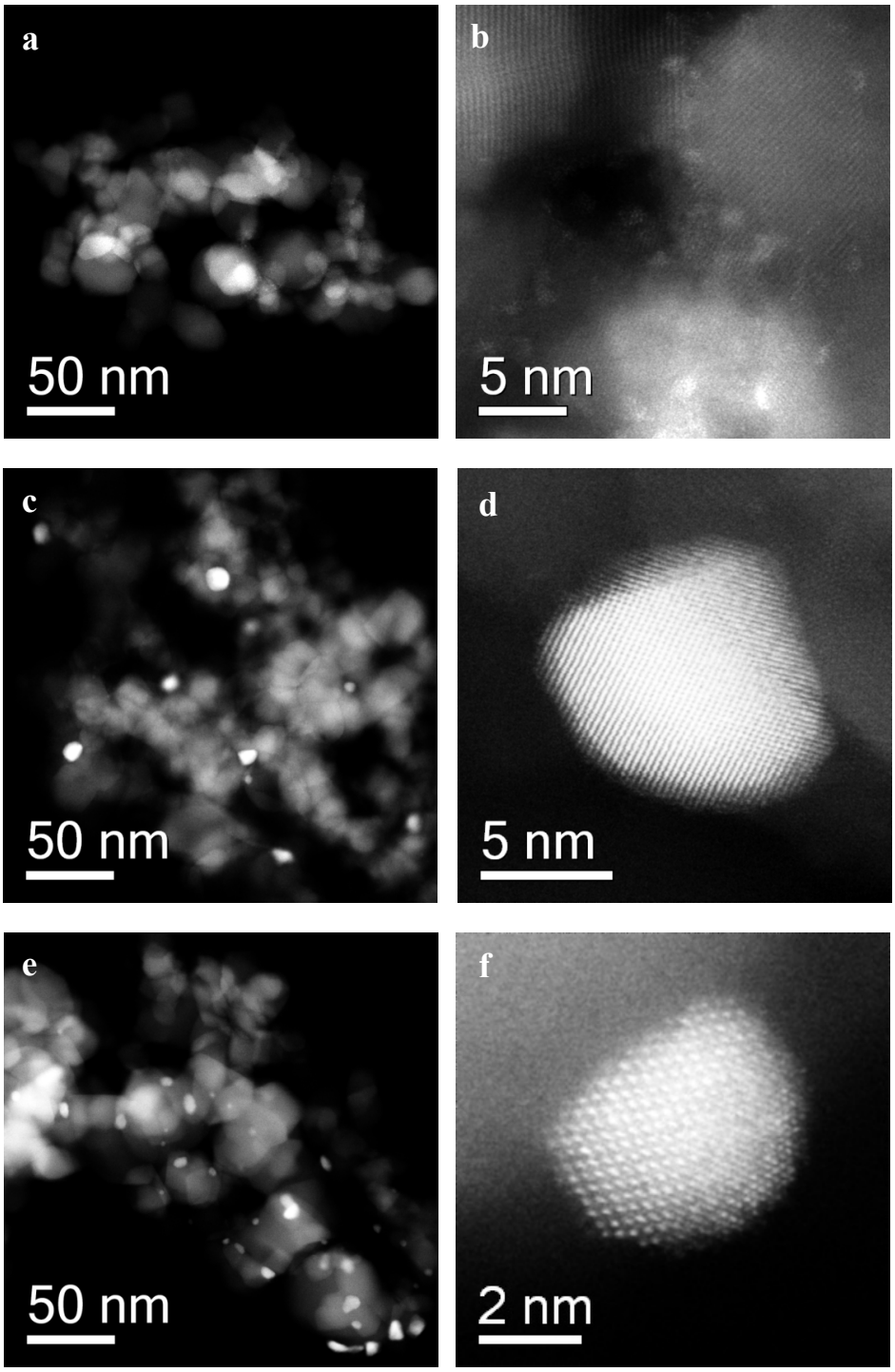

Figure 4.2: HAADF-STEM images of 0.5%Au+0.5%Pd/TiO_2 catalysts prepared by the C_{Im} method. (a, b) dried only at 120 °C; (c, d) calcined in air at 400 °C; (e, f) reduced in 5%H_2/Ar at 400 °C

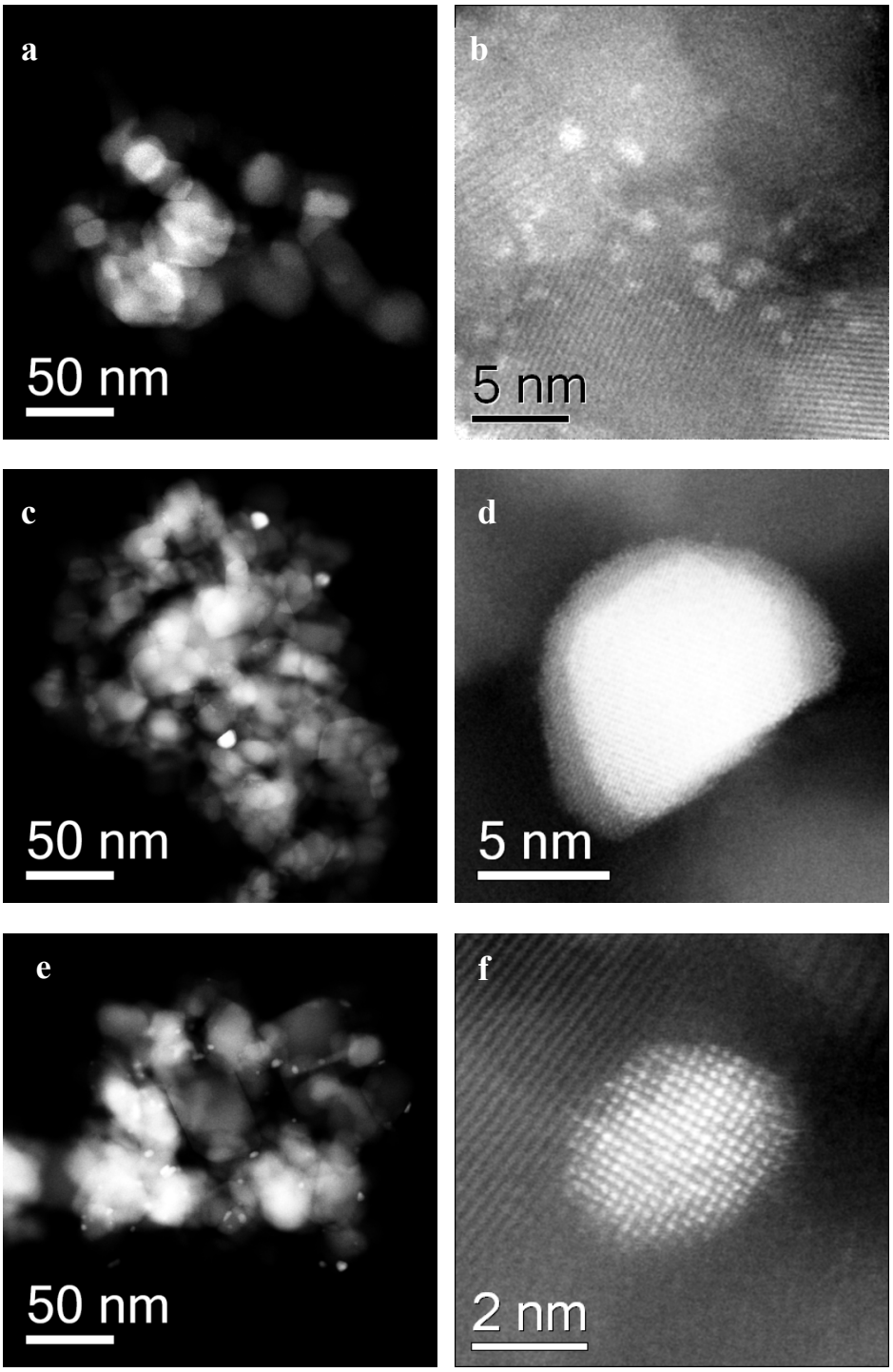

Figure 4.3: HAADF images of 0.5%Au + 0.5%Pd/TiO_2 catalysts prepared by the M_{Im} method with 0.58 M HCl. (a, b) dried only at 120 °C; (c, d) calcined in air at 400 °C; (e, f) reduced in 5%H_2/Ar at 400 °C

4.3.3- Effect of chloride ion concentration on catalytic activity

The standard 0.5wt%Au+0.5wt%Pd/TiO_2 M_{Im} catalyst reported above was prepared in an aqueous medium containing an "excess of chloride ions" generated by the addition of 0.58M HCl to the catalyst synthesis medium during the impregnation stage. To optimise the amount of "excess" chloride ions required to obtain the most active catalyst, a systematic series of samples were prepared in which a range of palladium stock solution in HCl *(i.e.* 0.1M, 0.58M, 1M and 2M) were added to the catalyst synthesis medium. These catalysts were then tested for the oxidation of benzyl alcohol, and the results are presented in **Figure 4.4**. It is apparent that increasing the chloride ion concentration increases the activity of the catalyst. However, although the catalysts prepared with 1M and 2M HCl solutions show a higher activity, they are not stable for reuse, whereas the 'standard M_{Im}' catalyst prepared with a 0.58 M HCl solution is stable for reuse as will be seen in the reusability effect, which will be presented later.

Moreover, with the synthesis of hydrogen peroxide, it has been found to show compatibility in the results to benzyl alcohol oxidation when the excess chloride ion is increased, which leads to an increase in the activity of the catalyst. However, although the catalysts prepared with 1M and 2M HCl solutions give a higher H_2O_2 productivity, they are also, as with benzyl alcohol, not stable for reuse, as will be shown in the reusability study [34].

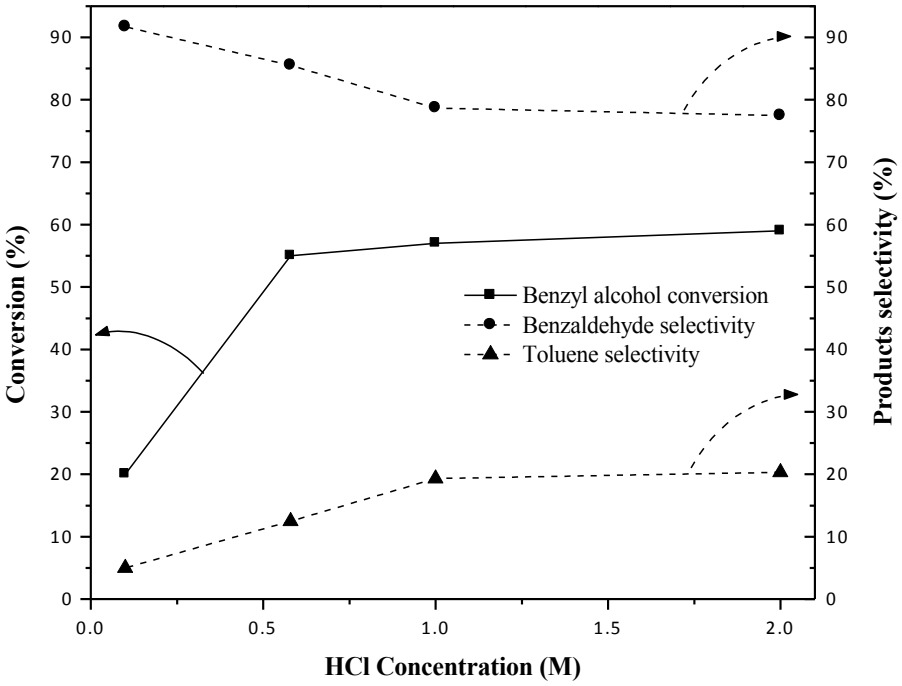

Figure 4.4: Effect of HCl amount, during catalyst preparation, on the catalytic performance of 0.5wt%Au+0.5wt%Pd/TiO_2 M_{Im}. Reaction conditions: 0.02g catalyst, 1 bar of O_2, 2g benzyl alcohol, 120 °C, stirring at 1000 rpm and 1hr of reaction time

It is possible that the role of the excess Cl^- is to permit the formation of the most effective $[AuCl_4]^-$ and $[PdCl_4]^{2-}$ precursor species in the aqueous medium. However, it is also plausible that the presence of excess Cl^- could improve the dispersion of the metal ions during the adsorption stage through competitive adsorption over the support. A similar effect has been observed during the preparation of mono-metallic gold catalysts that improved incipient wetness method, but here it is demonstrated that this "excess-anion" effect is very effective for the bimetallic gold-palladium catalysts [27].

Detailed high angle annular dark field (HAADF) imaging and STEM-XEDS studies have been carried out on a series of 0.5wt%Au+0.5wt%Pd/TiO_2 catalysts prepared using different [Cl] concentrations (namely (i) 0M HCl (*i.e.* C_{Im}), (ii) M_{Im}-0.58 M HCl and (iii) M_{Im}-2.0 M HCl). The results of these analyses are shown in **Figures 4.5** and **4.6**. All three samples in the dried-only state look very similar in the HAADF-STEM mode (**Figures 4.5 (a), (b)** and **(c)**), displaying 1-2 nm clusters and atomically dispersed species. After reduction in 5%H_2/Ar, all three materials show larger AuPd alloy particles (**Figures 4.5 (d, e, f)**) and a complete absence of clusters. Analysis of the particle size distributions from such micrographs (**Figures 4.6 (a, c, e)**) show that the mean particle size and spread of particle size decreases with increasing [Cl] concentrations (C_{Im} – mean 4.7 nm ; M_{Im} -0.58 M HCl – mean 2.9 nm; M_{Im} – 2.0M HCl – mean 2.6 nm). Representative images and XEDS spectra from individual particles from these three specimens are shown in **Figures 4.5** (C_{Im} - **Figures 4.5 (g, j)**; M_{Im} - 0.58 M HCl – **Figures 4.5 (h, k)**; M_{Im} – 2.0M HCl – **Figures 4.5 (i, l)**. All the particles are largely random alloys in nature, but they do show a systematic change in Pd:Au ratio with varying [Cl] concentration. A more statistically relevant analysis of composition with particle size for these three samples is presented in **Figures 4.6 (b, d** and **f)**. It is clear that increasing the amount of excess Cl^- used in the M_{Im} preparation causes a definite increase in Au content within the AuPd alloy particle. This compositional variation trend can be rationalised by analysing these samples using backscattered electron (BSE) imaging in an SEM to monitor the population of the larger scale (200 nm to 2.0 mm) Au particles (see **Figure 4.7**). It is clear that the C_{Im} material contains a significant population of poorly dispersed Au, but the effect of the excess Cl^-

in the M_{Im} materials is to progressively disperse (*i.e.,* eventually eliminate) these large Au species. As this Au is no longer associated with large inactive particles, it can be incorporated into the nm scale AuPd alloy particles, thereby increasing their mean gold content. Increasing the Au content in the particle improves the benzyl alcohol activity and H_2O_2 productivity, but simultaneously decreases the catalyst's reusability. The M_{Im} (2M HCl) catalyst showed in the study a decrease in productivity upon reuse. At this stage, the reason for this observed instability of the M_{Im} 2M catalyst is unknown, but detailed characterisations of these fresh and reused materials are currently underway. However, this implies that the intermediate (0.58 M HCl) M_{Im} sample has an AuPd particle composition that is a good compromise for yielding a catalyst that simultaneously has a reasonable benzyl alcohol and H_2O_2 productivity and effective reusability characteristics.

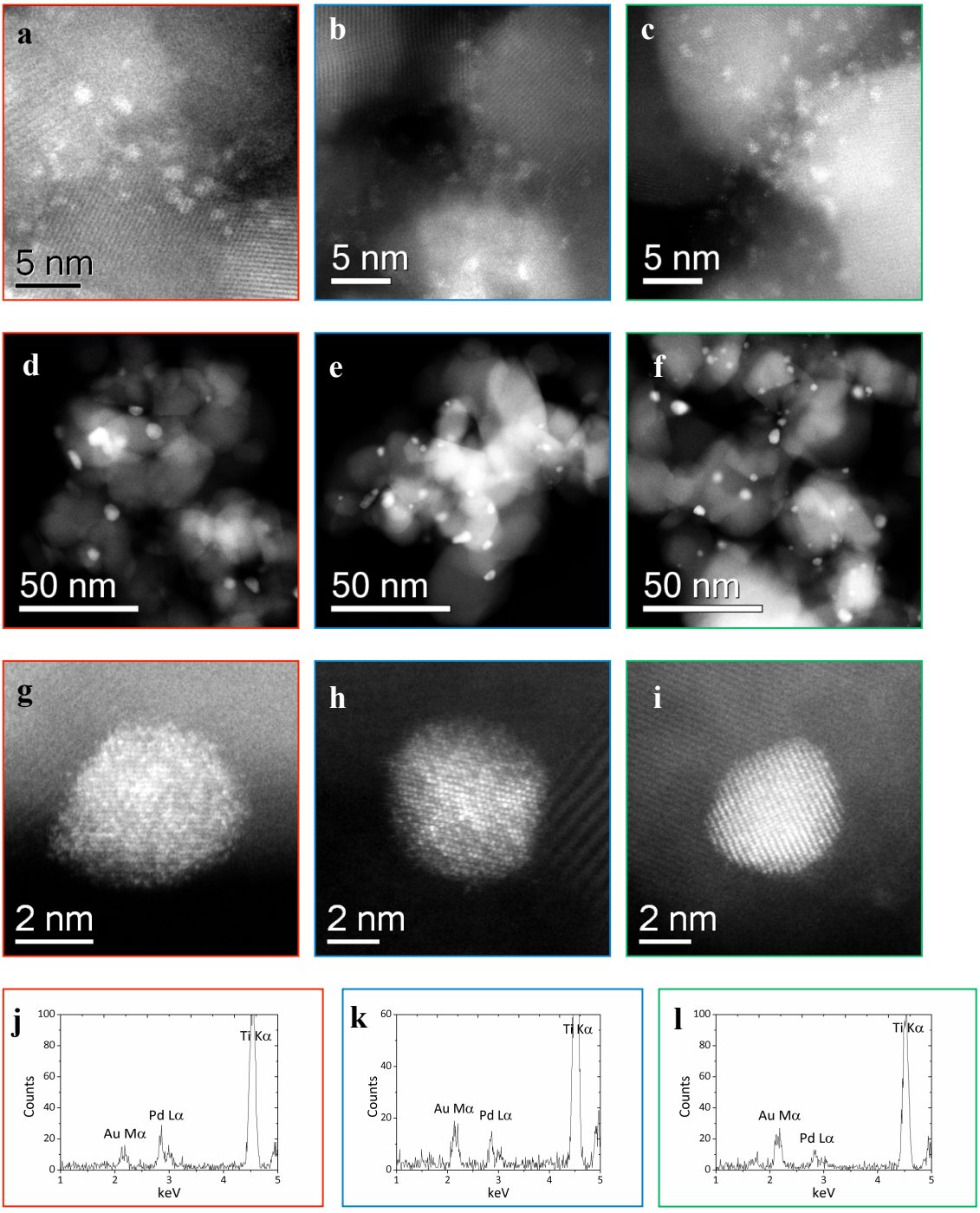

Figure 4.5: 0.5%Au+0.5%Pd/TiO_2 samples prepared with no HCl (*i.e.* C_{Im}) – red column, 0.58 M HCl (M_{Im}) – blue column and 2.0M HCl (M_{Im}) – green column: (a, b, c) HAADF images of dried only samples; (d, e, f, g, h, i) HAADF images of samples reduced in 5%H_2/Ar at 400 °C (j, k, l) XEDS spectra from the particles shown in (g), (h) and (i) respectively in which a systematic increase in Au content correlates with increasing HCl concentration used in the preparation

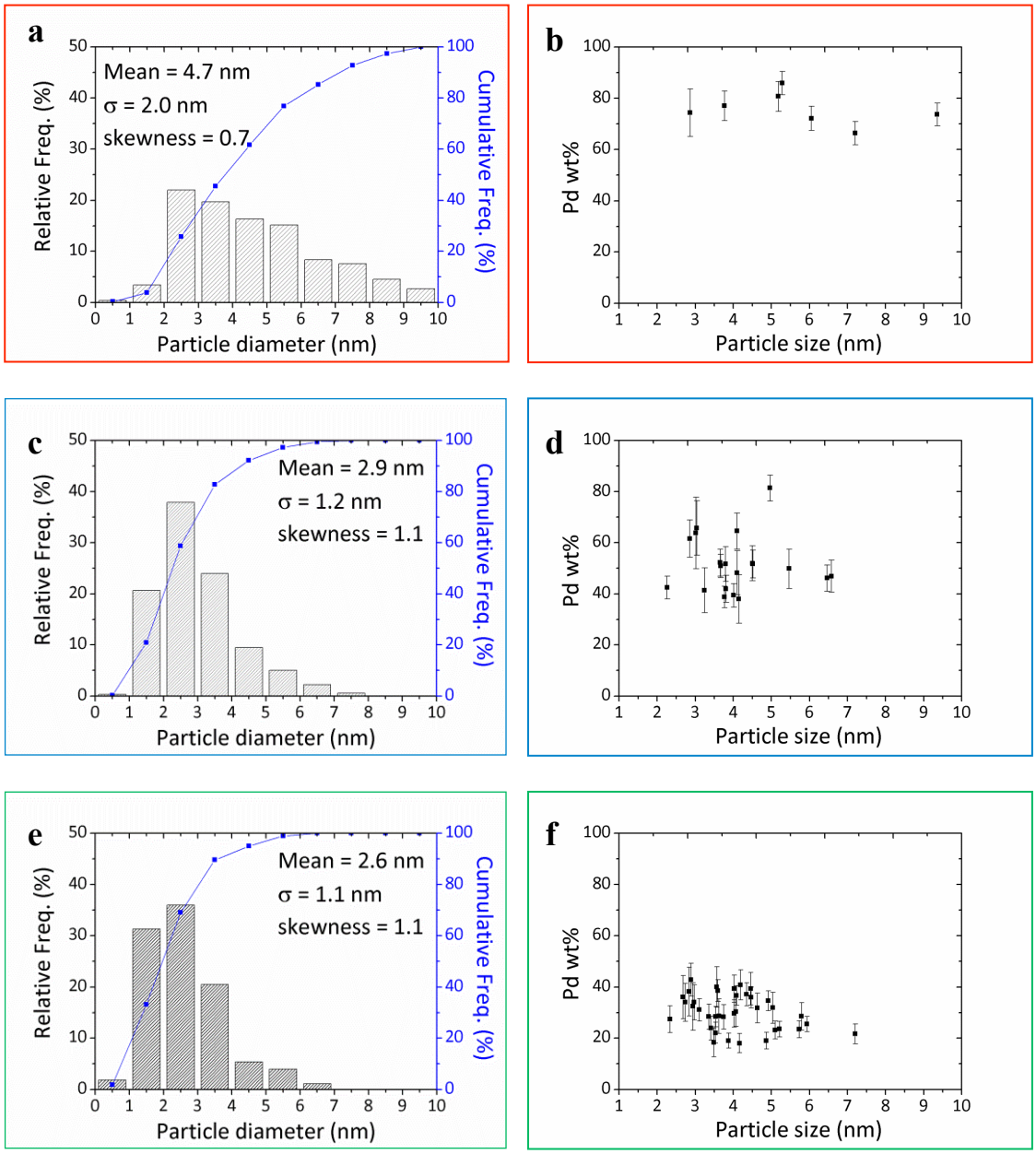

Figure 4.6: Particle size distributions for 0.5%Au+0.5%Pd/TiO_2 samples prepared with (a) no HCl (*i.e.* C_{Im}), (c) 0.58 M HCl (M_{Im}) and (e) 2.0M HCl (M_{Im}); Particle size/composition diagrams for AuPd/TiO_2 samples prepared with (b) no HCl (*i.e.* C_{Im}), (d) 0.58 M HCl (M_{Im}) and (f) 2.0M HCl (M_{Im}). All samples have been reduced in 5%H_2/Ar at 400 °C. Note that increasing the HCl concentration in the preparation causes a progressive increase in the gold content within the alloy particles

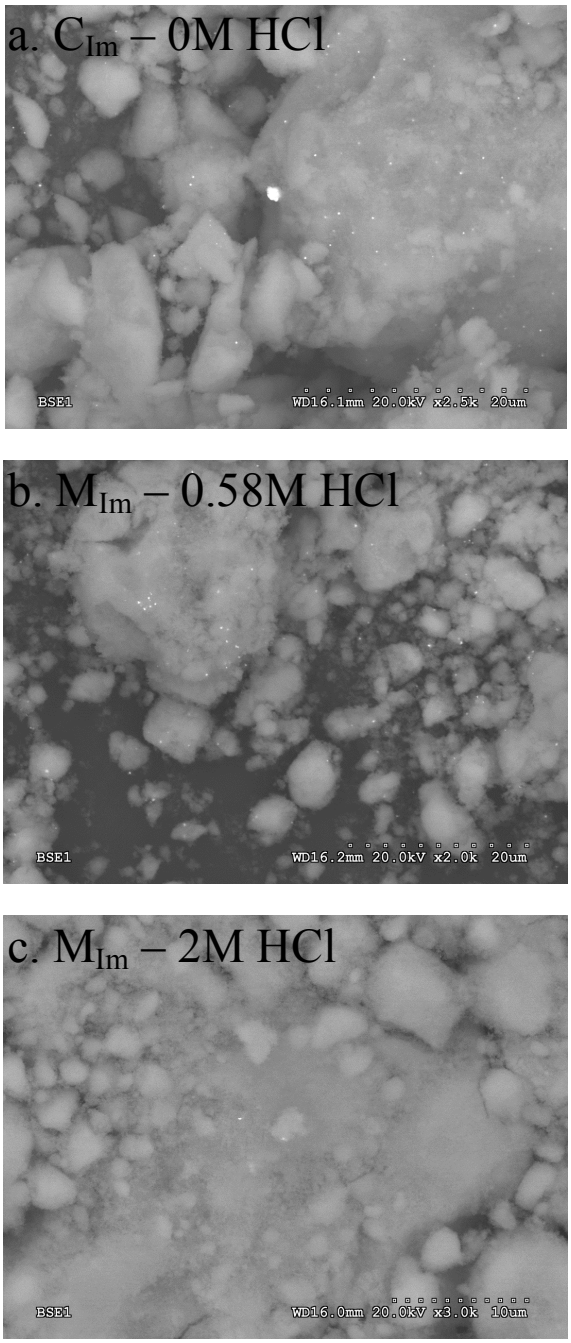

Figure 4.7: Backscattered electron (BSE) images taken in a Hitachi 4300LV SEM of 0.5%Au+0.5%Pd/TiO_2 catalysts prepared by (a) the C_{Im} method, (b) the M_{Im} method (using 0.58M HCl) and (c) the M_{Im} method (using 2M HCl). Note that the number of large (200nm – 2mm) gold-rich particles decreases with the addition of increasing amounts of HCl, from (a) to (c), which means that this Au becomes available for incorporation in the active AuPd nanoparticles in the M_{Im} sample

4.3.4- Effect of different palladium precursors

To investigate the hypothesis that the formation of a palladate precursor is essential to enable the most active catalyst to be formed, a range of palladium precursors were tried for the synthesis of 0.5wt%Au+0.5wt%Pd/TiO_2 catalysts, and the results are presented in **Table 4.3**. A catalyst prepared by dissolving Na_2PdCl_4 in water gave a lower benzyl alcohol oxidation activity (34.5%) to that of the standard M_{Im} catalyst, which gave 55%. The higher activity of the standard M_{Im} catalyst can be attributed to the effect of the additional chloride ions present in the aqueous medium as dilute HCl, which were not present for the catalyst prepared using Na_2PdCl_4. Another 0.5wt%Au+0.5wt%Pd/TiO_2 catalyst was also prepared using $Pd(NO_3)_2$ as palladium precursors, and an "excess" of Cl^- anions was provided by adding a 0.58M aqueous HCl solution. The activity of the catalyst was 16.6% which showed lower activity compared to the catalyst prepared using Na_2PdCl_4 for benzyl alcohol oxidation. Moreover, a catalyst was also prepared using $AuBr_3$ and $PdBr_2$ as the metal precursors; an "excess" of Br^- anions was provided by adding a 0.58M aqueous HBr solution. The activity of the Br^- excess sample was 25% which is inferior to that found for materials prepared with excess Cl^- anions. It therefore appears that this "excess anion" strategy is only effective when using chloride ions and palladium chloride as palladium precursors.

Table 4.3: Effect on benzyl alcohol oxidation using different palladium precursors in the synthesis of the 0.5%Au + 0.5%Pd/TiO_2 catalyst [a]

Palladium precursor	Conversion (%)	Selectivity (%)	
		Benzaldehyde	Toluene
$PdCl_2$	55	74	24.4
Na_2PdCl_4	34.5	83.8	14.4
$Pd(NO_3)_2$	16.6	82.4	16
$PdBr_2$*	25	65	34.7

[a] Reaction conditions: 0.02g catalyst, 1 bar of O_2, 2g benzyl alcohol, 120 °C, stirring at 1000 rpm and 1hr of reaction time

* Gold precursor is $AuBr_3$ in the presence of 0.58M of HBr

4.3.5- Effect of materials prepared using reagents other than HCl

To further investigate the role of the chloride ions, 0.58 M aqueous sodium chloride solution was used during the M_{Im} catalyst synthesis in place of the aqueous HCl. Here, NaCl provided the chloride ions but in a neutral pH environment. The catalyst prepared in presence of NaCl was found to be slightly less active compared to that prepared by the standard M_{Im} catalyst prepared in 0.58M HCl, displaying an activity of 41.5%. Two other catalysts were also prepared in the presence of 0.58M HNO_3 and 0.29M H_2SO_4 instead of 0.58M HCl in order to study the role of the pH of the synthesis medium in the resultant catalytic activity. These two catalysts were found to have the lowest activity amongst all the catalysts screened, having an activity of only 9% and 5% respectively, as shown in **Table 4.4**. This demonstrates that an excess of chloride ions is associated

with the higher activity displayed by the catalysts prepared by M_{Im}. But unfortunately, the catalyst prepared using NaCl derived material deactivated upon reuse, which will be studied later on, even after the H_2 reduction treatment at 400 °C, which afforded stability to the M_{Im} catalyst prepared using HCl.

Table 4.4: Effect of different reagent and anion on benzyl alcohol oxidation during the synthesis of the 0.5%Au + 0.5%Pd/TiO_2 catalyst [a]

Palladium precursor	Conversion (%)	Selectivity (%)	
		Benzaldehyde	Toluene
$PdCl_2$	55	74	24.4
NaCl	41.5	88.5	10.3
HNO_3	9	82.3	16.1
H_2SO_4	4	88.1	10

[a] Reaction conditions: 0.02g catalyst, 1 bar of O_2, 2g benzyl alcohol, 120 °C, stirring at 1000 rpm and 1hr of reaction time

For further investigation into the role of the chloride ions, the catalyst prepared using NaCl was also evaluated for the direct synthesis of hydrogen peroxide. It was found to be even better than the standard M_{Im} catalyst prepared using 0.58M HCl, displaying a productivity of 154 mol H_2O_2 kg-cat^{-1} h^{-1}. Unfortunately, the catalyst prepared using NaCl, as with benzyl alcohol, was not reusable. The catalyst prepared using H_2SO_4 was also synthesised in the presence of 0.29M H_2SO_4 as equal to the pH of 0.58M HCl to study the role of the pH of the synthesis medium in the resultant catalytic activity. This catalyst was found to be comparatively inactive for direct synthesis of hydrogen peroxide, having an activity of only 16 mol H_2O_2 kg-cat^{-1} h^{-1} [34].

The modified impregnation samples prepared using NaCl and H_2SO_4 in place of HCl were also examined by STEM. These two samples, designated M_{Im}-NaCl and M_{Im}-H_2SO_4 respectively, were studied in the unused state after having been reduced at 400 °C in H_2/Ar. Representative HAADF images of the M_{Im}-NaCl and M_{Im}-H_2SO_4 samples (**Figures 4.8 (a)** and **(b)** respectively) show them to have very similar 2-6 nm particle size distributions. **Figure 4.8** shows representative atomic resolution HAADF images of some small (2 nm) and large (5 nm) particles along with their corresponding XEDS spectra for the M_{Im}-NaCl sample. It is clear that the metal particles in M_{Im}-NaCl are all homogeneous Au-Pd alloys, which is a characteristic that it has in common with the M_{Im}-HCl derived sample. This is consistent with the fact that both these samples show good catalytic activity. By way of contrast, similar HAADF images and XEDS spectra of small (2 nm) and larger (6 nm) particles from the M_{Im}-H_2SO_4 sample are presented in **Figure 4.10**. It is clear that the metal particles in this case are comprised almost entirely of Au, and any Pd, if present at all, is below the detectability limit of the XEDS technique. This finding correlates very well with the poor catalytic activity displayed by the M_{Im}-H_2SO_4 sample, since AuPd alloy particles are not generated. The mystery of the Pd location in the M_{Im}-H_2SO_4 sample was easily resolved by examining the M_{Im}-H_2SO_4 material at lower magnification in the SEM, where occasional μm-scale particles of $PdSO_4$ were observed (**Figures 4.11**).

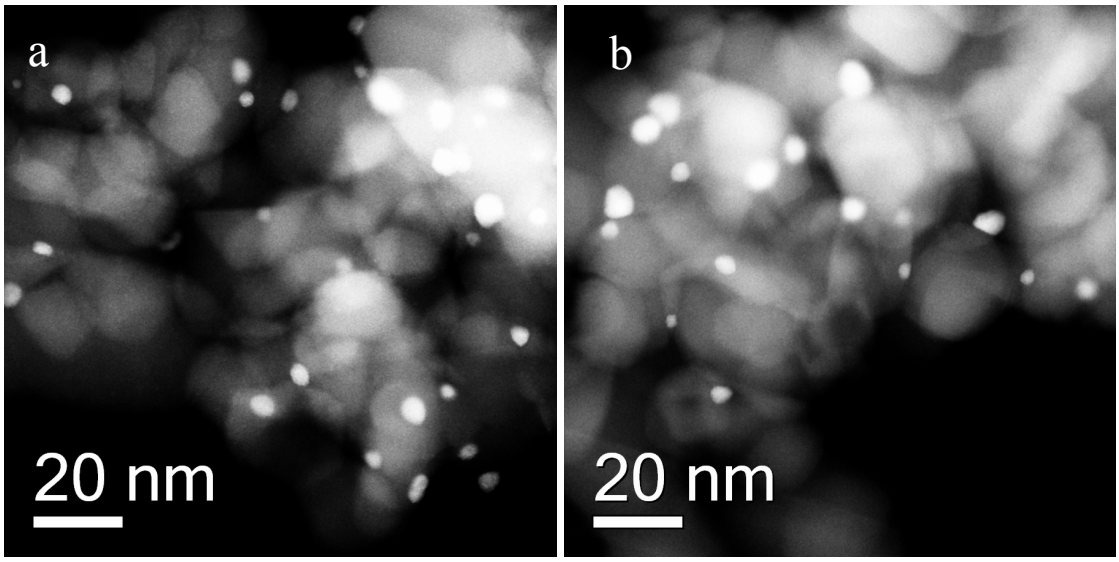

Figure 4.8: STEM-HAADF images of unused 0.5%Au+0.5%Pd/TiO_2 prepared by the (a) M_{Im}-NaCl and (b) M_{Im}-H_2SO_4 routes, both of which were reduced in 5%H_2/Ar at 400 °C. The nanoparticles in both samples have very similar particle size distributions

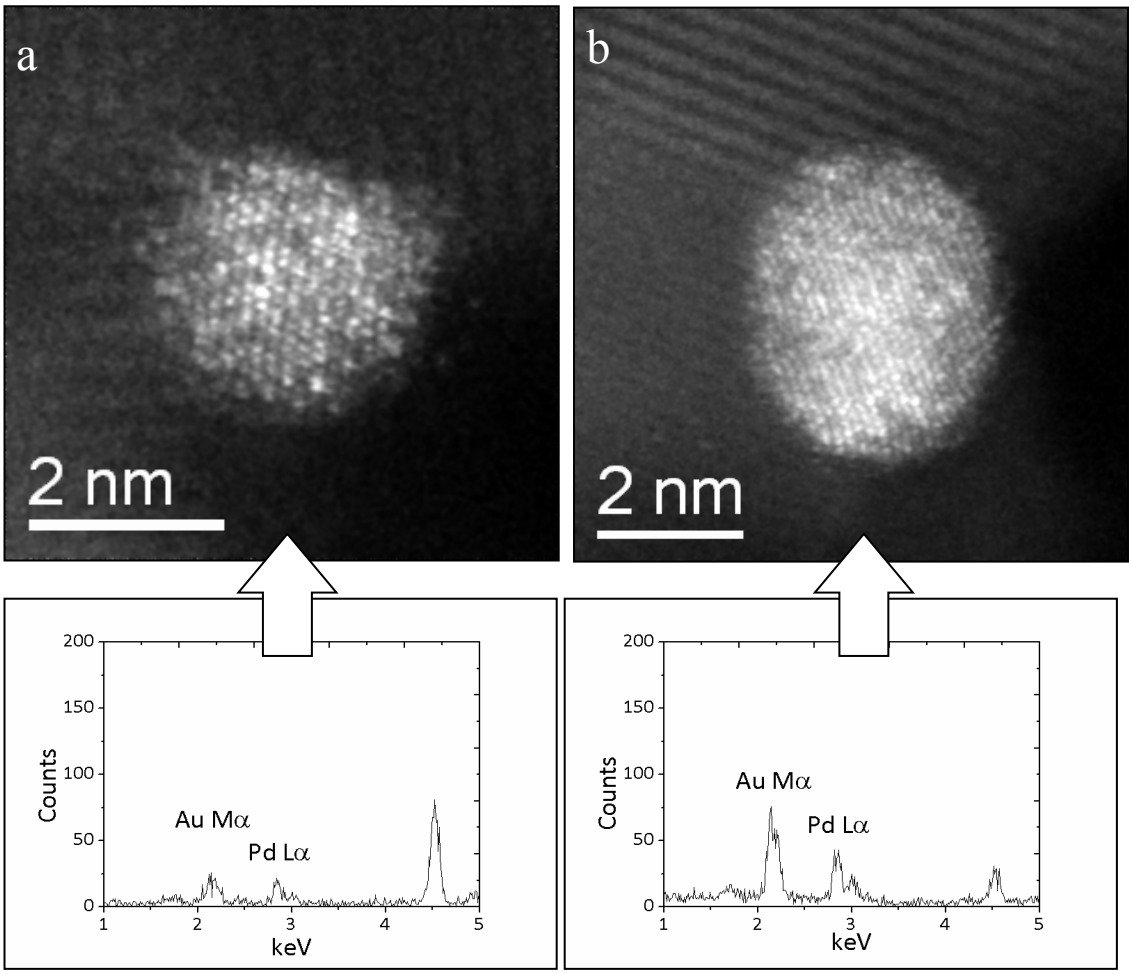

Figure 4.9: High magnification STEM-HAADF images and corresponding XEDS spectra from individual metal particles in the unused 0.5%Au+0.5%Pd/TiO_2 sample prepared by the M_{Im}-NaCl route and reduced at 400 °C in 5%H_2/Ar. Data obtained from (a) small (2nm) and (b) larger (5nm) particles in the M_{Im}-NaCl sample, showing that both are AuPd alloys

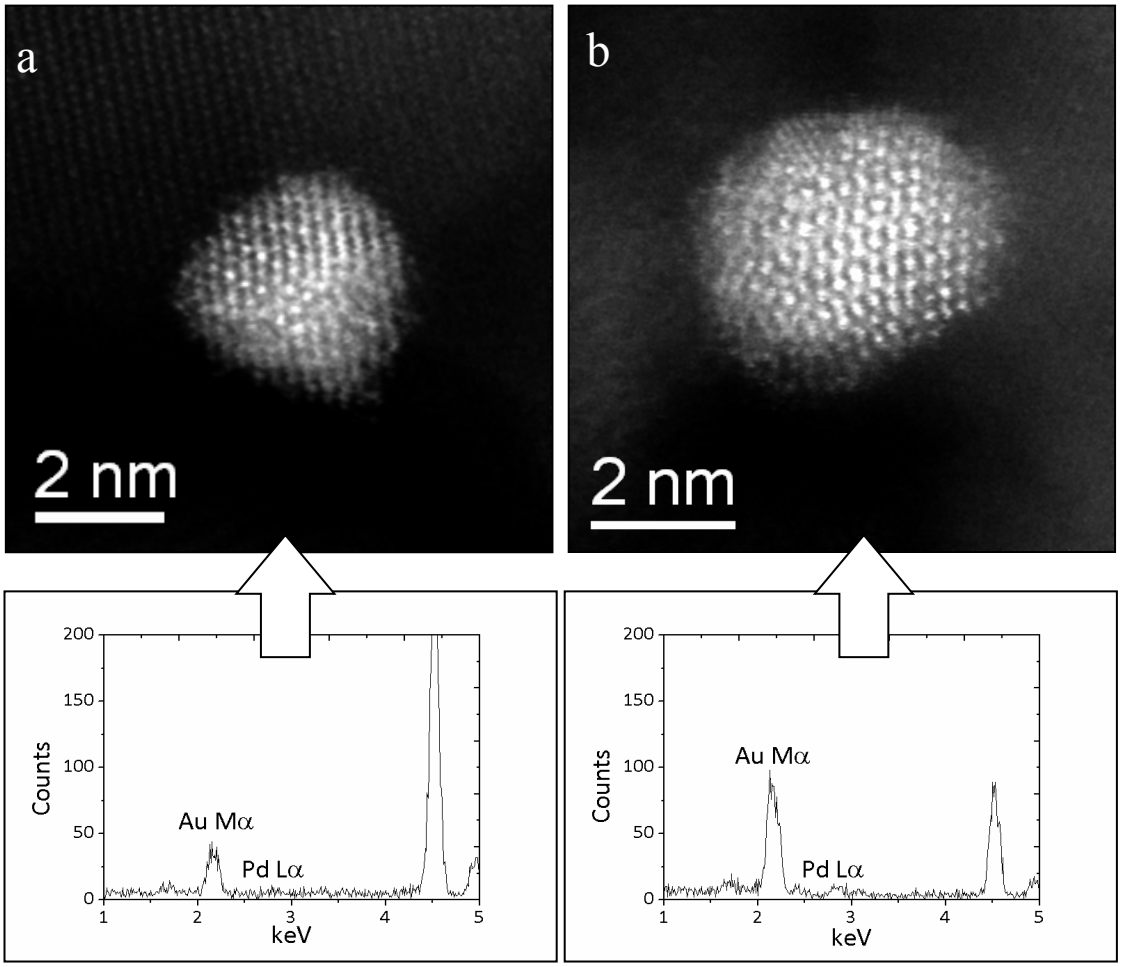

Figure 4.10: High magnification STEM-HAADF images and corresponding XEDS spectra from individual metal particles in the unused 0.5%Au+0.5%Pd/TiO_2 sample prepared by the M_{Im}-H_2SO_4 route and reduced at 400 °C in 5%H_2/Ar. Data obtained from (a) small (3nm) and (b) larger (5nm) particles in the M_{Im}-H_2SO_4 sample, showing that the particles in this case are Au. Any Pd, if present, is below the detectability limit of the XEDS technique

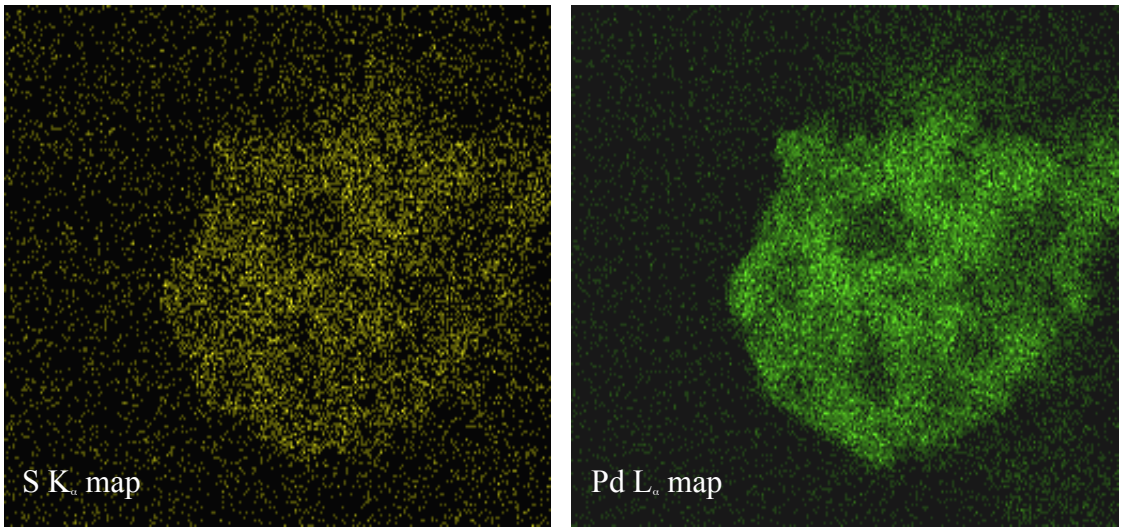

Figure 4.11: Backscattered electron (BSE) SEM image and the corresponding S K_a and Pd L_a XEDS-maps from a micron-scale $PdSO_4$ particle found in the 0.5%Au+0.5%Pd/TiO_2 sample prepared by the M_{Im}-H_2SO_4 route

4.3.6- Stability of the catalysts for reuse

The procedure adapted for studying the reusability of the catalysts is presented in chapter 2 (section 2.3.2). The catalysts have been investigated for first use and the subsequent activity of its used material. The results are shown in **Figure 4.12**. The conventional impregnation (C_{Im}) catalyst is reusable and does not show any decrease in activity, but this catalyst is least active compared to other catalysts prepared by modified impregnation (M_{Im}) methods or the sol immobilisation (S_{Im}) method. But among the other catalysts, most of the catalysts, especially catalysts prepared using NaCl or 2M HCl show a decrease in activity when reused. Sol immobilisation (S_{Im}) catalysts can be reused, but they also show lower activity (by a factor of 10%) than the fresh catalyst. However, the modified impregnation standard catalyst can be reused with a marginal loss (1.5%) in activity.

For further investigation into reusability, the catalysts were also evaluated for synthesis of hydrogen peroxide (**Figure 4.13)**, which shows compatibility in the results. The conventional impregnation (C_{Im}) catalyst was reusable and does not show any decrease in activity, but the productivity of this catalyst is comparable to sol immobilisation (S_{Im}) catalyst. Moreover, both (C_{Im}) and (S_{Im}) catalysts were least active when compared to other catalysts prepared by modified impregnation (M_{Im}) methods. But among the other catalysts, most of them, especially the dried catalyst and the catalysts prepared using NaCl or 2M HCl showed a decrease in activity when reused. However, the catalyst prepared using the (S_{Im}) method can be reused, but it also shows slightly lower activity than the fresh catalyst. The modified impregnation standard catalyst can be reused.

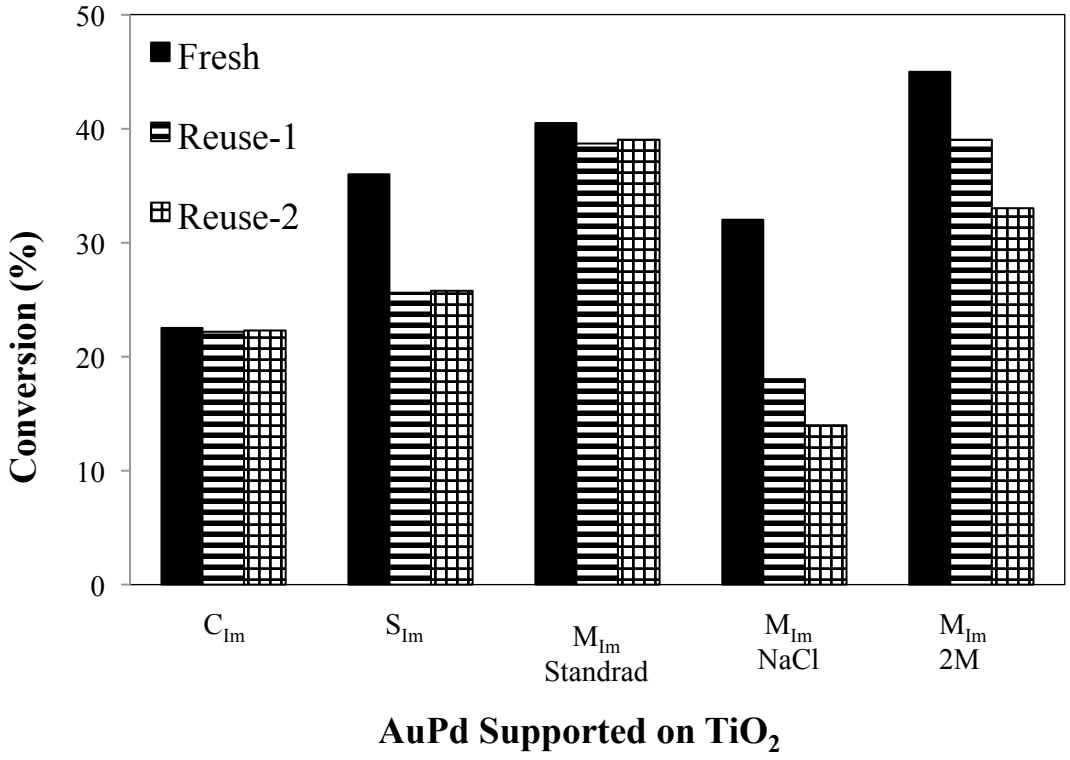

Figure 4.12: Comparison of activity and reusability data for benzyl alcohol oxidation with supported 0.5%Au+0.5%Pd/TiO_2 catalysts prepared by: sol immobilisation (S_{Im}), conventional impregnation (C_{Im}) and modified impregnation M_{Im} in three methodologies which are: standard modified impregnation reduced under H2/Ar in 400 °C (M_{Im} standard), M_{Im} prepared by NaCl excess (M_{Im} NaCl) and M_{Im} prepared by 2M HCl (M_{Im} 2M). Reaction conditions: 0.02g catalyst, 1 bar of O_2, 2g benzyl alcohol, 120 °C, stirring at 1000 rpm and 30min of reaction time

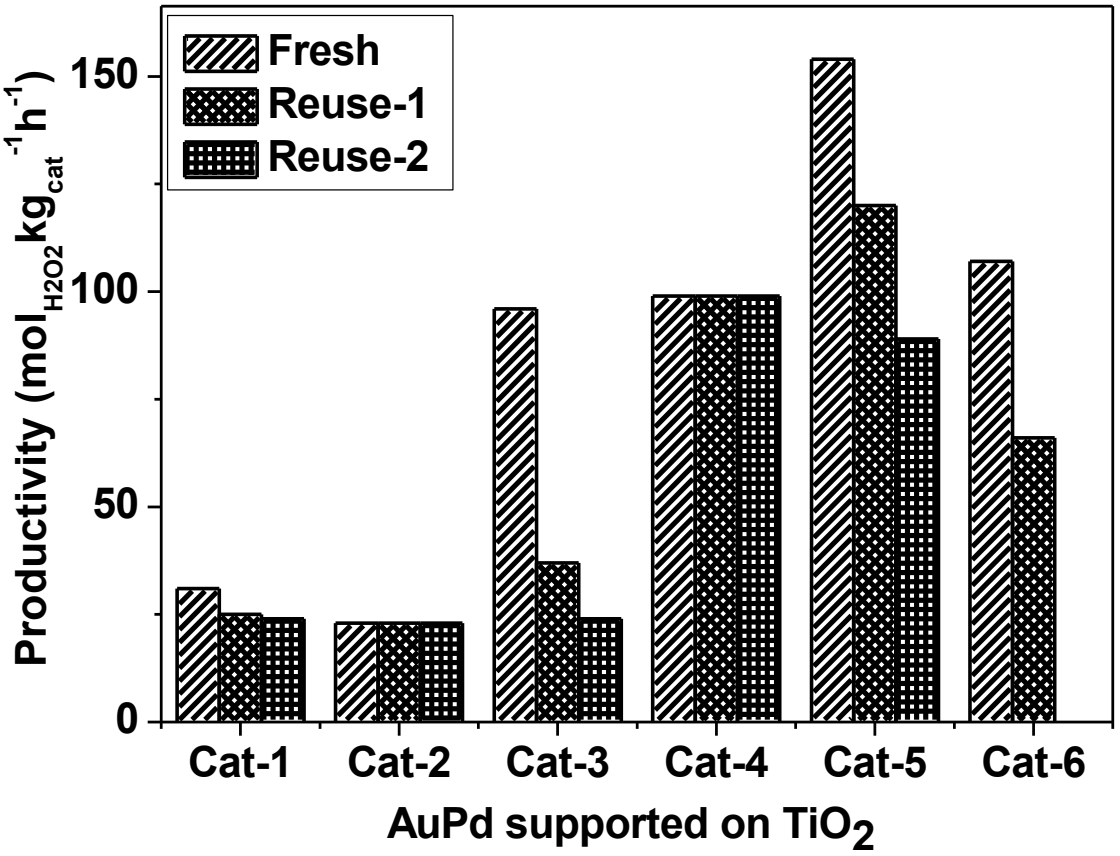

Figure 4.13: Comparison of activity and re-usability data for the direct synthesis of hydrogen peroxide for supported 0.5%Au + 0.5%Pd/TiO_2 catalysts prepared by: sol immobilisation S_{Im} (Cat-1), conventional impregnation C_{Im} (Cat-2), and modified impregnation M_{Im} methodologies (Cat-3 through 6). The modified impregnation catalysts tested are standard M_{Im} dried only (Cat-3), reduced in 5% H/Ar at 400 °C /4h (Cat-4) [Hydrogen conversion and selectivity for this catalyst are 18% and 70% respectively], M_{Im} prepared by NaCl excess (Cat-5) and M_{Im} prepared by 2M HCl (Cat-6). Reaction conditions*:* 5% H_2/CO_2 and 25% O_2/CO_2, 50% H_2/O_2 at 3.7 MPa, MeOH (5.6 g), H_2O (2.9 g), catalyst (0.01 g), 2 °C, 1200 rpm and 30min of reaction time

Using aberration corrected STEM, the dried only 0.5wt%Au+0.5wt%Pd/TiO_2 M_{Im} material, and the 0.5wt%Au+0.5wt%Pd/TiO_2 M_{Im} catalyst reduced at 400 °C in H_2/Ar, were studied both in their fresh and used states. **Figures 4.14 (a)** and **(b)** show representative HAADF images of the nanostructure of the unused, dried 0.5wt%Au+0.5wt%Pd/TiO_2 M_{Im} catalyst. There are two types of metal species present in these images, namely (i) 1-2 nm metallic clusters and (ii) isolated Au or Pd atoms. After use (**Figures 4.14 ((c)** and **(d)**), neither 1-2 nm clusters nor individual metal atoms could be found on the support, implying that these metal species were unstable and have leached from the catalyst during the catalytic testing. Hence, it is the loss of the active metal component that is responsible for the observed deactivation of the dried-only material.

Representative STEM-HAADF images of the 0.5wt%Au+0.5wt%Pd/TiO_2 material prepared by M_{Im} (0.58 M HCl) and reduced at 400 °C in an H_2/Ar mixture, in the fresh and used states, are shown in **Figures 4.15 (a)** and **(b)** respectively. In both cases, a homogeneous dispersion of metal nanoparticles was noted that had a 2-5 nm size range. Furthermore, no obvious metal leaching or particle coarsening was noticed in the used samples when compared to the fresh ones. Interestingly, no 1-2 nm clusters and very few individual metal atoms were noted in either of these reduced samples, implying that these species had been incorporated into the 2-5 nm particles by sintering during the 400 °C H_2/Ar reduction step.

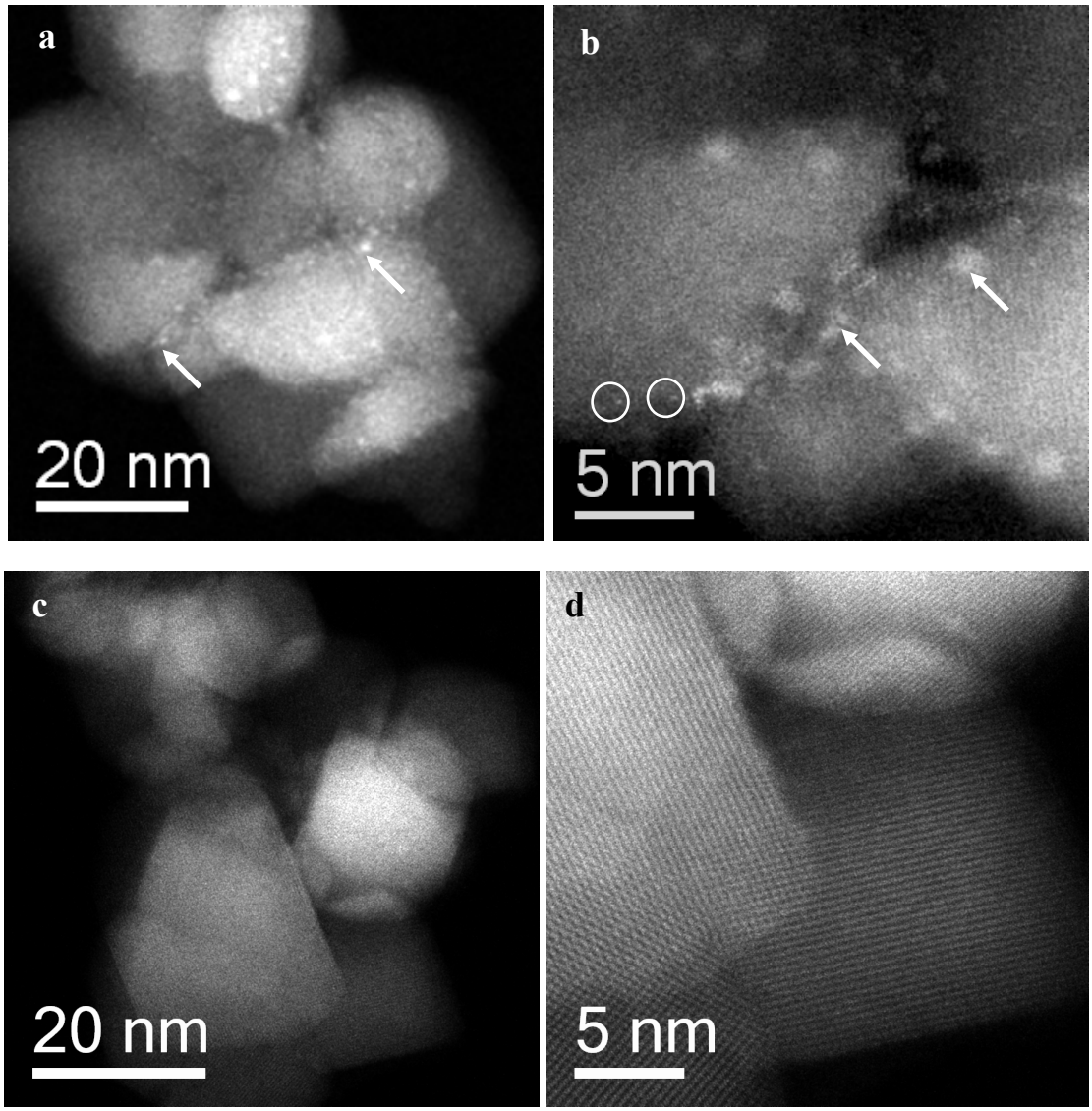

Figure 4.14: (a, b) STEM-HAADF images of the unused, dried only 0.5wt%Au+0.5wt%Pd/TiO_2 prepared by the M_{Im} route (0.58 M HCl); 1-2 nm rafts (arrowed in white) and isolated atoms (circled in white) are clearly visible in the fresh sample. (c, d) STEM-HAADF images of the corresponding material after one usage cycle in which all the supported Au species have been lost

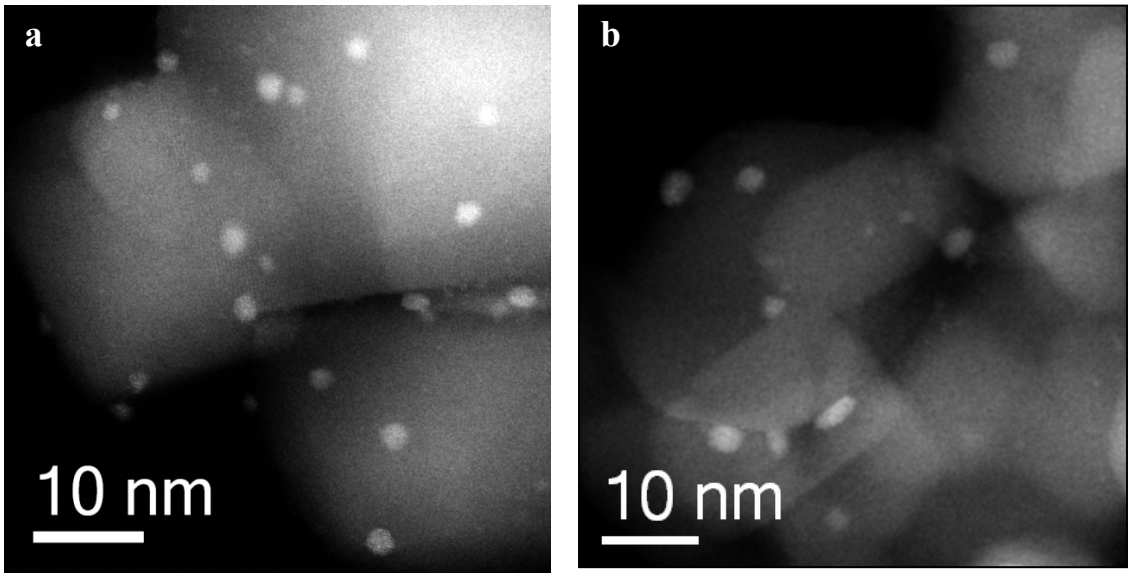

Figure 4.15: STEM-HAADF images of 0.5wt%Au+0.5wt%Pd/TiO_2 prepared by the M_{Im} route (0.58 M HCl) which were reduced in H_2/Ar at 400 °C: (a) fresh and (b) after one usage cycle

Compositional information from individual particles was also obtained by STEM-XEDS for these latter samples, as shown in **Figure 4.16**. X-ray signals were collected while scanning the electron beam over the entire particle, so the XEDS spectrum presented should be treated as an average composition over the entire particle. It was found that small (~2 nm) and larger (~6 nm) particles from the fresh (**Figure 4.16 (a), (b)**) and used samples (**Figures 4.16 (c), (d)**) are all AuPd alloys of relatively similar composition. Importantly, these alloyed particles show a higher catalytic activity than the corresponding 'dried-only' catalysts and are totally reusable. Furthermore, based on the intensity ratios between the Au M_{α} and Pd L_{α} lines, there seems to be no significant size dependent composition variation. This is quite a significant result as catalysts prepared by the sol immobilisation (S_{Im}) and conventional impregnation methods have previously been shown to display systematic composition variations in particle size. For S_{Im} catalysts, the larger particles were always Pd-rich, and the smaller ones were Au-rich [46, 47]. For the conventional impregnation route, the situation is reversed, with the larger particles reported as being Au-rich, and the smaller ones Pd-rich [48, 49]. These results clearly demonstrate that the modified impregnation route represents an effective new method for producing AuPd nanoparticles with a tight size distribution, along with minimal composition variation across this size range.

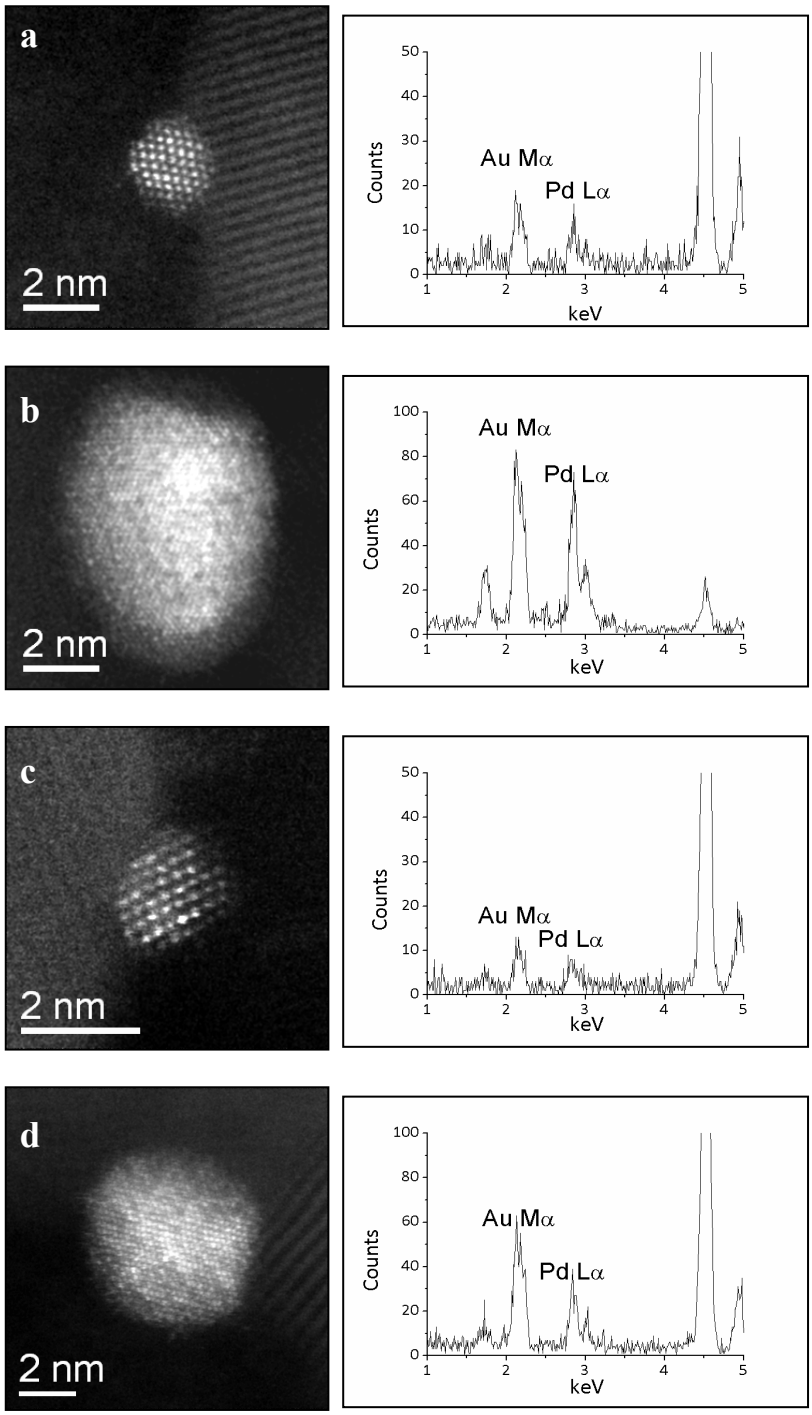

Figure 4.16: High magnification STEM-HAADF images and corresponding XEDS spectra from individual metal particles in the 0.5%Au+0.5%Pd/TiO_2 samples prepared by M_{Im} (0.58 M HCl) and reduced at 400 °C in H_2/Ar. (a, b) Data obtained from small (2nm) and larger (6nm) particles in the fresh sample: (c, d) Data obtained from small (2nm) and larger (7nm) particles in the used sample

However, it has not been possible to measure the compositions of the ultra-small 1-2 nm metallic clusters present in the dried-only M_{Im} samples simply because they were mobile under the electron beam and produced too little signal for meaningful XEDS analysis. Therefore, the corresponding monometallic Au/TiO_2 and Pd/TiO_2 M_{Im} systems were studied by STEM-HAADF imaging in order to evaluate how the modified impregnation method affected the distribution of each metal component individually. It was found that the dried only Au/TiO_2 M_{Im} sample contains 1-2 nm Au clusters and individual Au atoms (**Figure 4.17 (a), (b)**), while after reduction at 400 °C in H_2/Ar, these species aggregated and formed nanoparticles which were 2-6 nm in diameter (**Figure 4.17 (c), (d)**). The monometallic Pd/TiO_2 M_{Im} sample seemed to behave in a subtly different manner, in that 1-2 nm Pd rafts dominated with little evidence of individual Pd atoms (**Figure 4.18 (a), (b)**). After reduction at 400 °C in 5% H_2/Ar, 2-6 nm Pd nanoparticles were formed as expected (**Figure 4.18 (c), (d)** and **Figure 4.19**). From these studies of the two monometallic systems, it can be inferred that both Au and Pd can be finely dispersed into 1-2 nm clusters in the presence of excess Cl^- species. During reduction at 400 °C in 5% H_2/Ar, where the residual Cl^- had been largely removed, the clusters sinter to form nanoparticles. Since the two metals were so well dispersed initially, the resultant alloy nanoparticles can be well controlled both in terms of size and composition.

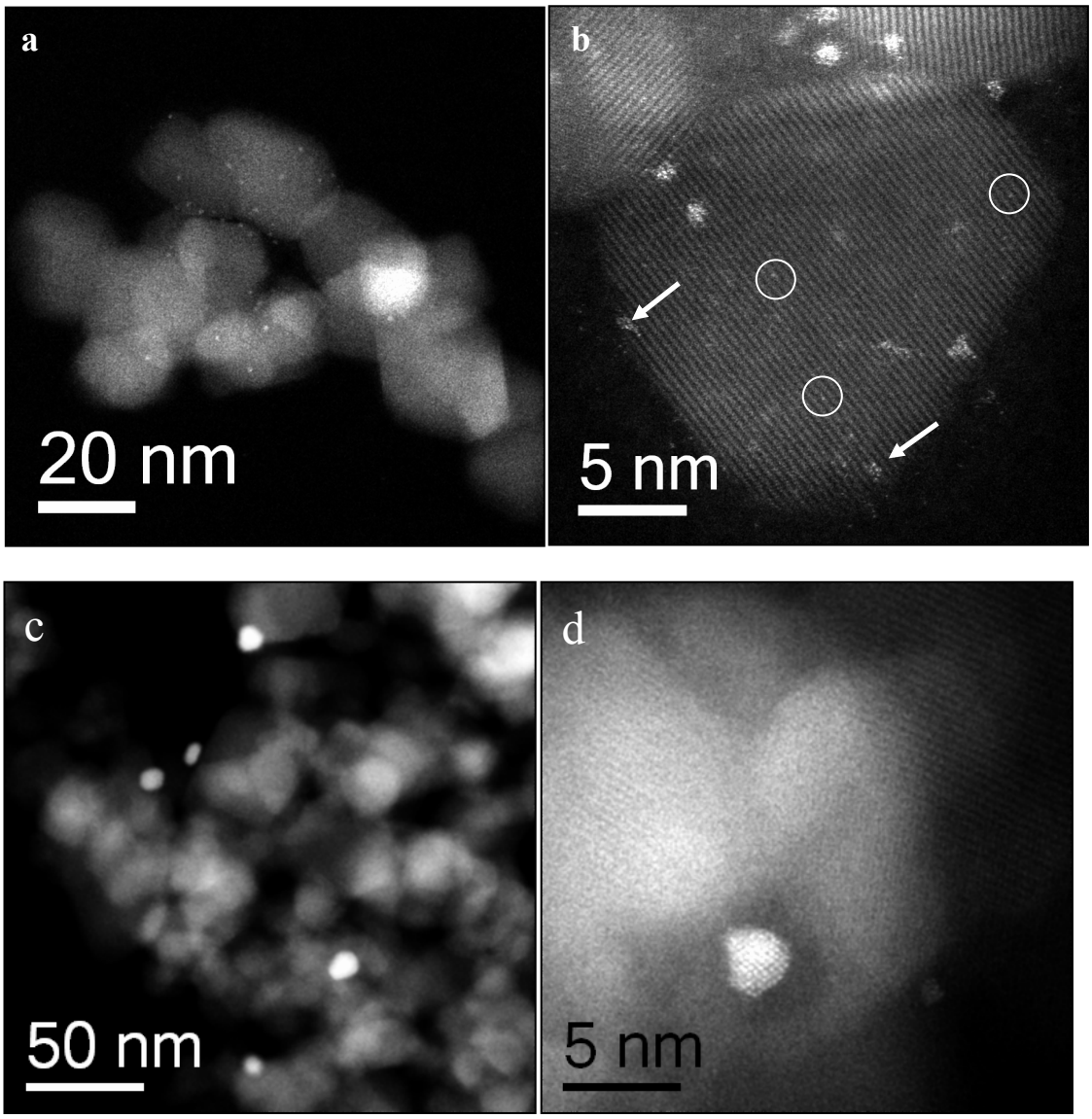

Figure 4.17: STEM-HAADF images of the monometallic 1wt%Au/TiO_2 sample prepared by M_{Im}. In the dried only sample (a, b) 1-2 nm Au clusters (arrowed in white) and isolated Au atoms (circled in white) were present; in the sample reduced at 400 °C in H_2/Ar (c, d) 2-6nm nanoparticles were formed at the expense of the clusters and atomically dispersed species

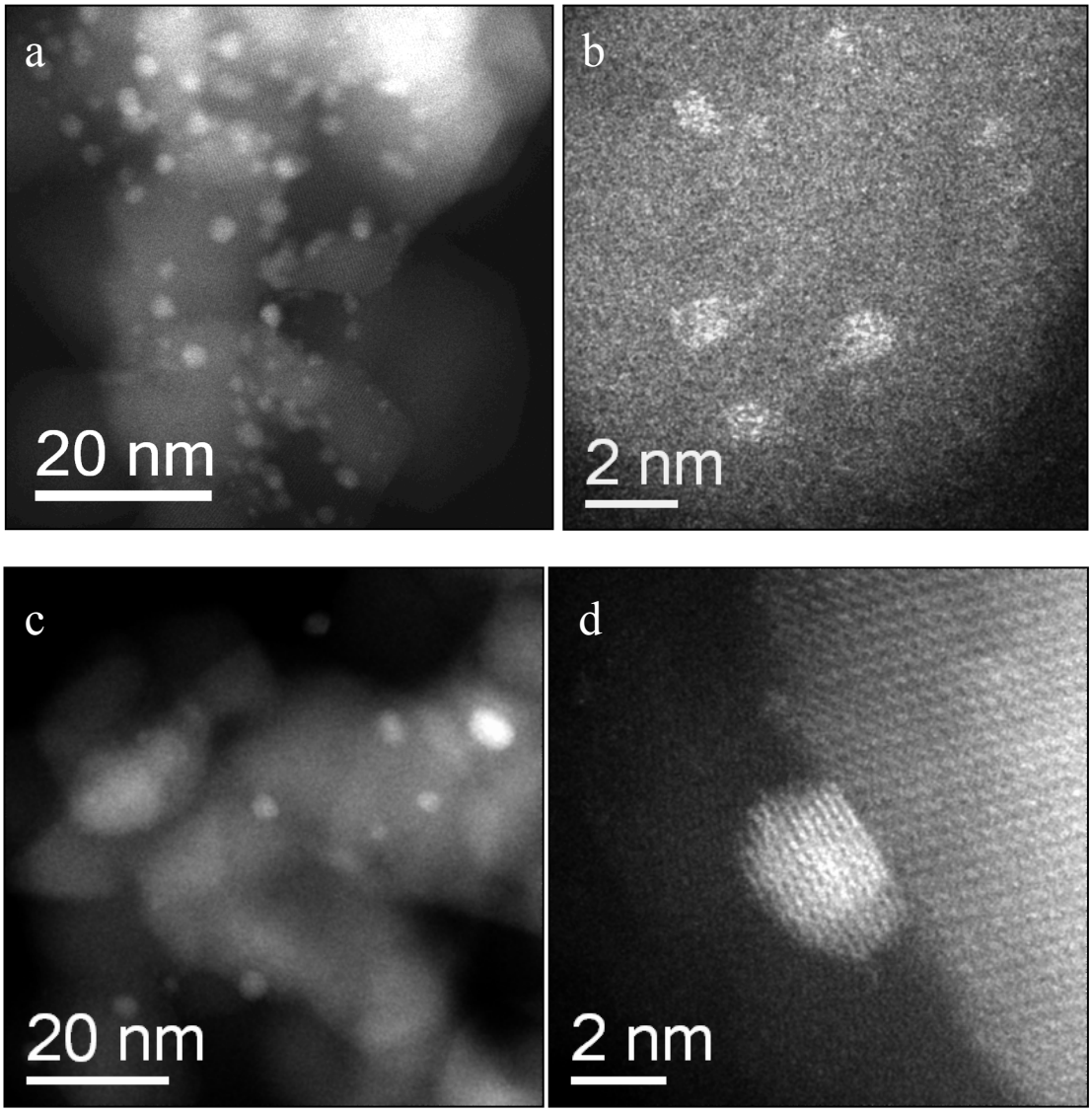

Figure 4.18: STEM-HAADF images of the monometallic 1wt% Pd/TiO_2 catalyst prepared by the M_{Im} route. In the dried only sample (a, b) the majority of the metal species were 1-2nm clusters. For the material reduced at 400 °C in H_2/Ar, (c, d) 2-6nm Pd nanoparticles were formed at the expense of the 1-2nm Pd clusters

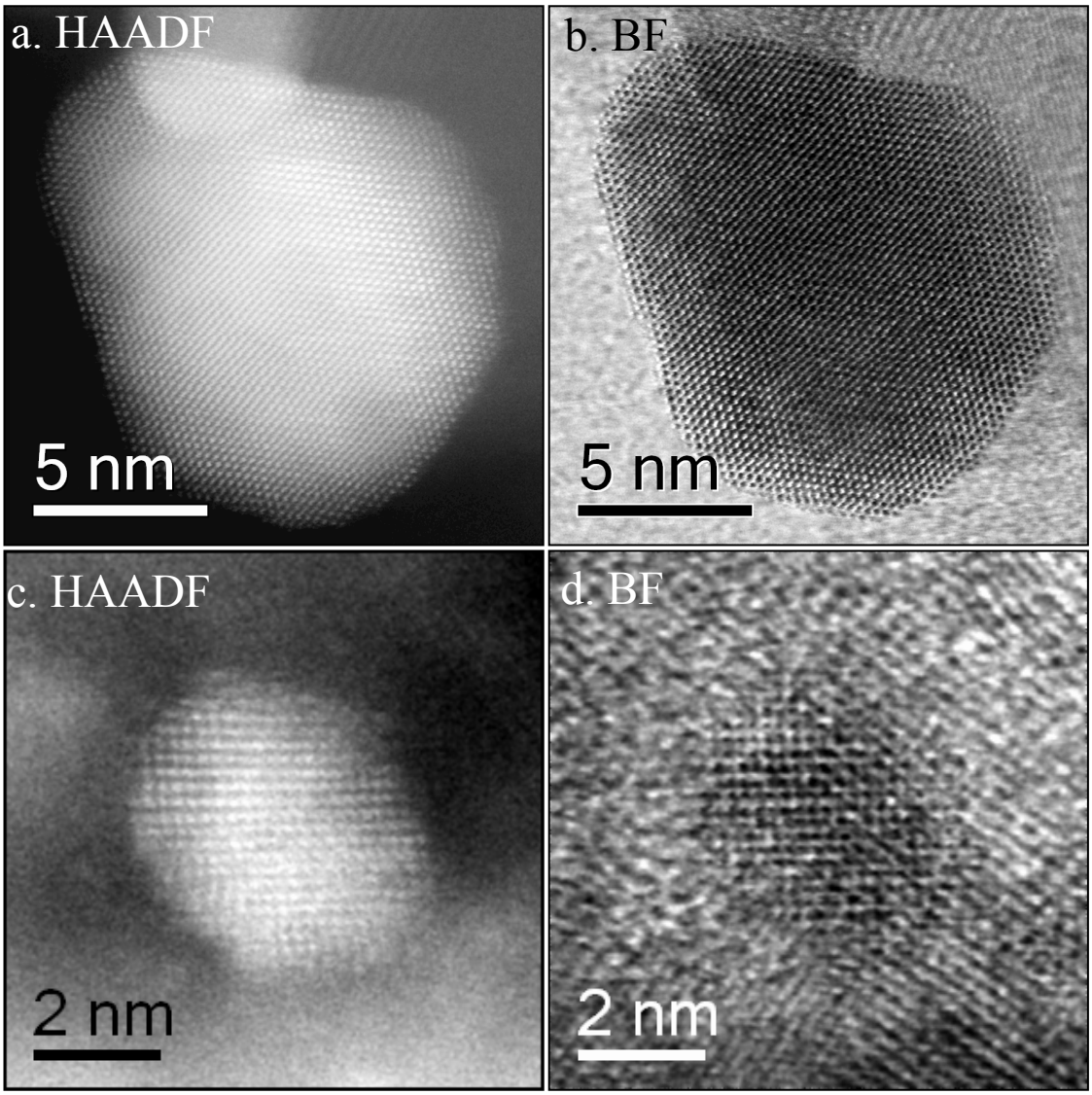

Figure 4.19: STEM-HAADF and STEM-BF image pairs from two particles in the 1wt% Pd/TiO_2 sample prepared by M_{Im}-HCl and reduced at 400 °C in H_2/Ar. The metallic Pd particles have an FCC structure, and are viewed along [110] in (a, b) and [100] in (c,d)

4.3.7- X-ray photoelectron spectroscopy (XPS) study of M_{Im} and C_{Im} materials

The 0.5%Au+0.5%Pd/TiO_2 catalysts prepared by the M_{Im} route, using different excess anions, and by the C_{Im} route were analysed by X-ray photoelectron spectroscopy (XPS). Quantified data showing derived surface compositions (at. %) and corrected Pd/Au ratios are shown in **Table 4.5**, and detailed spectra for the C_{Im} and M_{Im} (0.58 M HCl) samples are presented in **Figures 4.20** and **4.21**. The catalysts that have been analysed are: the dried and calcined/reduced catalysts, both fresh and after use for hydrogen peroxide synthesis. The behaviour of the C_{Im} samples has been reported previously [45]; calcination of the dried C_{Im} sample leads to a significant increase in the Pd:Au ratio due to the formation of particles with a Pd-rich shell/Au-rich core morphology. Furthermore, use of the dried-only C_{Im} catalyst for benzyl alcohol and H_2O_2 synthesis results in significant leaching, as reflected in the decrease in the [Au]+[Pd] value, whereas the calcined sample was stable. In marked contrast, the M_{Im} samples derived from HCl or NaCl show no strong evidence for core-shell formation on reduction at 400 °C (for a random alloy the expected Pd:Au ratio is 1.9:1), but in common with the C_{Im} materials, it does show leaching after use for the dried-only catalyst, but not for the 400 °C reduced samples. The C_{Im} and M_{Im}–HCl and M_{Im}-NaCl catalysts exhibit similar Cl^- surface concentrations for the dried materials, and only the latter shows no significant decrease after heat treatment. Interestingly, both oxidative (C_{Im}) and reductive (M_{Im}-HCl) heat treatments are able to decrease the residual [Cl] concentration. For all dried-only samples, the Cl^- concentration decreases significantly after use for

H_2O_2 synthesis. The low Pd signals for the M_{Im} (H_2SO_4) samples are in keeping with the results of the STEM-XEDS studies, which identified large microscopic $PdSO_4$ particles, where most of the Pd atoms would be not detected by XPS, since the mean free path for photoelectrons is in orders of magnitude smaller than the $PdSO_4$ particle size.

Quantified XPS data, together with the corrected Pd:Au ratios for M_{Im} samples prepared with varying HCl concentration, are shown in **Table 4.6**. After reduction in 5%H_2/Ar at 400 °C, the observation was only minor differences between the Pd/Au ratios for the 0.1M, 0.58M and 2M materials. This is in contrast with the STEM observation that large Au particles are not present in the 2M catalyst, the gold having been dispersed and incorporated into Pd-Au alloy nanoparticles. Although increased dispersion of the gold will lead to an increase in the Au(4f) signal intensity for those gold atoms, which might be reflected in a decrease in the Pd/Au ratio, XPS provides information averaged over a relatively large area and in this case is dominated by the AuPd nanoparticles. For all three preparations, the [Cl] concentration decreases significantly after reduction. The observed Au($4f_{7/2}$) binding energies, 82.6 – 83.1 eV, are lower than the expected bulk value of 84.0 eV. Some groups have related this negative shift to the change in electronic structure as a function of cluster size [50, 51], whilst other groups attribute it to (i) electron transfer from the support to the nanoparticles [52], (ii) an initial state effect resulting from H_2 pre-treatment [53] or (iii) charge transfer from Pd to Au, increasing the *s*-state occupancy for Au and indicating alloy formation [54]. Clearly, based on the STEM results and the sample preparation, both of the latter two explanations could be applicable here.

The measured Pd($3d_{5/2}$) binding energies lie in the range 336.0± 0.2 eV, somewhat lower than what has frequently been observed for Pd^{2+} in Pd and Pd-Au nanoclusters, at around 336.5 - 337 eV [48]. In light of the STEM results, the consideration of this energy may be indicative of two possibilities: (i) particle-size effects, wherein the Pd core-hole screening during photoemission results in a higher binding energy for small particles [55] or (ii) Pd^{d+} formation through charge transfer with adsorbed Cl [56], although whether this Cl is adsorbed on the Pd itself or neighbouring sites, is inconclusive from the XPS data alone. This latter point is in some agreement with Shen *et al.* [57] who reported similar Pd binding energies for Cl^- containing catalysts, and suggests the Pd has a more positive valency resulting in a more stable Pd surface structure than the corresponding halide free system.

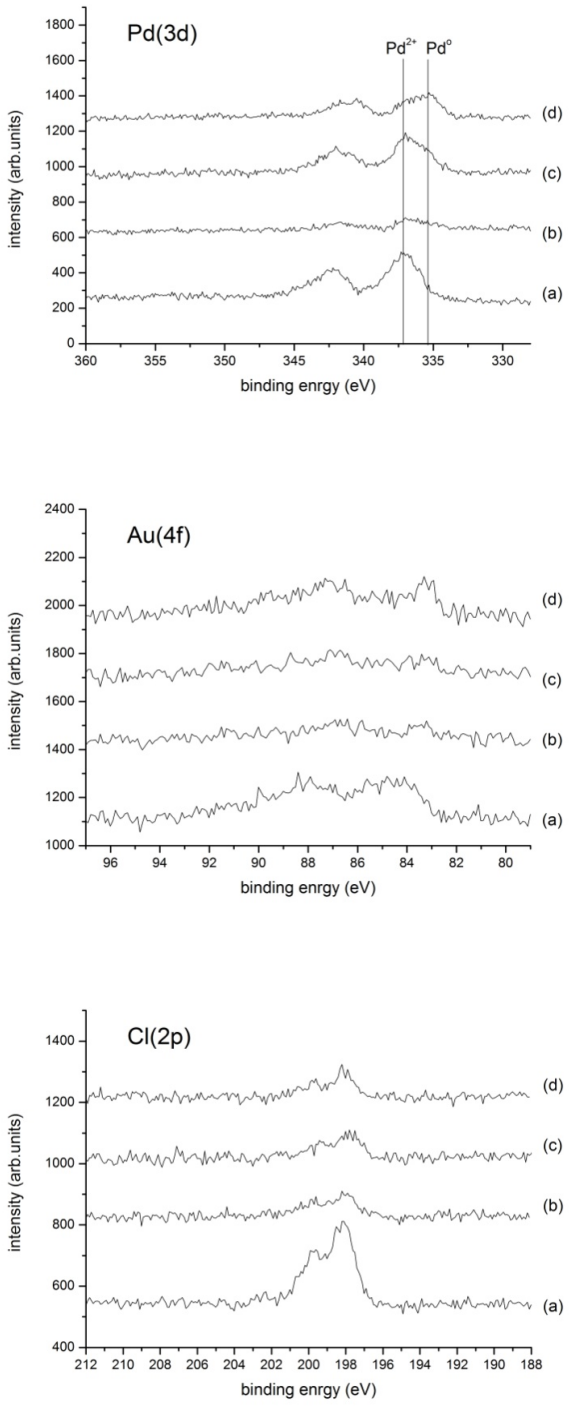

Figure 4.20: Pd(3d), Au(4f) and Cl(2p) spectra for 0.5%Au+0.5%Pd/TiO_2 samples prepared by conventional impregnation (C_{Im}): (a) dried sample; (b) catalyst *(a)* after being used for H_2O_2 synthesis; (c) catalyst *(a)* after calcination in air at 400 °C; (d) catalyst (c) after use for H_2O_2 synthesis

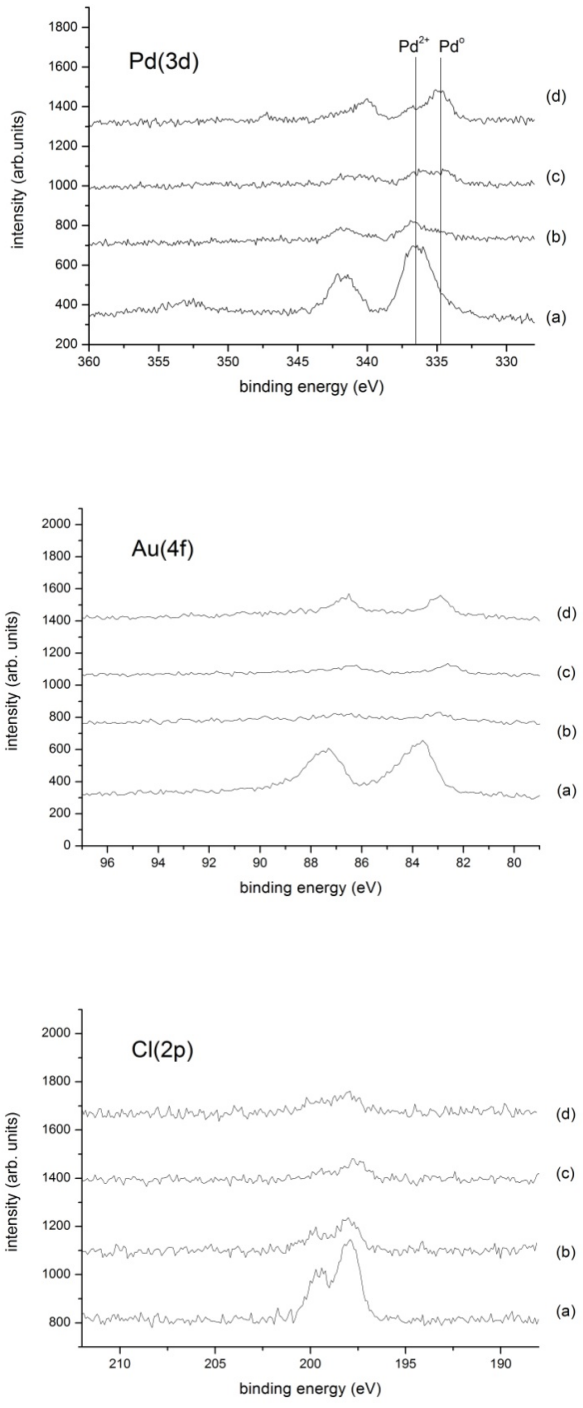

Figure 4.21: Pd(3d), Au(4f) and Cl(2p) spectra for 0.5%Au+0.5%Pd/TiO_2 samples prepared by modified impregnation (M_{Im}) using excess HCl: (a) dried sample; (b) catalyst *(a)* after being used for H_2O_2 synthesis; (c) catalyst *(a)* after heating in H_2/Ar at 400 °C; (d) catalyst (c) after use for H_2O_2 synthesis

Table 4.5: Quantified XPS results for the samples prepared by C_{Im} and M_{Im}. The Cl, Pd and Au atom % compositions are mean values for the surface region sampled by XPS

Treatment	C_{Im}				M_{Im} (HCl)				M_{Im} (NaCl)				M_{Im} (H_2SO_4)			
	%Cl	%Pd[a]	%Au	Pd/Au[b]	%Cl	%Pd[a]	%Au	Pd/Au[b]	%Cl	%Pd[a]	%Au	Pd/Au[b]	%Cl	%Pd[a]	%Au	Pd/Au[b]
Dried	1.6	0.66	0.16	3.7	1.1	0.68	0.35	1.4	1.7	0.67	0.31	1.6	0.0	0.16	0.18	0.33
Dried + syn x 1[c]	0.50	0.18	0.06	2.5	0.48	0.20	0.05	3.4	0.59	0.17	0.07	2.0	0.0	0.11	0.07	0.93
400 °C in air	0.34	0.50	0.06	8.1	0.22	0.32	0.08	3.3	-	-	-	-	-	-	-	-
400 °C in H_2/Ar	0.37	0.85	0.09	9.3	0.4	0.39	0.11	2.9	1.5	0.48	0.12	3.4	0.50	0.12	0.12	0.44
400 °C + syn x 1[c]	0.49	0.44	0.08	5.1	0.31	0.27	0.11	2.0	0.47	0.39	0.14	2.3	0.33	0.10	0.11	0.38

[a] calculated from the total apparent Pd(3d) intensity, which incorporates intensity from the Au($4d_{5/2}$) component

[b] ratio corrected for the overlap of the Pd(3d) doublet and the Au($4d_{5/2}$) component

[c] "syn x 1" means used once for H_2O_2 synthesis

Table 4.6: Quantified XPS results for the samples prepared *via* the M_{Im} route using different HCl concentrations. The Cl, Pd and Au atom % compositions are mean values for the surface region sampled by XPS

Treatment	M_{Im} (0.1M HCl)				M_{Im} (0.58M HCl)				M_{Im} (2M HCl)			
	%Cl	%Pd[a]	%Au	Pd/Au[b]	%Cl	%Pd[a]	%Au	Pd/Au[b]	%Cl	%Pd[a]	%Au	Pd/Au[b]
Dried	0.35	0.19	0.07	2.2	1.1	0.68	0.35	1.4	0.54	0.28	0.13	1.7
400 °C in air	0.34	0.31	0.03	9.8	0.22	0.32	0.08	3.3	0.41	0.30	0.06	4.5
400 °C in H_2/Ar	0.23	0.18	0.06	2.5	0.4	0.39	0.11	2.9	0.34	0.25	0.09	2.3

[a] calculated from the total apparent Pd(3d) intensity, which incorporates intensity from the Au($4d_{5/2}$) component

[b] ratio corrected for the overlap of the Pd(3d) doublet and the Au($4d_{5/2}$) component

4.3.8- Powder X-ray Diffraction (XRD)

The XRD data for the 0.5%Au+0.5%Pd/TiO_2 catalysts carried out for the powder X-ray diffraction (XRD) patterns show the metallic Au and Pd were dispersed over the support for all catalysts. The main reflections of Au are expected to be 2θ = 38° (111), 44° (200), 64° (220) and 77° (311), whereas the main reflections of Pd are expected to be 2θ = 40° (111), 46° (200) and 68° (220) where other reflections stem from the support. The purpose of the characterization was to determine the crystal structure and their oxidation state. **Figure 4.22** shows the XRD pattern for 1wt%AuPd/TiO_2 catalyst prepared by C_{Im} (dried and calcined), S_{Im} (dried) and C_{Im} (dried and reduced).

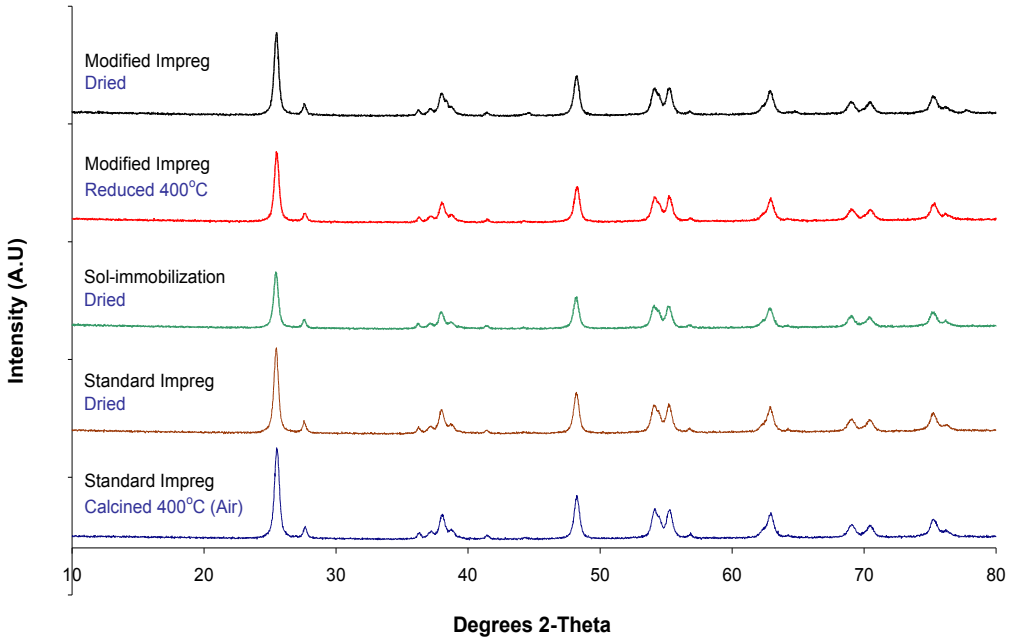

Figure 4.22: XRD patterns (with 2 Theta range 10°–80°) of 0.5wt%Au+0.5wt%Pd/TiO_2 catalysts prepared by modified impregnation (M_{Im}) (black and red lines denote dried only and 5%H_2/Ar reduced variants), sol immobilisation (S_{Im}) (green) and conventional/standard impregnation (C_{Im}) (brown and blue lines denote dried-only and calcined variants respectively)

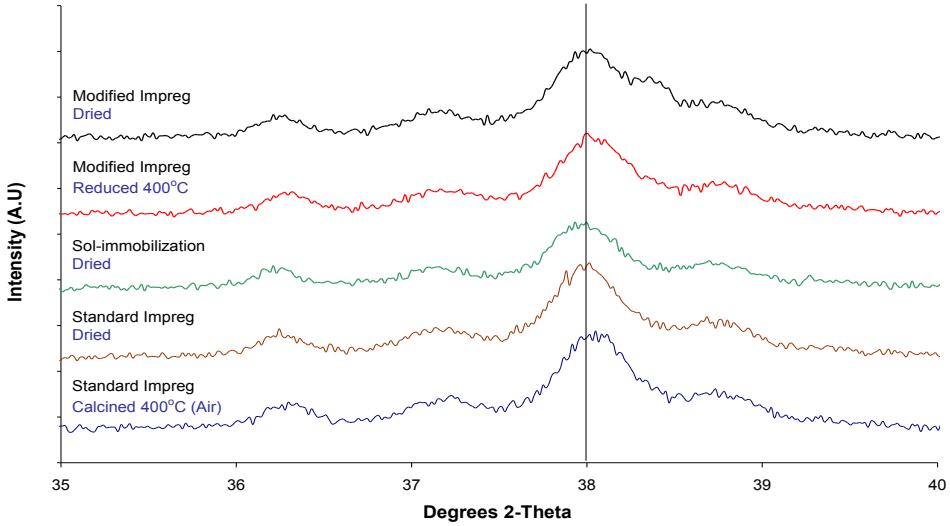

Figure 4.23: XRD patterns (with 2 Theta range 35°–40°) of 0.5wt%Au+0.5wt%Pd/TiO_2 catalysts prepared by modified impregnation (M_{Im}) (black and red lines denote dried and 5%H_2/Ar reduced variants), sol immobilisation (S_{Im}) (green) and conventional impregnation (C_{Im}) (brown and blue lines denote dried and calcined variants respectively)

The XRD pattern of the uncalcined sample indicated the presence of a characteristic peak of Au at 2θ = 38° (111) which became more intense after the thermal treatment process. The observation Pd peak was not detected because of the attribution smaller crystallite size that is lower than detectability limit of XRD (<5 nm) or due to the high metal dispersion on the TiO_2 support. The expanded region in **Figure 4.23** shows the position of (111) cubic metal phase reflection indicating the presence of Au or AuPd alloy peaks, whereas the Pd species were not detected probably due to the detectability limitation. The S_{Im} was determined by the lack of diffraction peaks due to the deposited metals (Au, Pd) in the XRD spectra and also could be due to the detectability limit of XRD instrument as detailed above and as the STEM produced metal catalyst with mean particle size 4.7 nm.

4.3.9- Effect of thermal treatment conditions

Another crucially important stage in the preparation of the catalysts by the M_{Im} method is the gas phase reduction in 5% H_2/Ar. The effect of thermal treatment on the material was studied by varying the temperature and the gas environment of this step. A 0.5wt%Au+0.5wt%Pd/TiO_2 catalyst prepared by the M_{Im} method was reduced at temperatures of 250, 300, 400 and 500 °C in flowing 5% H_2/Ar. The aerobic oxidation of benzyl alcohol was carried out to examine the performance of the reduced catalysts. The result is given in **Table 4.7**, and shows that the best performance is from the catalyst which was treated at 400 °C in H_2/Ar flow, achieving a conversion of 55% with selectivity 85.5% to benzaldehyde and 12.5% to toluene. Further increasing the thermal treatment temperature to 500 °C causes a marked drop in conversion to ~20% which was assumed to be due to sintering of the metal particles, or it is possibly due to the formation of larger particles at the expense of the most active small particles at the higher reduction temperatures. With the thermal treatment at 400 °C in flowing air, the conversion of benzyl alcohol decreases to almost half of that obtained at a similar temperature with H_2/Ar flow, to 27.5%, although the selectivity to benzaldehyde increases to 92.1%. This demonstrates that the thermal treatment of the catalysts plays an important role in the activity, and furthermore, that reduction treatment should be considered as an alternative to oxidation treatments when preparing gold palladium bimetallic catalysts for oxidation reactions.

Table 4.7: Effect of thermal treatment on benzyl alcohol oxidation in synthesis of the 0.5%Au+0.5%Pd/TiO_2 M_{Im} catalyst [a]

Catalyst	Heat Treatment temperature (^{o} C)	Heat Treatment atmosphere	Conversion (%)	Selectivity (%)	
				Benzaldehyde	Toluene
0.5%Au+0.5%Pd / TiO_2 (M_{Im})	250	H_2/Ar	32.2	74.5	23.5
	300	H_2/Ar	33	81.5	16.3
	400	H_2/Ar	55	85.5	12.5
	500	H_2/Ar	20.7	96	1.4
	400	Air	27.5	92.1	5

[a] Reaction conditions: 0.02g Catalyst, 1 bar of O_2, 2g Benzyl alcohol, 120 °C, Stirring at 1000 rpm and 1hr of reaction time

4.3.10- Effect of the support

A number of different AuPd catalysts were prepared on alternative supports by this M_{Im} method, and tested for benzyl alcohol oxidation. The results are presented in **Table 4.8**. When TiO_2 and MgO were used as supports, the M_{Im} catalysts are substantially more active than the corresponding S_{Im} catalysts. The table also shows that the activity was lower for the ZnO, C and Nb_2O_5 supported M_{Im} materials. However, the M_{Im} method's advantage here is that it can be used for an unlimited number of supports, while the S_{Im} catalysts can only be used on a very limited number of supports because the efficiency of deposition or immobilisation of these pre-formed colloids is highly dependent on the iso-electric point (IEP) of the support. Due to the amphoteric properties of $Au(OH)_3$, the pH of aqueous $HAuCl_4$ solution is amended at a fixed point in the range of 6 to 10. It is

not applicable to metal oxides, the IEPs of which are below 5, for example, for SiO_2 (IEP=2), SiO_2-Al_2O_3 (IEP=1), or WO_3 (IEP=1), the gold hydroxide cannot be deposited on the supports [32].

Table 4.8: Effect of support on benzyl alcohol oxidation using different methods in the synthesis of the 1%mol AuPd/TiO_2 catalyst [a]

Catalyst	M_{Im}			S_{Im}		
	Conv. (%)	Selectivity (%)		Conv. (%)	Selectivity (%)	
		Benzaldehyde	Toluene		Benzaldehyde	Toluene
1%(Au-Pd)/TiO_2	88	77	21	65	80	18
1%(Au-Pd)/MgO	33	98	0.5	26	99	0.4
1%(Au-Pd)/ZnO	27	97	0.5	39	99	0.3
1%(Au-Pd)/C	32	73	25	89	69	26
1%(Au-Pd)/Nb_2O_5	10	92	4.5	66	74	23
1%(Au-Pd)/Al_2O_3	68	82	16	NA	-	-
1%(Au-Pd)/Ga_2O_3	50	84	15	NA	-	-
1%(Au-Pd)/CeO_2	32	87	10	NA	-	-
1%(Au-Pd)/ZrO_2	22	85	14	NA	-	-
1%(Au-Pd)/MnO_2	20	99	0.7	NA	-	-
1%(Au-Pd)/SiO_2	10	92	5	NA	-	-
1%(Au-Pd)/WO_3	10	83	16	NA	-	-
1%(Au-Pd)/Gd_2O_3	7	95	2	NA	-	-
1%(Au-Pd)/SrO	5	100	0	NA	-	-

[a] Reaction conditions: 0.02g catalyst, 1 bar of O_2, 2g benzyl alcohol, 120 °C, stirring at 1000 rpm and 2hr of reaction time

4.4- Conclusions

A "stabiliser-free", modified impregnation methodology has been developed for the preparation of supported gold-palladium nano-alloy catalysts. The impregnation medium in this method contains a large excess of anionic ligands, namely Cl^-, which helps to improve the dispersion of the Au species in particular. The reduction treatment at 400 °C in a 5% H_2/Ar atmosphere is effective for removing the excess Cl^- from the catalyst, as well as efficiently 'sweeping-up' the very highly dispersed, predominantly Pd-rich species, and aiding their efficient incorporation into the 2-5 nm AuPd alloy nanoparticles. Catalysts prepared by the M_{Im} method are found to be four times more active for the direct synthesis of hydrogen peroxide from H_2 and O_2 than those made with C_{Im} and S_{Im} methods. They are also more active for the solvent-free oxidation of benzyl alcohol, although some loss of specificity to the desired benzaldehyde product has been noted. The metal nanoparticles in these M_{Im} materials have a tight distribution of particle sizes ranging from 2-6 nm, with only very occasional very large particles, that is, their size range is much better controlled than the C_{Im} materials and they are more akin in this respect to S_{Im} derived catalysts. Furthermore, the bimetallic alloy composition is relatively invariant from particle-to-particle in these M_{Im} materials, in contrast to the C_{Im} and S_{Im} materials, where systematic particle size/composition variations have previously been noted. In addition, it has been found that the Au:Pd ratio of the alloy particles can to some extent be controlled by varying the concentration of excess [Cl^-] anions employed in the M_{Im} process. In summary, this new M_{Im} route permits the generation of a catalyst, which has a small average particle size, an

optimised random alloy composition, and improved compositional uniformity from particle-to-particle. This new preparation protocol provides both the academic research community and the industrial community, with a very convenient and reproducible methodology for preparing supported Au-Pd nanoalloy catalysts with high activity and stability; without using any exotic ligands or stabilisers, while at the same time not compromising their catalytic activity.

4.5- References

[1] M. Haruta, T. Kobayashi, H. Sano, N. Yamada, Chem. Lett., (1987) 405-408.

[2] G.J. Hutchings, J. Catal., 96 (1985) 292-295.

[3] T.V. Choudhary, D.W. Goodman, Top. Catal., 21 (2002) 25-34.

[4] M. Haruta, N. Yamada, T. Kobayashi, S. Iijima, J. Catal., 115 (1989) 301-309.

[5] G.C. Bond, D.T. Thompson, Catal. Rev. - Sci. Eng., 41 (1999) 319-388.

[6] M. Haruta, M. Date, Appl. Catal., A, 222 (2001) 427-437.

[7] S. Carrettin, P. Concepcion, A. Corma, N.J.M. Lopez, V.F. Puntes, Angew Chem Int Ed Engl, 43 (2004) 2538-2540.

[8] Q. Fu, H. Saltsburg, M. Flytzani-Stephanopoulos, Science, 301 (2003) 935-938.

[9] P. Landon, J. Ferguson, B.E. Solsona, T. Garcia, A.F. Carley, A.A. Herzing, C.J. Kiely, S.E. Golunski, G.J. Hutchings, Chem. Commun. (Cambridge, U. K.), (2005) 3385-3387.

[10] A. Corma, H. Garcia, Chem. Soc. Rev., 37 (2008) 2096-2126.

[11] A. Corma, P. Serna, Science (Washington, DC, U. S.), 313 (2006) 332-334.

[12] P.C. Della, E. Falletta, L. Prati, M. Rossi, Chem. Soc. Rev., 37 (2008) 2077-2095.

[13] J.K. Edwards, G.J. Hutchings, Angew. Chem., Int. Ed., 47 (2008) 9192-9198.

[14] A. Corma, R. Juarez, M. Boronat, F. Sanchez, M. Iglesias, H. Garcia, Chem. Commun. (Cambridge, U. K.), 47 (2011) 1446-1448.

[15] D.I. Enache, J.K. Edwards, P. Landon, B. Solsona-Espriu, A.F. Carley, A.A. Herzing, M. Watanabe, C.J. Kiely, D.W. Knight, G.J. Hutchings, Science (Washington, DC, U. S.), 311 (2006) 362-365.

[16] H. Kobayashi, M. Yamauchi, R. Ikeda, H. Kitagawa, Chem. Commun. (Cambridge, U. K.), (2009) 4806-4808.

[17] S. Alayoglu, A.U. Nilekar, M. Mavrikakis, B. Eichhorn, Nat. Mater., 7 (2008) 333-338.

[18] R. Ferrando, J. Jellinek, R.L. Johnston, Chem. Rev. (Washington, DC, U. S.), 108 (2008) 845-910.

[19] M.-C. Daniel, D. Astruc, Chem. Rev. (Washington, DC, U. S.), 104 (2004) 293-346.

[20] J.M. Campelo, D. Luna, R. Luque, J.M. Marinas, A.A. Romero, ChemSusChem, 2 (2009) 18-45.

[21] R. Zanella, S. Giorgio, C.R. Henry, C. Louis, J. Phys. Chem. B, 106 (2002) 7634-7642.

[22] M. Okumura, S. Nakamura, S. Tsubota, T. Nakamura, M. Azuma, M. Haruta, Catal. Lett., 51 (1998) 53-58.

[23] C.J. Serpell, J. Cookson, D. Ozkaya, P.D. Beer, Nat. Chem., 3 (2011) 478-483.

[24] A. Villa, D. Wang, D.S. Su, L. Prati, ChemCatChem, 1 (2009) 510-514.

[25] M. Comotti, W.-C. Li, B. Spliethoff, F. Schueth, J. Am. Chem. Soc., 128 (2006) 917-924.

[26] W.-C. Li, M. Comotti, F. Schueth, J. Catal., 237 (2006) 190-196.

[27] C. Baatz, N. Decker, U. Pruesse, J. Catal., 258 (2008) 165-169.

[28] N. Zheng, G.D. Stucky, J. Am. Chem. Soc., 128 (2006) 14278-14280.

[29] W. Yan, S. Brown, Z. Pan, S.M. Mahurin, S.H. Overbury, S. Dai, Angew. Chem., Int. Ed., 45 (2006) 3614-3618.

[30] J.K. Edwards, B. Solsona, N.E. Ntainjua, A.F. Carley, A.A. Herzing, C.J. Kiely, G.J. Hutchings, Science (Washington, DC, U. S.), 323 (2009) 1037-1041.

[31] J.K. Edwards, A.F. Carley, A.A. Herzing, C.J. Kiely, G.J. Hutchings, Faraday Discuss., 138 (2008) 225-239.

[32] M. Haruta, Gold Bull. (London, U. K.), 37 (2004) 27-36.

[33] J.A. Lopez-Sanchez, N. Dimitratos, C. Hammond, G.L. Brett, L. Kesavan, S. White, P. Miedziak, R. Tiruvalam, R.L. Jenkins, A.F. Carley, D. Knight, C.J. Kiely, G.J. Hutchings, Nat. Chem., 3 (2011) 551-556.

[34] M. Sankar, Q. He, M. Morad, J. Pritchard, S.J. Freakley, J.K. Edwards, S.H. Taylor, D.J. Morgan, A.F. Carley, D.W. Knight, C.J. Kiely, G.J. Hutchings, ACS Nano, 6 (2012) 6600-6613.

[35] S.C. Carabineiro, D. Thompson, Catalytic Applications for Gold Nanotechnology, in: U. Heiz, U. Landman (Eds.) Nanocatalysis, Springer Berlin Heidelberg, 2007, pp. 377-489.

[36] H.H. Kung, M.C. Kung, C.K. Costello, J. Catal., 216 (2003) 425-432.

[37] H.S. Oh, J.H. Yang, C.K. Costello, Y.M. Wang, S.R. Bare, H.H. Kung, M.C. Kung, J. Catal., 210 (2002) 375-386.

[38] M.C. Kung, R.J. Davis, H.H. Kung, J. Phys. Chem. C, 111 (2007) 11767-11775.

[39] M. Bowker, A. Nuhu, J. Soares, Catal. Today, 122 (2007) 245-247.

[40] S. Ivanova, C. Petit, V. Pitchon, Appl. Catal., A, 267 (2004) 191-201.

[41] C.R. Adhikari, D. Parajuli, K. Inoue, K. Ohto, H. Kawakita, H. Harada, New Journal of Chemistry, 32 (2008) 1634-1641.

[42] S. Meenakshisundaram, E. Nowicka, P.J. Miedziak, G.L. Brett, R.L. Jenkins, N. Dimitratos, S.H. Taylor, D.W. Knight, D. Bethell, G.J. Hutchings, Faraday Discuss., 145 (2010) 341-356.

[43] M. Sankar, E. Nowicka, R. Tiruvalam, Q. He, S.H. Taylor, C.J. Kiely, D. Bethell, D.W. Knight, G.J. Hutchings, Chem. - Eur. J., 17 (2011) 6524-6532.

[44] N. Dimitratos, F. Porta, L. Prati, Appl. Catal., A, 291 (2005) 210-214.

[45] J.C. Pritchard, Q. He, E.N. Ntainjua, M. Piccinini, J.K. Edwards, A.A. Herzing, A.F. Carley, J.A. Moulijn, C.J. Kiely, G.J. Hutchings, Green Chem., 12 (2010) 915-921.

[46] J. Pritchard, L. Kesavan, M. Piccinini, Q. He, R. Tiruvalam, N. Dimitratos, J.A. Lopez-Sanchez, A.F. Carley, J.K. Edwards, C.J. Kiely, G.J. Hutchings, Langmuir, 26 (2010) 16568-16577.

[47] R.C. Tiruvalam, J.C. Pritchard, N. Dimitratos, J.A. Lopez-Sanchez, J.K. Edwards, A.F. Carley, G.J. Hutchings, C.J. Kiely, Faraday Discuss., 152 (2011) 63-86.

[48] J.K. Edwards, B.E. Solsona, P. Landon, A.F. Carley, A. Herzing, C.J. Kiely, G.J. Hutchings, J. Catal., 236 (2005) 69-79.

[49] A.A. Herzing, M. Watanabe, J.K. Edwards, M. Conte, Z.-R. Tang, G.J. Hutchings, C.J. Kiely, Faraday Discuss., 138 (2008) 337-351.

[50] F.-W. Chang, H.-Y. Yu, R.L. Selva, H.-C. Yang, Appl. Catal., A, 290 (2005) 138-147.

[51] P. Konova, A. Naydenov, C. Venkov, D. Mehandjiev, D. Andreeva, T. Tabakova, J. Mol. Catal. A: Chem., 213 (2004) 235-240.

[52] S. Arrii, F. Morfin, A.J. Renouprez, J.L. Rousset, J Am Chem Soc, 126 (2004) 1199-1205.

[53] J. Radnik, C. Mohr, P. Claus, Phys. Chem. Chem. Phys., 5 (2003) 172-177.

[54] R. Liu, Y. Yu, K. Yoshida, G. Li, H. Jiang, M. Zhang, F. Zhao, S.-i. Fujita, M. Arai, J. Catal., 269 (2010) 191-200.

[55] W.F. Egelhoff, Jr., G.G. Tibbetts, Phys. Rev. B: Condens. Matter, 19 (1979) 5028-5035.

[56] H.-F. Wang, H. Ariga, R. Dowler, M. Sterrer, H.-J. Freund, J. Catal., 286 (2012) 1-5.

[57] Y. Shen, S. Wang, K. Huang, Appl. Catal., 57 (1990) 55-70.

Chapter five:

Solvent-free aerobic oxidation of alcohols using supported gold-palladium in nanoalloys of different ratios prepared by a modified impregnation method

5.1- Introduction

The exceptional catalytic activity of gold nanoparticles has been reported in the literature for more than a quarter of a century [1, 2]. Since the crucial pre-requisite of these gold nanoparticles to be catalytically active is their size, numerous attempts have been made to make these nanoparticles as small as possible and with a very narrow particle size distribution [3, 4]. It is important to note here that the catalytic activity of gold nanoparticles having a particle size larger than 10nm decreases dramatically [5]. Hutchings and co-workers have reported that by combining gold with palladium at the nanoscale, the catalytic activity of these particles can be increased several fold for the selective aerobic oxidation of alcohols [6, 7]. The catalytic activity of these bimetallic nanoparticles follows a similar trend to that of supported monometallic gold particles; that is, catalytic activity increases with decreasing particle size. Due to this similarity, many methods of preparing supported monometallic gold nanoparticles have been directly translated to prepare supported bimetallic nanoparticles [4, 8]. However, the presence of a second metal can impose significant complications in terms of the particle size distribution, the mode of the arrangement of these two metals and the compositional variation from particle to particle [9]. The previous chapter showed a simple excess anion modification to the impregnation method to prepare supported gold-palladium, referred to as modified impregnation catalysts, which have been found to be exceptionally active and stable catalysts that also give very good control over the nanostructure particle size and the composition without using any stabiliser ligands in the preparation. The bimetallic catalysts prepared using this modified impregnation

(M_{Im}) method outperformed the identical catalysts prepared by the C_{Im} and S_{Im} methods for the direct synthesis of hydrogen peroxide from a dilute mixture of hydrogen and oxygen [10]. In this chapter, the work of the new method will be extended by using a modified impregnation catalyst This will be used to study the effect of the ratio between Au and Pd on catalytic performance compared with reduced wet-conventional impregnation catalysts using TiO_2 as a support for aerobic benzyl alcohol oxidation, as well as the anaerobic conditions, for the modified impregnation catalysts. The effect of the chloride ion during the preparation using a constant Cl^- amount for different Au:Pd ratios has also been examined. In addition, the effect of different Au:Pd ratios on the new catalysts using MgO have been evaluated for benzyl alcohol oxidation reaction. The new catalysts have also been evaluated for the solvent-free aerobic oxidation of alcohols, namely a crotyl alcohol reaction, and compared with sol immobilisation catalysts using TiO_2 and MgO as supports in a Radleys carousel glass-stirred reactor.

5.2- Experimental

5.2.1- Catalyst preparation

The catalysts were prepared using three different preparation methods, mainly the sol immobilisation S_{Im} method as described in chapter 2 (section 2.2.1), the conventional wet-impregnation C_{Im} method as described in chapter 2 (section 2.2.2), and the modified impregnation M_{Im} method as described in chapter 2 (section 2.2.3).

5.2.2- Catalyst testing

The catalysts were evaluated for the solvent-free aerobic oxidation of alcohols in a 50 mL glass-stirred (Radleys carousel) reactor system (GSR). Details of the reactor set-up are presented in chapter 2 (section 2.3.1) and the sample reaction is analysed as described in chapter 2 (section 2.4.1.4).

5.2.3- Catalyst characterisation

The catalysts were widely characterised in the previous chapter using scanning transmission electron microscopy (STEM) as described in chapter 2 (section 2.5.3); X-ray photoelectron spectroscopy (XPS) as described in chapter 2 (section 2.5.2), and powder X-ray diffraction (XRD) as described in chapter 2 (section 2.5.1).

5.3- Results and discussion

5.3.1- Benzyl alcohol oxidation

Hutchings *et al*., previously reported the effect of Au:Pd composition supported on carbon by S_{Im} for the oxidation of benzyl alcohol and the direct synthesis of hydrogen peroxide [3]. In this chapter, the oxidation of benzyl alcohol using different compositions of Au/Pd catalysts supported on TiO_2 will be performed using different catalyst preparation methods. The performance of an Au:Pd catalyst ratio prepared by

M_{Im} will be examined on benzyl alcohol for aerobic and anaerobic oxidation. The effect of the Au:Pd composition on the MgO as a support will also be studied with respect to benzyl alcohol oxidation.

5.3.1.1- Effect of Au:Pd ratio using M_{Im} supported on TiO_2

A range of catalysts, monometallic Au, Pd and bimetallic in different Au:Pd ratios, were prepared using the M_{Im} methods, and the catalysts were evaluated for benzyl alcohol oxidation under free solvent conditions to explore the catalytic performance of the bimetallic Au:Pd ratio catalysts. The results of the catalytic performance are presented with the activity of the reaction and the selectivity of benzaldehyde and toluene, the two major products, as shown in **Figure 5.1**. The error bars are also quantified for the reaction conversion on the graph to indicate the extent of the estimator value likely to be from the true value.

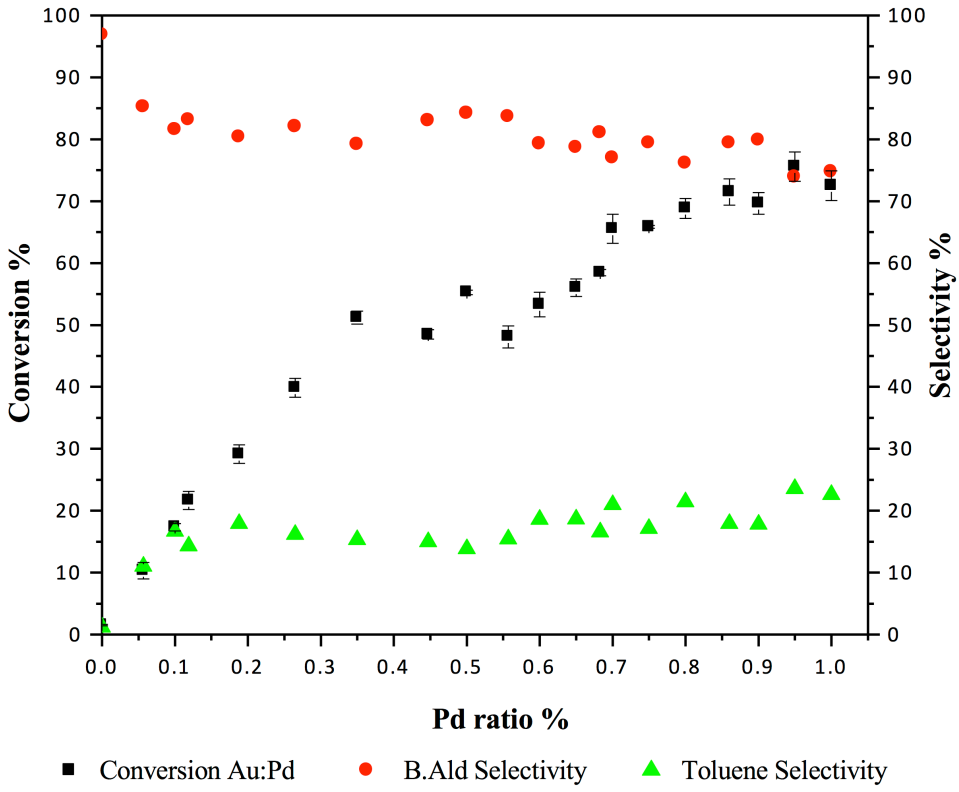

Figure 5.1: Benzyl alcohol oxidation using M_{Im} catalysts with different ratios, the activity with error bars and the major products selectivity. Reaction conditions: 0.02g catalyst, 1 bar of O_2, 2g of benzyl alcohol, 120 °C, 1hr and stirring at 1000 rpm

The monometallic 1wt% Au/TiO_2 yielded very poor activity and the best selectivity. However, increasing the Pd content led to a progressive increase in catalytic activity. This increase in activity reached a broad maximum with a Pd-rich composition with the ratio of 0.05 Au:0.95 Pd/TiO_2, with a value above 76% conversion. A further increase, yielding the monometallic 1wt% Pd/TiO_2, resulted in a slight decrease in catalytic activity. However, based on selectivity for the two major products, as the other by-products were formed with less than 5% selectivity, increasing the Pd content led to interruption of the aldehyde selectivity. This was due to the formation of toluene, formed by the disproportionation reaction, reaching a maximum with the monometallic

1wt% Pd/TiO_2 with a value of approximately of 25%. It is important to note that even in the presence of a minor amount of gold with palladium (*i.e.*, 0.05:0.95 Au:Pd wt ratio), a significant increase in catalytic activity occurred. Moreover, it is notable that the catalysts showed a significant increase in the activity for the Au-rich composition until the gold-palladium 0.5:0.5 Au:Pd wt ratio was reached, then a slight drop in activity occurred in the Pd-rich composition, followed by a gradual increase. It is possible that this is because of the narrow particle size and high gold distribution for the Au-rich composition compared to the Pd-rich composition for the M_{Im} method, as noted in the previous chapter [10]. However, for the bimetallic catalysts, a 0.5:0.5 Au/Pd wt ratio yielded a considerable selectivity of 85%. The product yields are shown in **Figure 5.2**, as is the oxidation yield of benzaldehyde, which is generated by the oxidation reaction only of benzyl alcohol; whereas the toluene yield was generated by the disproportionation reaction. The results show a linear increase in the yield in benzaldehyde and toluene. The error bars are also quantified for the product yield on the graph to indicate the error rate. However, the oxidation reaction yield shows a gradual increase in the Au-rich compositions, reaching the maximum at the position of the 1:1wt Au:Pd ratio, and then becoming unstable with Pd-rich compositions. This may mean that the 1:1wt Au:Pd ratio results in the best benzaldehyde oxidation yield with a limited toluene yield.

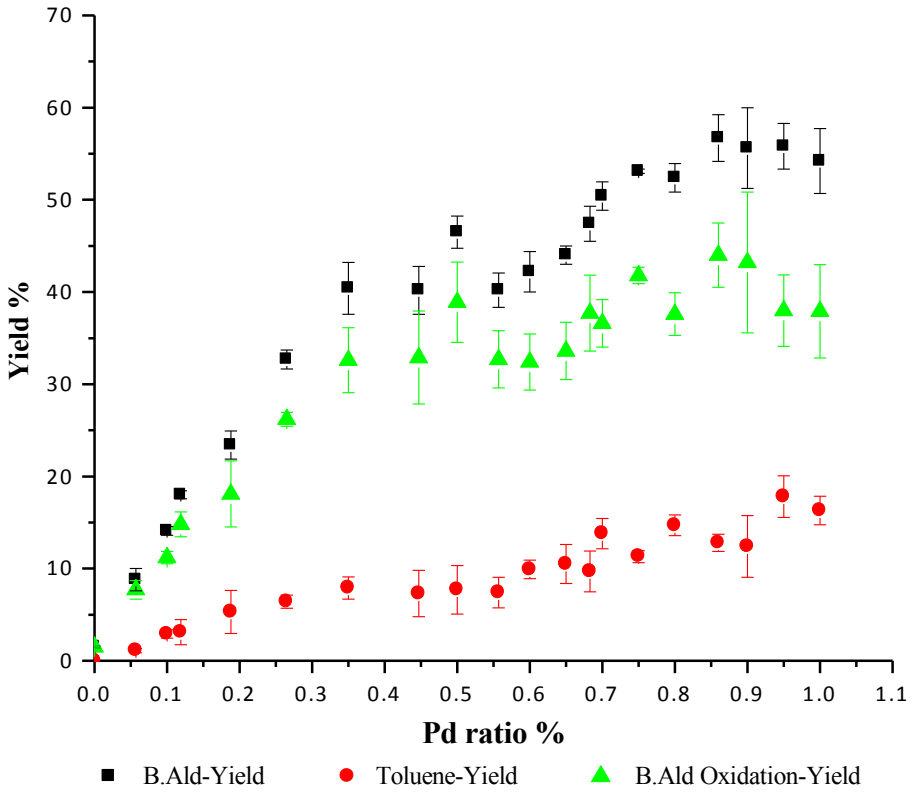

Figure 5.2: Benzyl alcohol oxidation using M_{Im} catalysts with different ratios, the yield with error bars for the major products' selectivity. Reaction conditions: 0.02g catalyst, 1 bar of O_2, 2 g of benzyl alcohol, 120 °C, 1hr and stirring at 1000 rpm

5.3.1.2- Effect of monometallic Pd/TiO_2 using M_{Im} with different ratios

To determine the effect of the gold on palladium, ranges of monometallic Pd were prepared with different ratios, namely 0.2%, 0.5% and 0.8%, on TiO_2 supports. The catalysts' performances are presented in **Figure 5.3**, with a comparison to the activity of the bimetallic Au:Pd with different ratios.

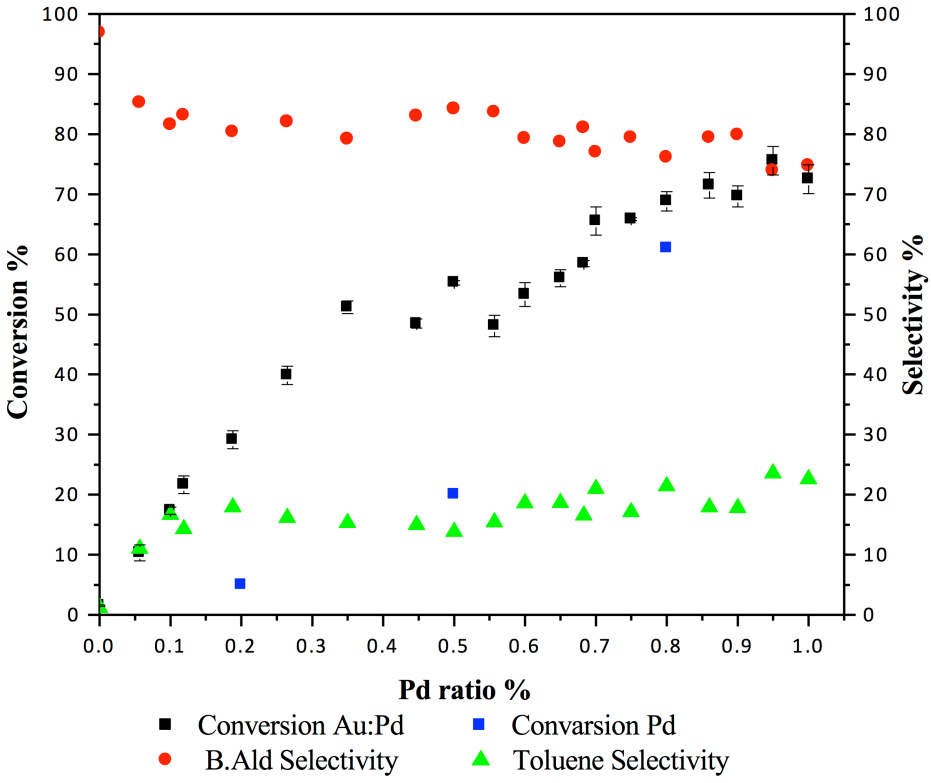

Figure 5.3: Comparison activity of monometallic Pd and bimetallic catalysts in different ratios for benzyl alcohol oxidation using M_{Im} catalysts. Reaction conditions: 0.02 g catalyst, 1 bar of O_2, 2 g of benzyl alcohol, 120 °C, 1hr and stirring at 1000 rpm

The results show, in general, that the activity of the monometallic Pd catalysts increases significantly on increasing the Pd amount. However, these results obviously prove that the gold plays an important role in promoting catalytic performance, as the monometallic Pd catalysts increased the activity by a factor of 35% when the gold was added to palladium in the 0.5:0.5 Au:Pd ratio catalyst. For the other monometallic Pd catalyst ratios, increases of a factor of 25% and 9% were observed with the catalysts prepared using an Au:Pd ratio of 0.8:0.2 and 0.2:0.8, respectively.

5.3.1.3- The effect on selectivity at iso-conversion using M_{Im}

To determine the effect of the Au:Pd wt ratio on selectivity, the catalytic data was compared with respect to the iso-conversion, and **Table 5.1** shows the catalytic data for the 10% conversion.

Table 5.1: The iso-conversion at 10% and selectivity and yield data for the oxidation of benzyl alcohol using 1wt% AuPd/TiO_2 prepared by the M_{Im} method [a]

Catalysts Ratio	Selectivity %		Yield %	
	Benzaldehyde	Toluene	Benzaldehyde	Toluene
0.65% Au + 0.35% Pd /TiO_2	92	5.7	9.2	0.6
0.5% Au + 0.5% Pd /TiO_2	93.2	4.1	9.3	0.4
0.316% Au + 0.683% Pd /TiO_2	90	7.2	9	0.7
0.2% Au + 0.8% Pd /TiO_2	90	7.4	9	0.7
1% Pd /TiO_2	85.7	12.9	8.6	1.3

[a] Reaction conditions: 0.02g catalyst, 1 bar of O_2, 2g benzyl alcohol, 120 °C and stirring at 1000 rpm

This data shows that the catalytic performance in terms of reaction selectivity is not particularly significant and that all bimetallic catalysts yield high selectivity to benzaldehyde, which is the primary product, especially with the 0.65:0.35 and 0.5:0.5 Au:Pd ratio catalysts. However, the main effect of alloying Au with Pd is the enhancing of activity and selectivity, particularly the formation of benzaldehyde, which increases at iso conversion. Whereas the formation of toluene, which is generated from the disproportionation reaction decreases at iso-conversion and a slight increases as the Pd content increases.

5.3.1.4- Effect of using constant Cl^- ions on M_{Im} with different Au:Pd ratios

The effect of Cl^- ion has been studied using a constant amount of Cl^- ions during the preparation of the modified impregnation catalysts. The 0.5 Au:0.5 Pd ratio, containing 9.7 $x10^{-4}$ mol of chloride ions, was selected as the constant Cl^- amount, and the catalysts were prepared with different Au:Pd ratios. The results are shown in **Table 5.2**.

Table 5.2: Conversion and selectivity data for the oxidation of benzyl alcohol using 1wt% $AuPd/TiO_2$ prepared by the M_{Im} method [a]

Catalyst Pd ratio (%)	M_{Im}				M_{Im} with Constant Cl^-			
	Cl^- mol	Conv. (%)	Selectivity (%)		Cl^- mol	Conv. (%)	Selectivity (%)	
			B.Ald	Toluene			B.Ald	Toluene
0	0	1.5	96.8	1.2	9.7 $x10^{-4}$	0.1	96	0.1
0.2	3.8 $x10^{-4}$	29	80	17.9	9.7 $x10^{-4}$	41	72	26
0.4	7.7 $x10^{-4}$	51.6	81	15.5	9.7 $x10^{-4}$	59	71	27
0.5	9.7 $x10^{-4}$	55	84	13.8	9.7 $x10^{-4}$	55	84	13.8
0.6	1.1 $x10^{-3}$	53	79	18.6	9.7 $x10^{-4}$	50	77.5	21
0.7	1.3 $x10^{-3}$	65.5	76.9	21.0	9.7 $x10^{-4}$	58	77.5	22
0.8	1.5 $x10^{-3}$	68.8	76	21.4	9.7 $x10^{-4}$	59	73	24
0.9	1.7 $x10^{-3}$	69.6	79.8	17.8	9.7 $x10^{-4}$	62	71	26
1	1.9 $x10^{-3}$	72.5	74.7	22.6	9.7 $x10^{-4}$	74.6	66	32

[a] Reaction conditions: 0.02g catalyst, 1 bar of O_2, 2g benzyl alcohol, 120 °C, 1hr of reaction time and stirring at 1000 rpm

This data shows that the catalysts in the Au-rich composition up to 0.5Au:0.5Pd showed better catalytic performance when the catalysts were prepared using a M_{Im} constant Cl^- amount than the normal M_{Im} catalysts. The activity may be associated with an increase

in the Cl^- ion amount; whereas the catalytic performance dropped with the Pd-rich compositions when the catalysts were prepared using the M_{Im} constant Cl^- amount compared to the normal M_{Im} catalysts as a result of the decrease in the Cl^- ion amounts. This data proves the previous study when the catalysts were prepared using excess amounts of Cl^-, more than 0.58M, for example 2M or 1M, as a significant increase in the activity was revealed, but unfortunately, the catalysts lose activity when they are reused, as explained in the previous chapter [10]. The current catalysts were also examined for reusability and showed results compatible with those observed previously, as shown in **Figure 5.4**.

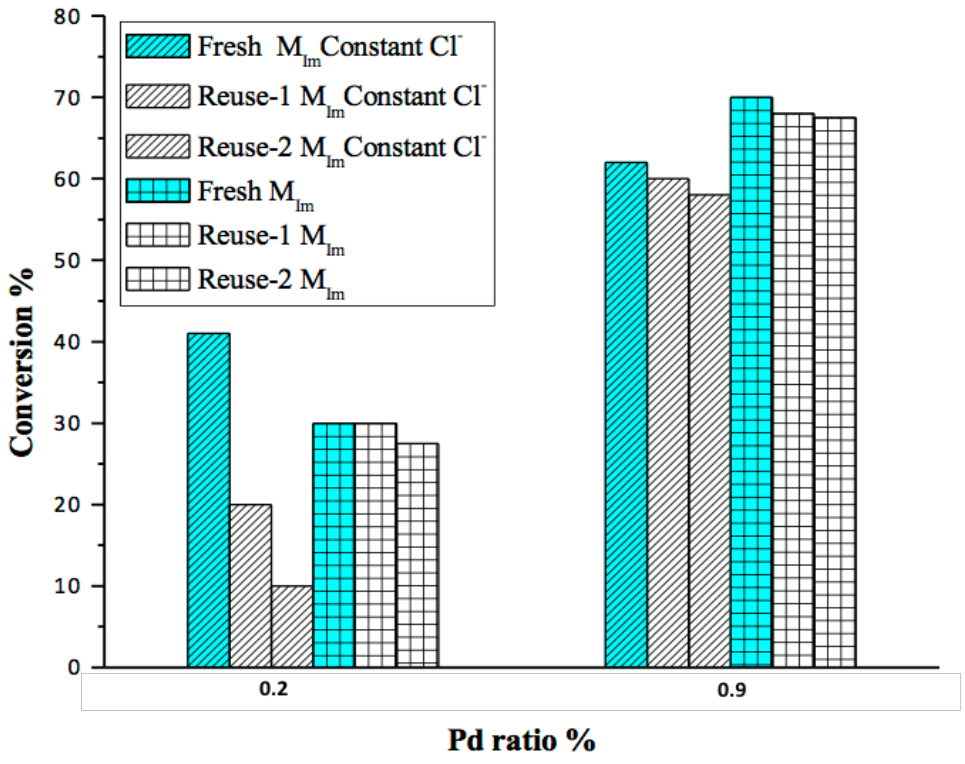

Figure 5.4: Comparison of activity and reusability data for benzyl alcohol oxidation. Reaction conditions: 0.02g catalyst, 1 bar of O_2, 2g benzyl alcohol, 120 °C, 1hr of reaction time and stirring at 1000 rpm

5.3.1.5- Effect of Au:Pd and Pd ratios on a reduced C_{Im} supported on TiO_2

A range of catalysts, monometallic Au and different Pd ratios and different bimetallic Au:Pd ratios, were prepared. The catalysts were prepared using C_{Im} methods and reduced under 5% H_2/Ar for 4 hr at 400 °C as per the treatment conditions for the M_{Im} catalysts. The catalysts were evaluated for benzyl alcohol oxidation under solvent free conditions to explore the catalytic performance of the bimetallic Au:Pd ratio catalysts. The results are presented with the activity of the reaction and the selectivity of the major products. The error bars are also quantified for the reaction conversion (see **Figure 5.5**).

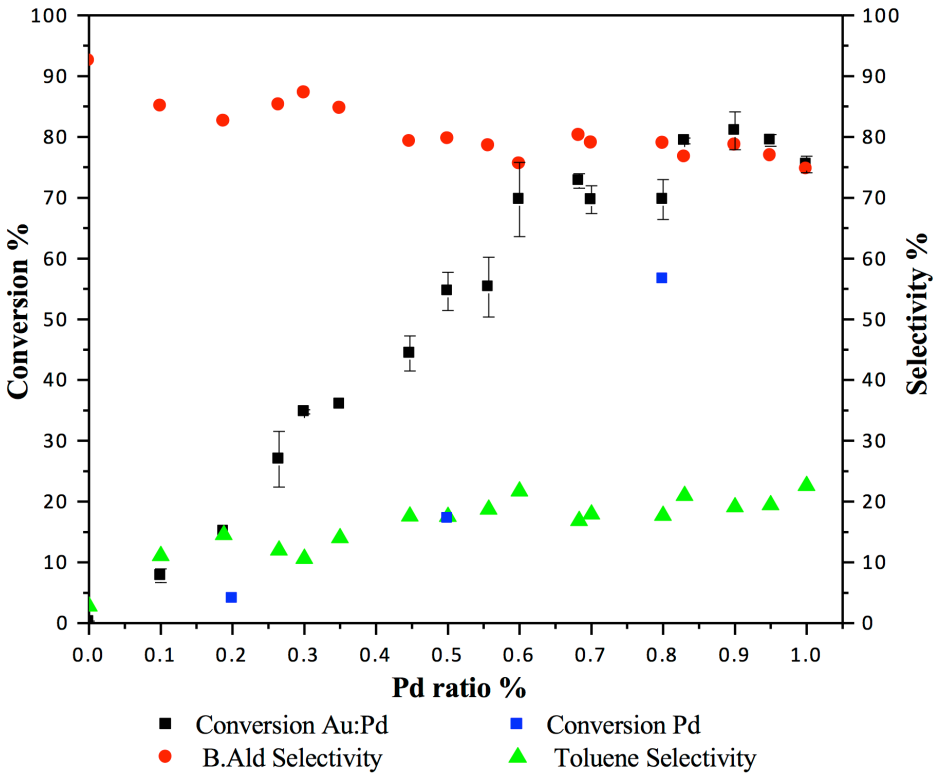

Figure 5.5: Comparison activity of monometallic Pd and bimetallic catalysts by C_{Im} in different ratios for benzyl alcohol oxidation using M_{Im} catalysts. Reaction conditions: 0.02g catalyst, 1 bar of O_2, 2g of benzyl alcohol, 120 °C, 1hr and stirring at 1000 rpm

The catalysts show a similar synergetic effect to the linear trend activity and the selectivity of the M_{Im} catalysts. The monometallic 1 wt% Au/TiO_2 yielded very poor activity and the best selectivity. However, increasing the Pd content led to a progressive increase in catalytic activity. On considering the percent activity increase, the highest effect for the Pd-rich composition was observed at about 80% conversion for the 0.1 Au:0.9 Pd ratio catalyst. Further increases in the Pd content led to a slight decrease in catalytic activity, which can be seen for the ratio of 0.05 Au:0.95 Pd and for the monometallic Pd catalysts.

Based on the selectivity for the two major products, as the other by-products were formed with less than 5% selectivity, the benzaldehyde appeared to yield the highest selectivity with the Au/TiO_2 dependent on the Au:Pd ratio. Au 0.9:Pd 0.1 showed a high selectivity to aldehyde close to that observed for pure gold catalyst, and the addition of Pd decreased this gradually; whereas 0.2 Au:0.8 Pd displayed similar selectivity to toluene to that observed for the pure palladium catalyst. However, among the bimetallic catalysts, for the 0.7:0.3 Au:Pdwt ratio, a high selectivity of 87% was observed.

It can be clearly seen in **Figure 5.5** that the addition of Au to Pd for the alloy catalysts yielded a similar synergetic effect to that observed for M_{Im} catalysts, with significant differences in the linear trend expected for the monometallic Pd using different ratios (0.2, 0.5 and 0.8) prepared by C_{Im} catalysts. It is obvious that gold nanoparticles can considerably promote the catalytic activity of the reaction.

5.3.1.6- Comparison of Au:Pd and Pd ratios between M_{Im} and reduced C_{Im}

To demonstrate the efficacy of the preparation methods on the different Au and Pd ratios, the bimetallic catalysts prepared using M_{Im}, M_{Im} constant Cl^- amounts, reduced C_{Im} methods as well as the monometallic Pd ratios. The catalysts were all compared with respect to the catalytic activity results for the aerobic oxidation of benzyl alcohol. For a judicious comparison, all catalysts were prepared using different metallic ratios. The results are shown in **Figure 5.6**.

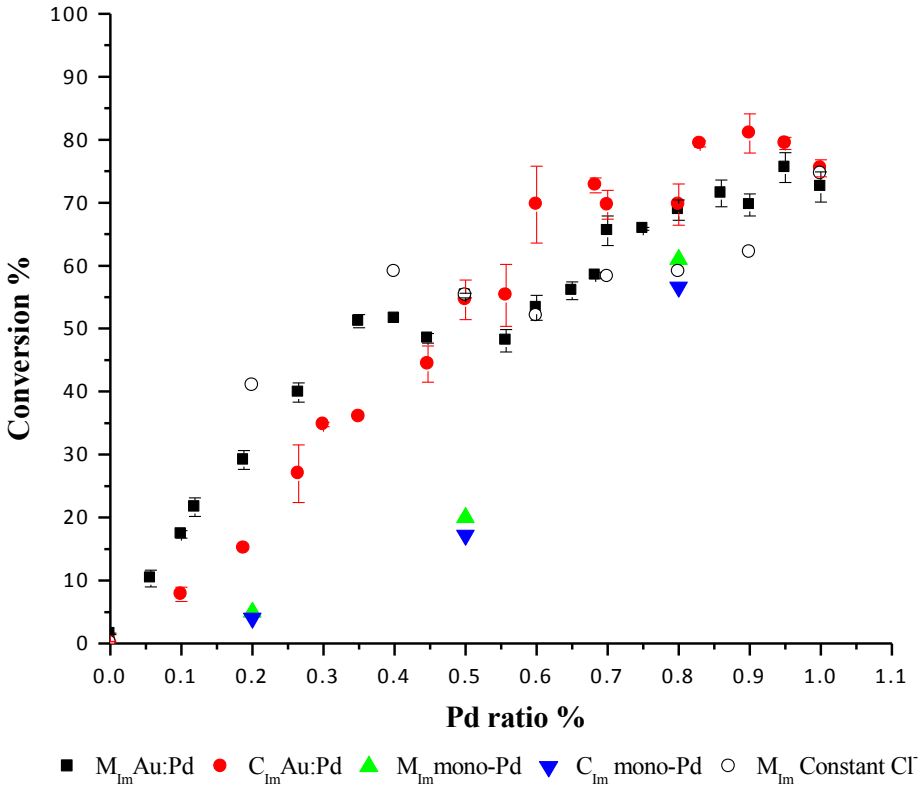

Figure 5.6: Comparison activity of M_{Im} and C_{Im} for benzyl alcohol oxidation. Reaction conditions: 0.02g catalyst, 1 bar of O_2, 2g benzyl alcohol, 120 °C, 1hr of reaction time and stirring at 1000 rpm

The comparison data show that there are two sides of the Au:Pd ratio trend. The first side is the trend of the Au-rich composition up to 0.5Au:0.5Pd ratio, which shows a distinction between the activity for the catalysts prepared by M_{Im} constant Cl^- amount compared to the catalysts prepared by M_{Im} and C_{Im} methods. The activity of the catalyst on the first side followed the order of M_{Im} constant $Cl^- > M_{Im} > C_{Im}$. However, for M_{Im} constant Cl^-, the activity could be due to the excess chloride ion, but it is not a stable catalyst, as shown previously in **Figure 5.4**. However, the superiority in the activity for M_{Im} than C_{Im} on the first side could be because the M_{Im} had a narrow particle size and higher gold distribution in the Au-rich composition than the catalysts prepared by the C_{Im} method [10]. On the second side of the Au:Pd ratio trend, the Pd-rich composition shows more distinction in the activity of the C_{Im} method than catalysts prepared by the M_{Im} and M_{Im} constant Cl^- amount methods. The activity of the catalyst on the second side followed the order of $C_{Im} > M_{Im} > M_{Im}$ constant Cl^-. However, the superiority of the activity of C_{Im} compared to M_{Im} could be as the C_{Im} had a good palladium distribution in the Pd-rich composition compared to the catalysts prepared by the M_{Im} method [10]. However, the catalysts prepared by M_{Im} constant Cl^- lose their activity due to the reduction of the chloride ion on this side which has a Pd-rich composition.

The characterisation described in the previous chapter, after 400 °C reducing treatments under 5% H_2/Ar the catalysts M_{Im} and $C_{Im,}$ show that all the AuPd metals have been efficiently subsumed into the larger random alloy particles with an absence of any clusters and atomic dispersed species. The reduced C_{Im} and M_{Im} materials show a distinct difference in AuPd particle size distribution, with mean values of 4.7 and 2.9

nm respectively. The difference in catalytic activity between the M_{Im} and C_{Im} catalysts was referred to the "excess" anion effect. The analysis of the particle size distributions in the previous chapter shows that the mean particle size and spread of particle size decreases with increasing [Cl] concentration; it also shows a systematic change in Pd:Au ratio. Moreover, it has been clearly shown that increasing the amount of excess [Cl] used in the M_{Im} preparation causes a definite increase in Au content within the AuPd alloy particle. The previous chapter clearly shows that the C_{Im} material contains a significant population of poorly dispersed Au, but the effect of the excess Cl^- in the M_{Im} materials is to progressively disperse (*i.e.,* eventually eliminate) these large Au species. As this Au is no longer associated with large inactive particles, it can be incorporated into the nm scale AuPd alloy particles, thereby increasing their mean gold content. Increasing the Au content in the particle improves the benzyl alcohol activity, but simultaneously decreases the catalyst's reusability when over ion excess is used (e.g the catalysts prepared using constant Cl^- with Au-rich composition and M_{Im} 2M HCl in previous studies). The reason for the observed instability of these catalysts is unknown, but a detailed characterisation of these fresh and reused materials is currently underway. However, this implies that the intermediate (0.58 M HCl) M_{Im} sample has a AuPd particle composition that is a good compromise for yielding a catalyst that simultaneously has a reasonable benzyl alcohol activity and effective reusability characteristics. The catalysts prepared using monometallic Pd with different ratios show comparable activity for both the M_{Im} and C_{Im} methods, yielding a general increase in the activities of all monometallic Pd catalysts with increases in the Pd amount in the

catalyst. Based on an overview of the testing of these various ratios of Au-Pd supported by TiO_2, it can be concluded that there was a synergistic effect between Au and Pd.

5.3.1.7- Anaerobic oxidation using M_{Im} with different Au:Pd ratios

The anaerobic oxidation of benzyl alcohol using M_{Im} catalysts has been studied using a range of Au:Pd ratios. The results of the catalytic performance are presented with the activity of the benzyl alcohol reaction and the yield of benzaldehyde and toluene as the only two products (**Figure 5.7**).

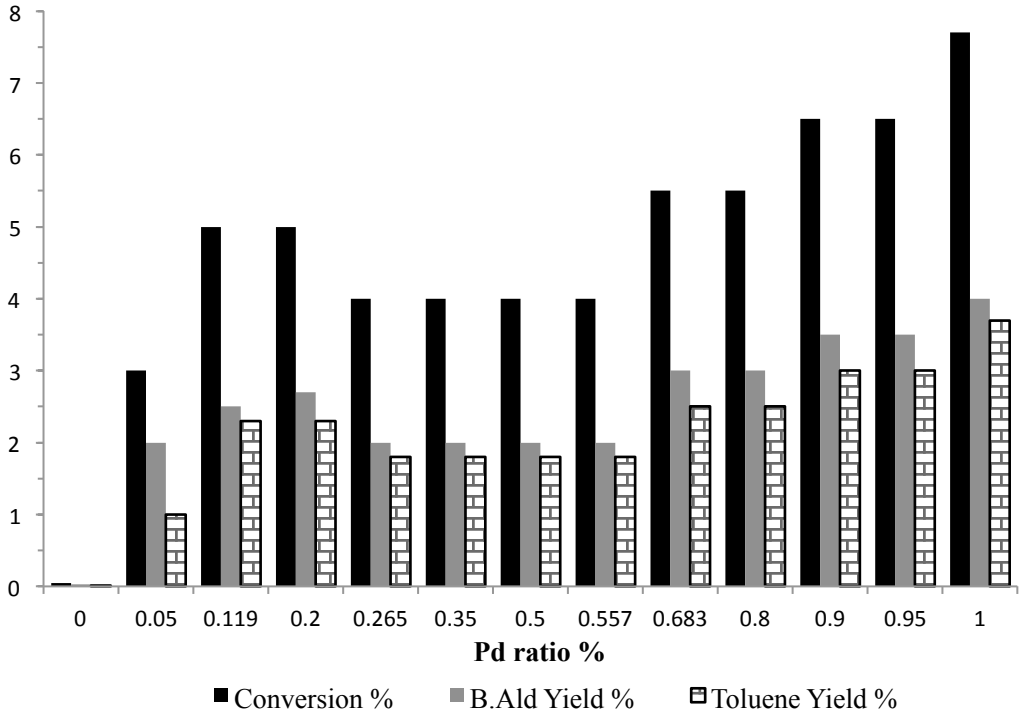

Figure 5.7: Benzyl alcohol oxidation activity and products yield. Reaction conditions: 0.02g catalyst, 1 bar of He, 2g benzyl alcohol, 120 °C, 1hr of reaction time and stirring at 1000 rpm

The results show that, under anaerobic conditions in the presence of He, the product mixture generally comprised nearly equivalent amounts of benzaldehyde and toluene, which means that the redox disproportionation reaction of benzyl alcohol to produce benzaldehyde and toluene is the only active reaction [11, 12]. However, there was a small positive value for the oxidation to aldehyde, which was attributed to the adsorbed O_2 on the surface of the catalyst, which could not be removed [12]. However, the data shows that the disproportionation reactions are more active with a Pd-rich composition than with an Au-rich composition. Moreover, with a Pd-rich composition, increased Pd content led to a slight increase in the catalytic activity of the disproportionation reaction and, hence, the toluene formation with a Pd-rich composition in the overall reactions. This is because benzaldehyde is formed by both oxidation and disproportionation reactions, while disproportionation is the only origin of toluene, as shown in **Scheme 5.1**.

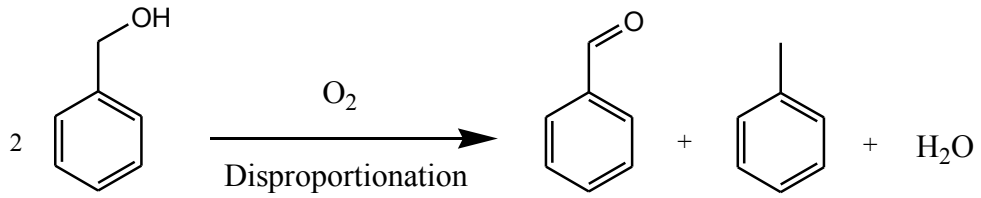

Scheme 5.1: Disproportionation of two moles of benzyl alcohol, leading to equimolar amounts of toluene and benzaldehyde

5.3.1.8- Effect of Au:Pd ratio using M_{Im} supported on MgO

An investigation was carried out into the oxidation side of benzyl alcohol, with no disproportionation reactions, and MgO was used as a support in place of TiO_2, as the titania support promotes both oxidation and disproportionation reactions. Catalysts prepared using the M_{Im} method were studied for this reaction with a range of Au:Pd ratios. The results of the catalytic performance are presented in **Figure 5.8**, with the activity of the reaction and the selectivity of benzaldehyde and toluene, the two major products.

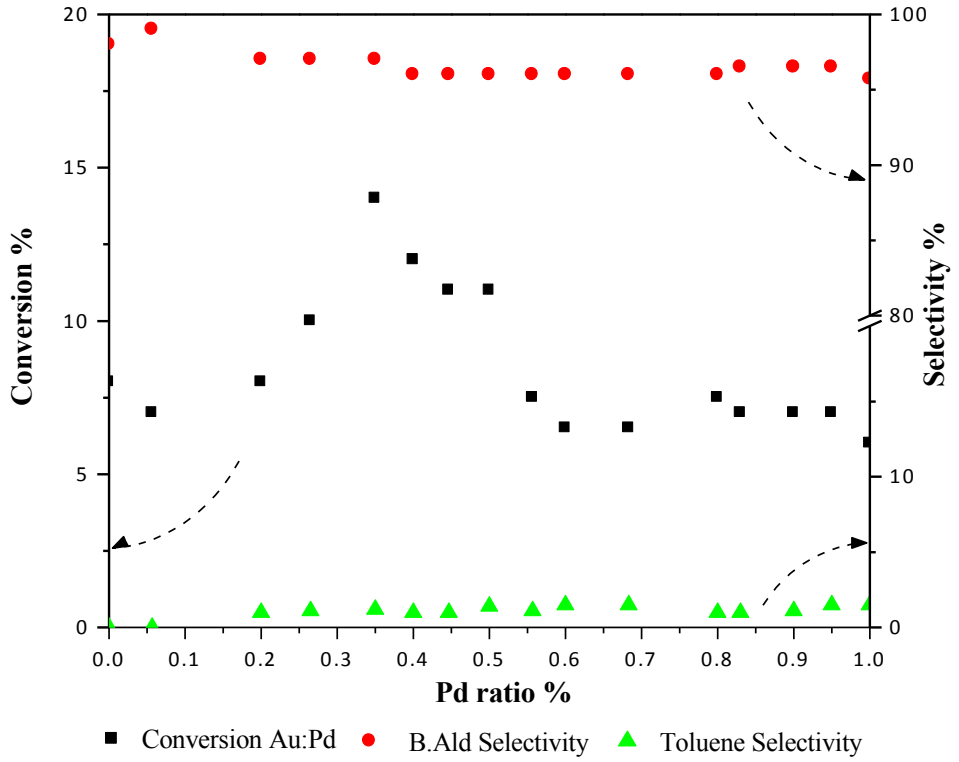

Figure 5.8: The activity and selectivity of benzyl alcohol oxidation using supported MgO by M_{Im} method. Reaction conditions: 0.02g catalyst, 1 bar of O_2, 2g benzyl alcohol, 120 °C, 1hr of reaction time and stirring at 1000 rpm

The performance of the catalysts in the oxidation of benzyl alcohol shows that the catalysts yield higher activity in the Au-rich composition ratio than in the Pd-rich composition. The results show that the 0.65 Au:0.35 Pd ratio, which is computationally equal to a 1:1 molar ratio of the metals, has a marked effect on the conversion of benzyl alcohol, with a maximum activity of 15% conversion and 97% aldehyde selectivity. The monometallic Pd shows the lowest activity among all the catalysts.

These ratio data demonstrate that the disproportionation reaction is switched off by the MgO support, and the only active reaction was the oxidative dehydrogenation reaction to form the aldehyde, as shown in **Scheme 5.2**.

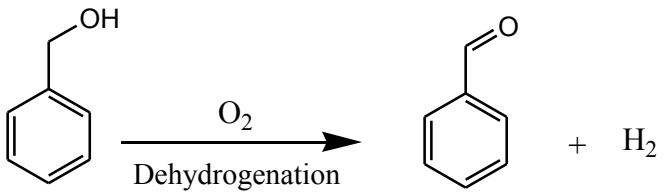

Scheme 5.2: Dehydrogenation of benzyl alcohol to benzaldehyde

5.3.2- Crotyl alcohol oxidation

Recent interest in nano-gold catalysed selective oxidation reactions has led to increased investigation into bimetallic catalysts. The most notable studies have involved the bimetallic catalysts gold and palladium. The addition of Au to Pd catalysts has been reported to improve both catalytic activity, as well as the selectivity to the desired product [13, 14]. In a comparison of Pd and Pt, gold is more resistant to deactivation by chemical poisoning or over-oxidation, and as a result, Au displays higher selectivity

[15]. However, gold selectivity for the oxidation of the hydroxyl group in the presence of other functional groups in the molecule is very high compared to Pd [16]. Recently, Bawaked *et al.* [17] showed that monometallic Au was observed to have low activity and high selectivity, whereas the activity of crotyl alcohol was significantly increased for a bimetallic catalyst supported on graphite, and it was highly dependent on the ratio between Au and Pd. In this part of the chapter, solvent-free crotyl alcohol oxidation using bimetallic AuPd catalysts will be performed. The effect of the preparation methods of Au-Pd catalysts using TiO_2 and MgO as supports on crotyl alcohol will also be examined.

5.3.2.1- Crotyl alcohol oxidation using M_{Im} compared to S_{Im} on TiO_2

The investigation into the new M_{Im} preparation method on the crotyl alcohol reaction, which was selected because it contains two functional groups, was carried out using catalysts prepared by the M_{Im} method and compared to the S_{Im} method in the 1:1 equal molar ratio 1% AuPd/TiO_2. The activity comparison is presented in **Figure 5.9**, and the selectivity for M_{Im} and S_{Im} are presented in **Figure 5.10** and **Figure 5.10** respectively.

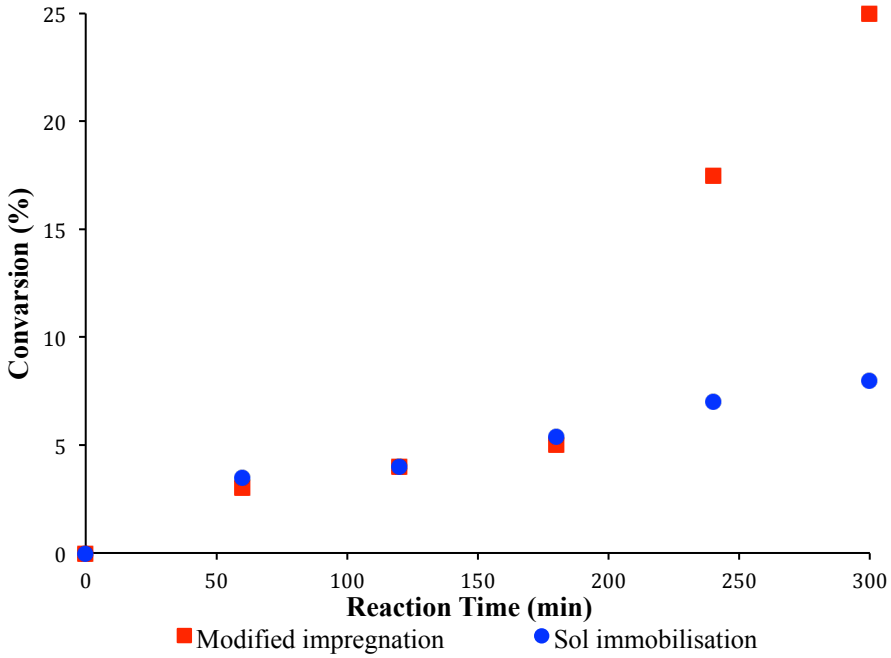

Figure 5.9: Crotyl alcohol oxidation the activity data comparison using 1% AuPd/TiO_2 catalyst. Reaction conditions: 0.02g catalyst, 1 bar of O_2, 2g benzyl alcohol, 100 °C and stirring at 1000 rpm

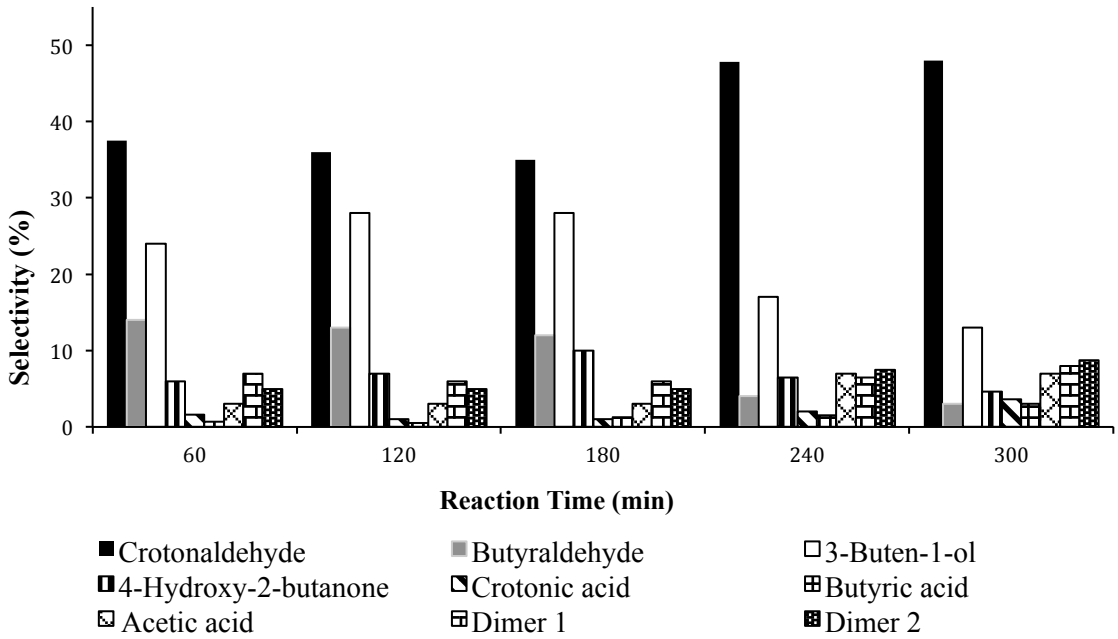

Figure 5.10: Selectivity of crotyl alcohol oxidation using 1% AuPd/TiO_2 by M_{Im} method. Reaction conditions: 0.02g catalyst, 1 bar of O_2, 2g benzyl alcohol, 100 °C and stirring at 1000 rpm

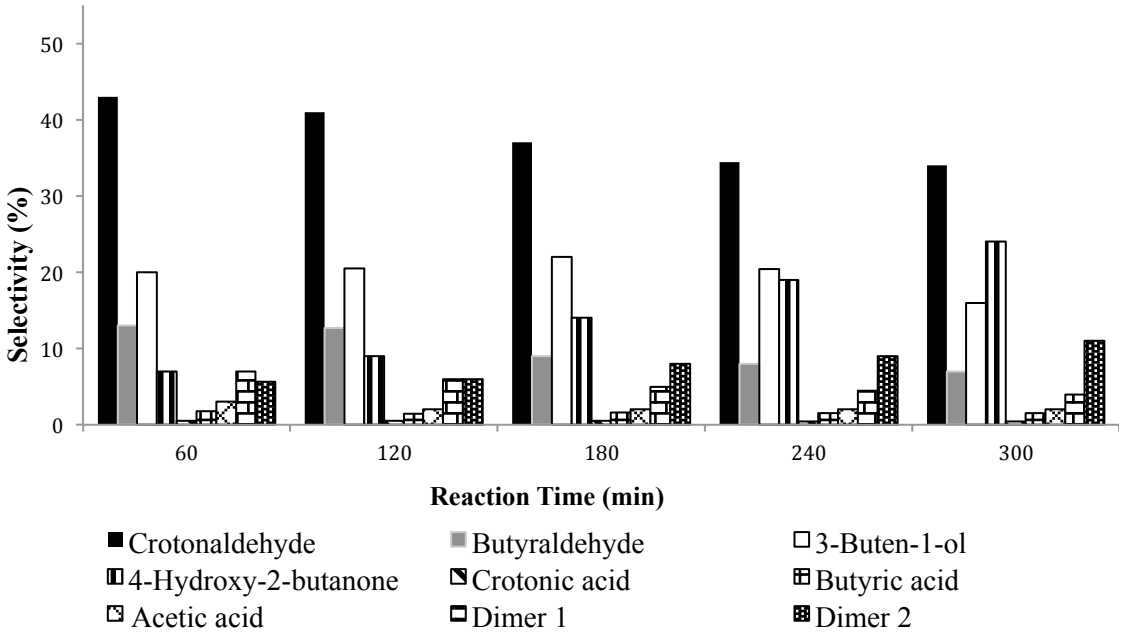

Figure 5.11: Selectivity of crotyl alcohol oxidation using 1% $AuPd/TiO_2$ by S_{Im} method. Reaction conditions: 0.02g catalyst, 1 bar of O_2, 2g benzyl alcohol, 100 °C and stirring at 1000 rpm

The activity data comparison shows a general increase in activity over the reaction time for both catalysts. However, during the first three hours of reaction time, the two catalysts show comparable activity. Then the catalysts prepared using the M_{Im} method showed an excellent improvement in catalytic performance, at four hours, compared to the S_{Im} method. The improvement of the M_{Im} catalytic performance continued and was nearly three times more effective at the end of the reaction time. The reusability test was conducted using the M_{Im} catalyst to confirm the previous results for three hours of reaction time as well as for five hours. This gave similar results to those observed with the fresh catalysts, having an activity of 5% for three hours and 22% conversion for five hours of reaction time.

Based on selectivity, the oxidation of the alcohol functional group was observed over the two M_{Im} and S_{Im} catalysts. The major product was crotonaldehyde, which increased over the reaction time in M_{Im} more than S_{Im} method; however, the over-oxidation of crotonaldehyde led to crotonic acid formation. The isomerisation reaction was dominant as 3-buten-1-ol, the second major product, which decreased more with the reaction time for the M_{Im} method than for the S_{Im} method. Further oxidation of the former led to 4-hydroxy-2-butanone formation through the Wacker oxidation type, as occurs when Pd is present [17-20]. The formation of 4-hydroxy-2-butanone increased significantly more over the reaction time for the S_{Im} method than for the M_{Im} method. This could mean that S_{Im} promotes the isomerisation reaction, whereas M_{Im} promotes oxidation. The formation of butyraldehyde occurs when palladium is present, which is the following alkene isomerisation, as shown in **Figure 5.12**. Subsequent oxidation of the former leads to butanoic acid formation.

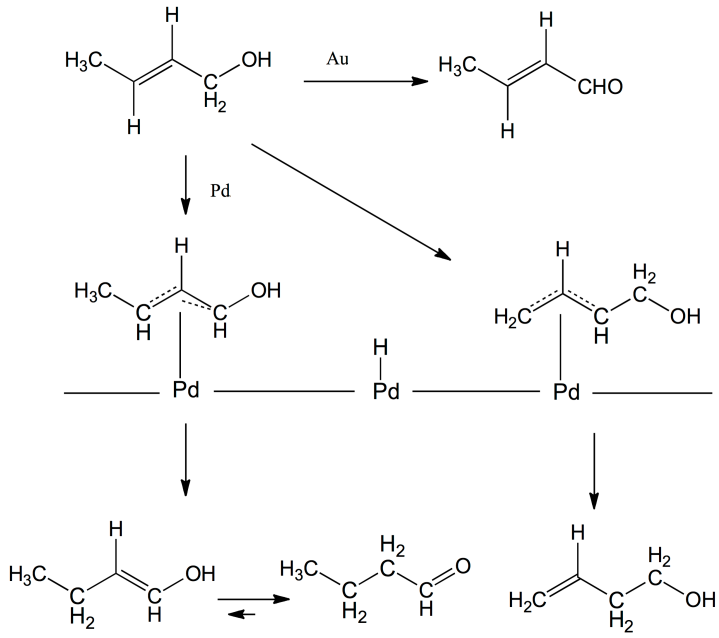

Figure 5.12: Principal pathways for transformation of crotyl alcohol [17]

Other by-products were observed in uneven amounts: acetic acid, dimer 1 and dimer 2. The dimmers are presented in **Figure 5.14**; these secondary products increased slightly over the reaction period. The summaries of these formations are as follows: the formation of crotonaldehyde was followed by the addition of water to the unsaturated bond, and then through the cleavage of hydrated crotonaldehyde (retro-aldol fragmentation), which may produce two acetaldehyde molecules, that could then transform into acetic acid [17] (as shown in **Figure 5.13**).

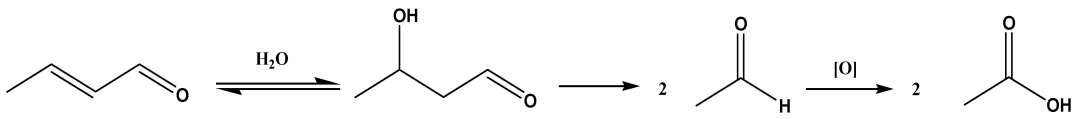

Figure 5.13: Potential pathway for the formation of acetic acid from crotonaldehyde [17]

The oxidation of acetaldehyde using the standard condition catalyst resulted in acetic acid as a minor product. The catalyst may facilitate the dimerisation of the oxidation product crotonaldehyde to 6-hydroxy-2,4-dimethyltetrahydro-2H-pyran-3-carbaldehyde through the Diels-Alder reaction, which occurs with acid or base catalysis [17, 21, 22], as presented in **Figure 5.14**. Summary scheme of crotyl alcohol oxidation and isomerisation reactions is presented in **Figure 5.15**.

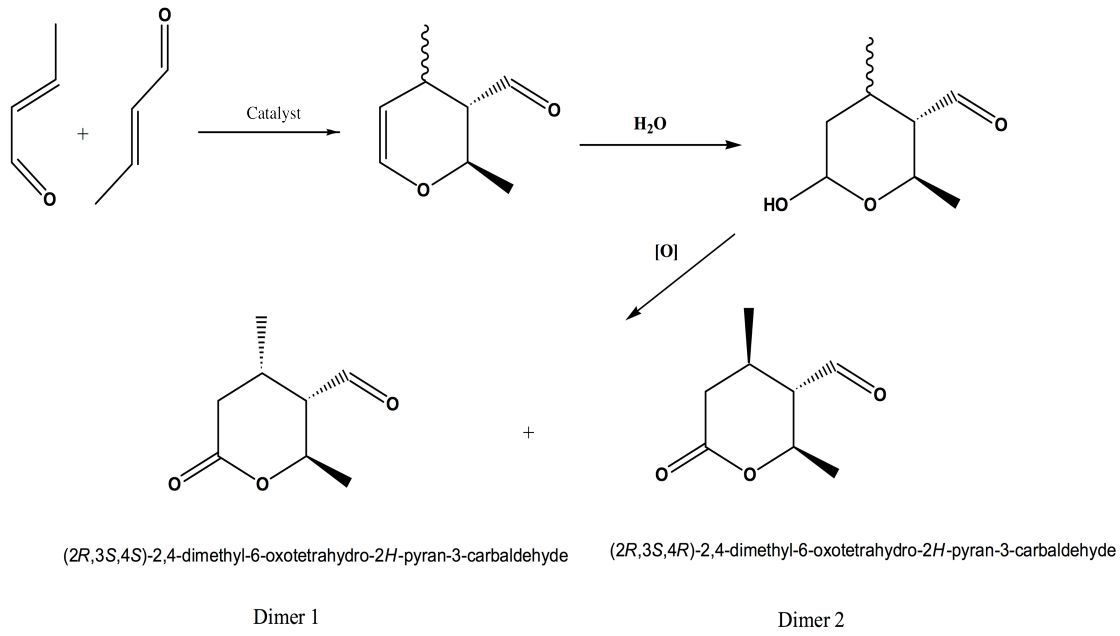

Figure 5.14: Potential Diels–Alder formation of epimeric products (2,4-dimethyl-6-oxotetrahydro-2H-pyran-3-carbaldehyde) from the crotonaldehyde oxidation product [17]

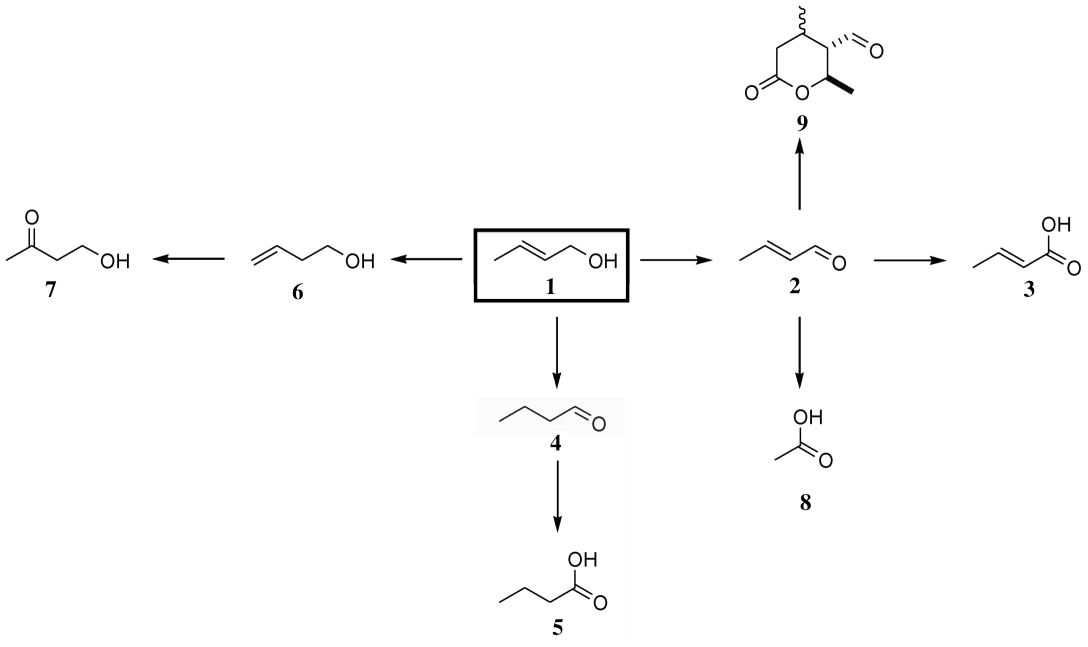

Figure 5.15: Crotyl alcohol (1) oxidation and isomerisation products. Crotonaldehyde (2), crotonic acid (3), butyraldehyde (4), butanoic acid (5), 3-buten-1-ol (6), 4-hydroxy-2-butanone (7), acetic acid (8), and lactons (9)

5.3.2.2- Crotyl alcohol oxidation using M_{Im} compared to S_{Im} on MgO

An investigation into the preparation methods for crotyl alcohol reaction using different supports was carried out. The catalysts were prepared using M_{Im} and S_{Im} in the 1:1 equal molar ratio of 1% AuPd/MgO. A comparison of the activity and selectivity of the reaction is presented in **Table 5.3**.

Table 5.3: Comparison of conversion and selectivity data for the oxidation of crotyl alcohol using 1% Au-Pd/MgO prepared by the M_{Im} and S_{Im} methods [a]

		Preparation methods			
		Modified impregnation		Sol immobilisation	
	Time (min)	60	120	60	120
	Conversion (%)	9	12	5	7
Selectivity (%)	Crotonaldehyde	49.6	47	40.6	41.3
	Butyraldehyde	19.5	21.7	19.4	20
	3-buten-1-ol	28	28.4	23.4	23.7
	4-hydroxy-2-butanone	0.5	0.5	1	1
	Crotonic acid	0	0	0.2	0.3
	Butyric acid	0	0	1.2	1
	Acetic acid	0.8	0.8	5	5
	Dimer 1	0.8	0.8	3	2
	Dimer 2	0.8	0.5	6.4	5.5

Reaction conditions: 0.02g catalyst, 1 bar of O_2, 2g crotyl alcohol, 100 °C and stirring at 1000 rpm

The activity data comparison shows a general increase in activity for both catalysts. However, the catalysts prepared using the M_{Im} method show a better catalytic performance than the S_{Im} method for all reaction times.

Based on selectivity, the oxidation of the alcohol functional group was observed for the two M_{Im} and S_{Im} catalysts. The major product was crotonaldehyde, for which the M_{Im} catalyst gave higher selectivity over the reaction time compared to the S_{Im} catalyst. In contrast, the isomerisation reaction of 3-buten-1-ol was the second major product, and exhibited more formation with the catalyst prepared using the M_{Im} method than with the S_{Im} method. The butanal was formed with comparable selectivity for both catalysts. However, it is notable that M_{Im} was selective, as it did not form much dimer or the acid products, which increased the activity toward the crotonaldehyde.

5.4- Conclusions

A modified impregnation methodology for preparing supported gold-palladium nanoalloy catalysts in the presence of an excess amount of anionic ligands in the impregnation medium has been developed. Catalysts prepared using this method have been tested with different Au:Pd ratios and found to be extremely active for the aerobic oxidation of benzyl alcohol, mainly with gold-rich composition. Eventually, the Cl^- ion had an effect on the catalysts, and the effect of Cl^- ions in this chapter has indicated that increasing the Cl^- ions led to an increase in the activity; however, over increasing of the Cl^- ions led to losing the stability of the catalysts. The anaerobic oxidation of benzyl alcohol shows an increasing disproportionation reaction with palladium-rich composition for the modified impregnation catalysts. However, the best catalytic performance can be observed for an Au:Pd ratio using MgO as a support when an equal 1:1 molar ratio is used. Moreover, the catalysts prepared using this new methodology are more active and stable for the oxidation of crotyl alcohol to its corresponding aldehyde, than a similar composition catalyst prepared by another methodology, such as a sol immobilisation catalyst.

5.5- References

[1] G.J. Hutchings, J. Catal., 96 (1985) 292-295.

[2] M. Haruta, T. Kobayashi, H. Sano, N. Yamada, Chem. Lett., (1987) 405-408.

[3] J. Pritchard, L. Kesavan, M. Piccinini, Q. He, R. Tiruvalam, N. Dimitratos, J.A. Lopez-Sanchez, A.F. Carley, J.K. Edwards, C.J. Kiely, G.J. Hutchings, Langmuir, 26 (2010) 16568-16577.

[4] P. Miedziak, M. Sankar, N. Dimitratos, J.A. Lopez-Sanchez, A.F. Carley, D.W. Knight, S.H. Taylor, C.J. Kiely, G.J. Hutchings, Catal. Today, 164 (2011) 315-319.

[5] N. Lopez, T.V.W. Janssens, B.S. Clausen, Y. Xu, M. Mavrikakis, T. Bligaard, J.K. Norskov, J. Catal., 223 (2004) 232-235.

[6] A. Villa, N. Janjic, P. Spontoni, D. Wang, D.S. Su, L. Prati, Appl. Catal., A, 364 (2009) 221-228.

[7] D.I. Enache, J.K. Edwards, P. Landon, B. Solsona-Espriu, A.F. Carley, A.A. Herzing, M. Watanabe, C.J. Kiely, D.W. Knight, G.J. Hutchings, Science (Washington, DC, U. S.), 311 (2006) 362-365.

[8] J.A. Lopez-Sanchez, N. Dimitratos, P. Miedziak, E. Ntainjua, J.K. Edwards, D. Morgan, A.F. Carley, R. Tiruvalam, C.J. Kiely, G.J. Hutchings, Phys. Chem. Chem. Phys., 10 (2008) 1921-1930.

[9] R.C. Tiruvalam, J.C. Pritchard, N. Dimitratos, J.A. Lopez-Sanchez, J.K. Edwards, A.F. Carley, G.J. Hutchings, C.J. Kiely, Faraday Discuss., 152 (2011) 63-86.

[10] M. Sankar, Q. He, M. Morad, J. Pritchard, S.J. Freakley, J.K. Edwards, S.H. Taylor, D.J. Morgan, A.F. Carley, D.W. Knight, C.J. Kiely, G.J. Hutchings, ACS Nano, 6 (2012) 6600-6613.

[11] E. Cao, M. Sankar, E. Nowicka, Q. He, M. Morad, P.J. Miedziak, S.H. Taylor, D.W. Knight, D. Bethell, C.J. Kiely, A. Gavriilidis, G.J. Hutchings, Catalysis Today, 203 (2013) 146-152.

[12] M. Sankar, E. Nowicka, R. Tiruvalam, Q. He, S.H. Taylor, C.J. Kiely, D. Bethell, D.W. Knight, G.J. Hutchings, Chem. - Eur. J., 17 (2011) 6524-6532.

[13] D. Wang, A. Villa, F. Porta, L. Prati, D. Su, J. Phys. Chem. C, 112 (2008) 8617-8622.

[14] X. Wang, N.S. Venkataramanan, H. Kawanami, Y. Ikushima, Green Chem., 9 (2007) 1352-1355.

[15] P.G.N. Mertens, M. Bulut, L.E.M. Gevers, I.F.J. Vankelecom, P.A. Jacobs, V.D.E. De, Catal. Lett., 102 (2005) 57-61.

[16] A. Abad, C. Almela, A. Corma, H. Garcia, Tetrahedron, 62 (2006) 6666-6672.

[17] S. Bawaked, Q. He, N.F. Dummer, A.F. Carley, D.W. Knight, D. Bethell, C.J. Kiely, G.J. Hutchings, Catal. Sci. Technol., 1 (2011) 71-83.

[18] H. Pellissier, P.-Y. Michellys, M. Santelli, Tetrahedron Lett., 35 (1994) 6481-6484.

[19] J. Tsuji, H. Nagashima, H. Nemoto, Org. Synth., 62 (1984) 9-13.

[20] T. Yokota, A. Sakakura, M. Tani, S. Sakaguchi, Y. Ishii, Tetrahedron Lett., 43 (2002) 8887-8891.

[21] D.W. Cameron, P.E. Schuetz, J. Chem. Soc., C, (1968) 1801-1802.

[22] A. Losse, Chem. Ber., 100 (1967) 1266-1269.

Chapter six:

Conclusions and future work

6.1- Conclusions

Until relatively recently, gold was thought of as too unreactive to be of interest chemically, but this perception changed with the discovery of its catalytic capabilities when reduced to the nano-scale [1, 2]. Subsequently, it has been demonstrated that the combination of Au and Pd as alloy nanoparticles can significantly enhance the catalytic activity for the oxidation of alcohols [4]. Moreover, it has been shown that the nature of the support can have a very important influence in determining the catalyst's performance [5, 6]. As outlined in chapter three, changing the support to MgO can stop the disproportionation reaction for benzyl alcohol oxidation; the objective was to investigate the toluene formation from the disproportionation reaction. This formation was inhibiting benzaldehyde selectivity when catalysts were prepared with Au-Pd/TiO_2. The other objectives for this thesis were to investigate the preparation methods for the catalysts, which also have been shown to be significant in terms of the activity of the catalysts, such as control of the gold particle size and the dispersion of gold on the support. Consequently, it is important to look for a simple and effective method for the reproducible preparation of highly active and stable gold-based nanoparticulate catalysts [7, 8]. As outlined in chapter 4, the main objective of the chapter was to study the effect of modifying the conventional impregnation method by adding excess amount of Cl^- ion during preparation, which showed promising results for benzyl alcohol oxidation. Finally, in chapter 5, the objective was to study bimetallic catalysts prepared using the modified impregnation method, in particular Au-Pd, and the effect of the ratio between the two metals on benzyl alcohol oxidation, in addition to studying the catalysts'

performance concerning alcohol oxidation, in particular crotyl alcohol oxidation.

In chapter 3, the disproportionation of benzyl alcohol under solvent-free conditions for reactions on a 1%AuPd/TiO_2 catalyst using the sol immobilisation method was confirmed experimentally in a glass stirred reactor under anaerobic conditions. This was in order to produce equimolar amounts of benzaldehyde and toluene, which proved that disproportionation of benzyl alcohol, is the source of toluene. The disproportionation reaction is promoted by increases in O_2 concentration pressure up to 1 bar, but this promotion effect was reduced by further increases in O_2 pressure. This dependence of the disproportionation reaction on O_2 pressure may imply the existence of two mechanisms of disproportionation – one aerobic and the other anaerobic. Moreover, increasing the temperature promotes disproportionation, and as a consequence, the toluene formation. However, the conclusion of this study is that the support plays an important role in the formation of the products, as it can stop the disproportionation and the formation of toluene. The consequence of this is that the selectivity increases toward benzaldehyde. Moreover, the characterisation of the catalysts suggests that the difference in promotional behaviour for the disproportionation reaction for these AuPd supported TiO_2 and MgO catalysts is not simply because of differences in particle size, but it could be related to the redox conductance or surface compositional characteristics of the oxide support.

Chapter 4 discussed the wet conventional impregnation methodology which has been developed by using a new method for preparing supported gold-palladium nano-alloy catalysts that are stabiliser-free. The impregnation medium in the new method contains

a large excess of anionic ligands, namely Cl^- ions, which help to improve the dispersion of the Au species in particular. The reduction treatment at 400 °C in a 5%H_2/Ar atmosphere is effective for removing the excess Cl^- from the catalyst, as well as efficiently sweeping-up the very highly dispersed, mostly Pd-rich species; this helps their efficient incorporation into the 2-5 nm AuPd alloy nanoparticles. Catalysts prepared using the M_{Im} method are found to be more active for the solvent-free oxidation of benzyl alcohol than those made by C_{Im} and S_{Im} methods, and also found to be four times more active for the direct synthesis of hydrogen peroxide from H_2 and O_2 than those methods. The metal nanoparticles in these M_{Im} materials have a tight distribution of particle sizes, ranging from 2-6 nm with only very occasional large particles, that is, their size range is much better controlled than the C_{Im} materials and they are more akin in this respect to S_{Im} derived catalysts. Furthermore, the bimetallic alloy composition is relatively invariant from particle-to-particle in these M_{Im} materials, in contrast to the C_{Im} and S_{Im} materials where systematic particle size/composition variations have previously been noted. In addition, it has been found that the Au:Pd ratio of the alloy particles can to some extent be controlled by varying the concentration of excess [Cl^-] anions employed in the M_{Im} process. This new preparation protocol could be of benefit for both the academic research community and the industrial community, with a very convenient and reproducible methodology for preparing supported Au-Pd nanoalloys catalysts with high activity and stability without using any ligands or stabilisers, while at the same time not compromising their catalytic activity.

In chapter 5, the work on the modified impregnation methodology for preparing supported gold-palladium nanoalloys catalysts in the presence of an excess amount of anionic ligands in the impregnation medium has been extended. Catalysts prepared through this method have been compared with reduced C_{Im} in different Au:Pd ratios and found to be extremely active for the aerobic oxidation of benzyl alcohol, mainly with gold-rich composition. The effect of Cl^- ions has shown that increasing the Cl^- ions led to increased activity, although a greater amount of Cl^- led to losing the stability of the catalysts. The anaerobic oxidation of benzyl alcohol shows an increasing disproportionation reaction with palladium-rich composition for the modified impregnation catalysts. However, the best catalytic performance can be observed for an Au:Pd ratio using MgO as a support when an equal 1:1 molar ratio was used. Moreover, the catalysts prepared using this new methodology are more active and stable for the oxidation of crotyl alcohol to its corresponding aldehyde than a similar composition catalyst prepared by another methodology, such as a sol immobilisation catalyst.

It can be concluded that using excess Cl^- anion during the catalyst's preparation is very effective, although a higher amount of Cl^- leads to losing the stability of the catalyst. The new method could be beneficial for alcohol oxidation, especially when ratios of Au-rich composition are used. However, the Pd-rich composition catalysts may be more suitable catalysts for hydrogenation reactions, and this possibility is something for future investigation.

6.2- Future work

The work in this thesis has demonstrated that supported nanoparticulate AuPd catalysts are promising for heterogeneous catalysts in selective oxidation of hydrocarbons under mild conditions, particularly from the viewpoint of green chemistry. The results obtained from these reactions and investigations have led to some possible questions and suggestions for further work and development. The following suggestions may be beneficial to understanding more about the mechanism of hydrocarbon reactions, to improve the selectivity, as well as improving the supported gold nanoparticles and gold bimetallic catalysts' performance.

a) It was shown in chapter 3 that using MgO as support could stop the disproportionation reaction and lead the oxidation reaction to be the only active reaction. Although the activity was reduced compared to that observed with TiO_2, using a mixed support may improve the activity.

b) To understand and explain the difference in the activity and selectivity that has been obtained using different supports, more high definition characterisation of STEM and the chemisorption analysis used *in situ* ATR-IR and DRIFT spectroscopic studies on catalysts prepared by different supports for alcohol oxidation, are also needed. Investigations from this aspect may help in understanding the support effect and the interface effect between the metals' nanoparticles and the supports, and also the products' molecular composition with the supports and metals. This will help in understanding the possible molecular mechanism processes of the reactions.

c) As shown in chapter 4, new preparation methods or even small modifications to methods, show promising results, which is related to the narrow nanopartical size and the metal distribution. Accordingly, modifying the S_{Im} by, for example, using a stabiliser that could easily be removed from the catalysts, or by designing additional new preparation methods, could lead to finding catalysts that have more enhancements for activity, selectivity and reusability. This would also contribute towards establishing a general relationship between catalyst structure and the activity of the catalysts.

d) Optimisation of the formulation of different gold bimetal supported catalysts, for example supported Au-Ag or Au-Cu catalysts with the new modified impregnation method for alcohol oxidation, may improve the activity of the reaction and the selectivity of the products. Moreover, using supported Au-Ag or Au-Cu for other reactions, for example CO oxidation and H_2O_2 synthesis, would also be a very important factor in influencing catalytic activity through supported gold bimetallic catalysts using the modified impregnation method.

e) As revealed in chapter 4 and chapter 5, increasing the Cl^- ion in the preparation medium was found to act towards promoting the catalyst's performance, although an over increase of the Cl^- ion concentration led to losing the reusability of the catalysts. This seems to be an area where further research would be worthwhile, as this could lead to better understanding of how these catalysts work when using the new method, and subsequently, the development of better catalyst reusability.

f) As shown in chapter 4, using NaCl in place of HCl during preparation of the M_{Im} catalyst makes an excellent active catalyst for H_2O_2 synthesis, but as yet, it has not been possible to stabilise the catalyst for reuse. However, working on the concentration could be one of the probabilities for creating stability, as this possibility was shown when HCl were used in this method.

g) As chapter 5 demonstrated the superiority of the new method with crotyl alcohol oxidation, it would be interesting to carry out an evaluation of the oxidation of other alcohols, or even test hydrogenation reactions with the catalyst prepared using the new preparation method.

h) As demonstrated in this thesis, the selectivity of the reaction is dependent on the Au:Pd ratio. Therefore, the catalysts with an Au-rich composition could be beneficial for oxidation reactions, whereas, the catalysts with a Pd-rich composition could be valuable for hydrogenation reactions; this needs to be studied in more detail.

6.3- References

[1] G.J. Hutchings, Dalton Transactions, (2008) 5523-5536.

[2] M. Haruta, T. Kobayashi, H. Sano, N. Yamada, Chemistry Letters, 16 (1987) 405-408.

[3] R.A. Sheldon, J.K. Kochi, Academic Press, (1981).

[4] D.I. Enache, J.K. Edwards, P. Landon, B. Solsona-Espriu, A.F. Carley, A.A. Herzing, M. Watanabe, C.J. Kiely, D.W. Knight, G.J. Hutchings, Science (Washington, DC, U. S.), 311 (2006) 362-365.

[5] G.C. Bond, C. Louis, D.T. Thompson, Editors, Catalysis by Gold, World Scientific, (2006).

[6] J. Huang, W.-L. Dai, K. Fan, Journal of Catalysis, 266 (2009) 228-235.

[7] N. Zheng, G.D. Stucky, J. Am. Chem. Soc., 128 (2006) 14278-14280.

[8] W. Yan, S. Brown, Z. Pan, S.M. Mahurin, S.H. Overbury, S. Dai, Angew. Chem., Int. Ed., 45 (2006) 3614-3618.